



OPTIMISATION OF FRAGMENTATION AT SOUTH DEEP GOLD FIELDS MINE. A CASE STUDY

Matsobane Nong
(306926)

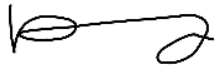
School of Mining Engineering
University of the Witwatersrand Johannesburg, South Africa.

A research report submitted to the Faculty of Engineering and the Built Environment, University of the Witwatersrand, in partial fulfilment of the requirements for the degree of Master of Science in Engineering.

Johannesburg, 2020

DECLARATION

I declare that this research report is my own, unaided work. It is being submitted to the Degree of Master of Science in Engineering to the University of the Witwatersrand, Johannesburg. It has not been submitted before, for any degree or examination to any other university.



(Signature of Candidate)

ABSTRACT

A fundamental aspect of an efficient mining operation is the steady movement of material throughout the mine system; particularly the flow of ore from the upstream excavation point to the downstream processing or stockpile site(s). This can be achieved by attaining an optimal fragmentation size from drilling and blasting suitable for subsequent mining process such as loading, hauling and crushing. Drilling and blasting are the first fragmentation process and is currently the most economical technique of fragmenting hard and competent rock especially for deep-level mines where operational costs are high.

The aim of this research is to analyse and optimise fragmentation to improve the ore flow efficiency at South Deep Mine in South Africa. The mine experiences coarse fragmentation that cannot pass through 300mm by 300mm grizzlies. As such, secondary blasting is often done to reduce the size of boulders either in the stopes or on top of the grizzly which leads to a reduction in productivity. Although coarse fragmentation is reported in the stopes and on top of grizzlies, the plant is reporting fine fragmentation that is not suitable for the ball mill. This results in reduced gold recoveries.

To get a better understanding of the fragmentation size distribution achieved, fifty-one images of the muckpile from five stopes were analysed using the Split-Desktop software. The analysis showed an overall F_{80} passing of 287.48mm, which is less than the 300mm grizzly size implying that the fragmentation size achieved is adequate. However, looking at the overall particle size, the Rosin-Rammler distribution was found to be 0.80. This infers an inconsistent fragmentation where the mine produces both coarse and fine fragmentation size.

The AEGIS Underground drill and blast software was used to analyse the drill and blast design patterns. The analysis showed that the design toe spacing varies from about 0.5m to 7.5m in the same blast. Due to the software's limitations, the break model analysis was only run for toe spacing between 2m and 7.5m. This showed that there is no overlap between blastholes which may be the source of the coarse fragmentation size. Fine fragment size may be as a result of blastholes which are close together, i.e. 0.5m.

Although not tested, the impact of blasting stresses emanating from primary stopes may result in fractures in secondary stopes which will have a greater impact on the propagation of the shock

wave and high-pressure gases between the blastholes and consequently the fragmentation distribution size.

It is recommended that the mine change their drill and blast pattern. The mine must change from 76mm blasthole diameters and introduce a larger blasthole diameter of 89mm blasthole diameter. Not only will this diameter improve drilling accuracies but will reduce the fragmentation size distribution. It is also recommended that the mine maintains a ring burden of 2m throughout despite an increase in the blasthole diameter. For the first design, the toe spacing must also be 2m followed by increments of 0.5m per blast until a suitable fragmentation distribution size is achieved. After which, the toe spacing must be kept constant. It is important that South Deep Mine continually evaluate the fragmentation size distribution achieved from each blast for optimisation purposes. Therefore, a blast management system is important.

ACKNOWLEDGEMENTS

I would like to extend my sincerest gratitude to institutions and individuals who assisted, guided and supported me throughout out my research. This report is because of their continuous inputs.

- Gold Fields, for the provision of data, financial support and the opportunity to undertake this research.
- Mapttek for the providence of the AEGIS Drill and Blast Software that enabled me to do the analysis.
- Mr. Erhan Uludag, my supervisor for his guidance and support.
- Gold Fields Executive and Management, Mr. Richard Butcher, Mr. Tim Rowland, Mr. Dave McMahan and Mr. Jonathan Bernitz for their invaluable input.
- Mr. Troy Williams from iRing INC who tirelessly trained me on using AEGIS Drill and Blast Software
- The South Deep Mine Drill and Blast department, especially Mr. Mzwakhe Tshabalala for his assistance during data collection.
- The South Deep Mine Quality Assurance/Quality Control department for taking their time to accompany me underground when collecting data.
- Paseka Leeuw, Tinashe Tholana, Yonela Mgwebi, Joseph Kwiri, Prince Mulenga and Tinashe Chingozha for their assistance in proofreading my report drafts and providing guidance.
- My family and friends for their continued motivation and support.
- My husband, Chris for his unfailing love, support and continuous encouragement throughout my years of study, the process of researching and writing this thesis.

DEDICATION

This thesis is dedicated to my late grandmother, Ramokone Nong

CONTENTS	Page
DECLARATION	I
ABSTRACT	II
ACKNOWLEDGEMENTS	IV
TABLE OF CONTENTS	VI
LIST OF FIGURES	XI
LIST OF TABLES	XIII
LIST OF ABBREVIATIONS AND SYMBOLS	XIV
1. INTRODUCTION	1
1.1 Chapter Overview	1
1.2 Research Background and Context	1
1.2.1 Mine Locality	2
1.3 Problem Statement	7
1.4 Research Aim and Objectives	8
1.5 Significance of the Research	9
1.6 Research Contents	9
1.7 Scope of the Research	10
2. ROCK FRAGMENTATION	11
2.1 Chapter Overview	11
2.2 Mechanism of Rock Breakage	11
2.3 Factors Affecting Rock Fragmentation	13
2.3.1 Uncontrollable Rock Variables	13

2.3.2	Controllable Rock Variables	16
2.4	Blastibility Index	20
2.5	Fragmentation Prediction and Modelling	22
2.5.1	Empirical Models	23
2.5.2	Numerical Models	30
2.5.3	Mechanistic Models	31
2.6	Fragmentation Analysis	39
2.6.1	Sieving	40
2.6.2	Visual Observations	40
2.6.3	Digital Image Analysis Techniques	40
2.7	Chapter Summary	43
3.	METHODOLOGY	45
3.1	Chapter Overview	45
3.2	Image Analysis and Fragmentation Size Distribution Determination	45
3.3	Geometric Blast Design and Explosives Data	46
3.4	Mechanical Properties of Rock	46
3.5	Drill and Blast Design Simulation	47
3.6	Chapter Summary	48
4.	RESULTS AND ANALYSIS	49
4.1	Introduction	49
4.2	Blast Planning	49
4.3	Oreflow System from the Stope to the Stockpile	51
4.4	Classification and Determination of Rock Mass Properties	52
4.5	Explosive Performance Characteristics	55
4.6	Blastibility Index	56

4.7	Analysis and Determination of the Current Fragmentation Size Distribution	58
4.8	Analysis of the Current Drill and Blast Patterns	63
4.9	Proposed Drill and Blast Patterns	70
4.10	Chapter Summary	73
5.	CONCLUSIONS AND RECOMMENDATIONS	75
5.1	Chapter Overview	75
5.2	Conclusions	75
5.3	Recommendations	76
6.	REFERENCES	78
7.	APPENDICES	88
	APPENDIX 7.1: A SCHEMATIC FLOW OF BROKEN ROCK FROM THE STOPE TO THE STOCKPILE AT THE METALLURGICAL PLANT	88
	APPENDIX 7.2: FRAGMENTATION SIZE DISTRIBUTION FOR LONGHOLE STOPE 100 4W CUT3 LHS 7W (SPLIT-DESKTOP, 2019)	89
	APPENDIX 7.3: FRAGMENTATION SIZE DISTRIBUTION FOR LONGHOLE STOPE 100 4W CUT4 LHS 07EMB (SPLIT-DESKTOP, 2019)	89
	APPENDIX 7.4: FRAGMENTATION SIZE DISTRIBUTION FOR LONGHOLE STOPE 95 3W MPR03 LHS 4S (SPLIT-DESKTOP, 2019)	90
	APPENDIX 7.5: FRAGMENTATION SIZE DISTRIBUTION FOR LONGHOLE STOPE 90 3W CUT2 LHS 12 (SPLIT-DESKTOP, 2019)	90
	APPENDIX 7.6: FRAGMENTATION SIZE DISTRIBUTION FOR LONGHOLE STOPE 95 3W MP2 LHS 2S (SPLIT-DESKTOP, 2019)	91
	APPENDIX 7.7: UNIAXIAL COMPRESSIVE TEST RESULTS FOR DETERMINING UCS, YOUNG’S MODULUS AND POISSON’S RATIO	92
	APPENDIX 7.8: BRAZILIAN TEST RESULTS	93

APPENDIX 7.9: RING PATTERN ITERATION AND SIMULATION FOR S/B RATIO OF 1 AND BLASTHOLE DIAMETER OF 76MM (AEGIS DRILL AND BLAST UNDERGROUND SOFTWARE, 2019)	94
APPENDIX 7.10: RING PATTERN ITERATION AND SIMULATION FOR S/B RATIO OF 1.2 AND BLASTHOLE DIAMETER OF 76MM (AEGIS DRILL AND BLAST UNDERGROUND SOFTWARE, 2019)	95
APPENDIX 7.11: RING PATTERN ITERATION AND SIMULATION FOR S/B RATIO OF 1.4 AND BLASTHOLE DIAMETER OF 76MM (AEGIS DRILL AND BLAST UNDERGROUND SOFTWARE, 2019)	96
APPENDIX 7.12: RING PATTERN ITERATION AND SIMULATION FOR S/B RATIO OF 1.6 AND BLASTHOLE DIAMETER OF 76MM (AEGIS DRILL AND BLAST UNDERGROUND SOFTWARE, 2019)	97
APPENDIX 7.13: RING PATTERN ITERATION AND SIMULATION FOR S/B RATIO OF 1.8 AND BLASTHOLE DIAMETER OF 76MM (AEGIS DRILL AND BLAST UNDERGROUND SOFTWARE, 2019)	98
APPENDIX 7.14: RING PATTERN ITERATION AND SIMULATION FOR S/B RATIO OF 2.0 AND BLASTHOLE DIAMETER OF 76MM (AEGIS DRILL AND BLAST UNDERGROUND SOFTWARE, 2019)	99
APPENDIX 7.15: RING PATTERN ITERATION AND SIMULATION FOR S/B RATIO OF 1.0 AND BLASTHOLE DIAMETER OF 76MM (AEGIS DRILL AND BLAST UNDERGROUND SOFTWARE, 2019)	100
APPENDIX 7.16: RING PATTERN ITERATION AND SIMULATION FOR S/B RATIO OF 1.0 AND BLASTHOLE DIAMETER OF 76MM (AEGIS DRILL AND BLAST UNDERGROUND SOFTWARE, 2019)	101
APPENDIX 7.17: RING PATTERN ITERATION AND SIMULATION FOR S/B RATIO OF 1.0 AND BLASTHOLE DIAMETER OF 89MM (AEGIS DRILL AND BLAST UNDERGROUND SOFTWARE, 2019)	102
APPENDIX 7.18: RING PATTERN ITERATION AND SIMULATION FOR S/B RATIO OF 1.2 AND BLASTHOLE DIAMETER OF 89MM (AEGIS DRILL AND BLAST UNDERGROUND SOFTWARE, 2019)	103
APPENDIX 7.19: RING PATTERN ITERATION AND SIMULATION FOR S/B RATIO OF 1.4 AND BLASTHOLE DIAMETER OF 89MM (AEGIS DRILL AND BLAST UNDERGROUND SOFTWARE, 2019)	104

APPENDIX 7.20: RING PATTERN ITERATION AND SIMULATION FOR S/B RATIO OF 1.6 AND BLASTHOLE DIAMETER OF 89MM (AEGIS DRILL AND BLAST UNDERGROUND SOFTWARE, 2019)	105
APPENDIX 7.21: RING PATTERN ITERATION AND SIMULATION FOR S/B RATIO OF 1.8 AND BLASTHOLE DIAMETER OF 89MM (AEGIS DRILL AND BLAST UNDERGROUND SOFTWARE, 2019)	106
APPENDIX 7.22: RING PATTERN ITERATION AND SIMULATION FOR S/B RATIO OF 2.0 AND BLASTHOLE DIAMETER OF 89MM (AEGIS DRILL AND BLAST UNDERGROUND SOFTWARE, 2019)	107
APPENDIX 7.23: RING PATTERN ITERATION AND SIMULATION FOR S/B RATIO OF 1.0 WITH BURDEN AND SPACING OF 3M AND BLASTHOLE DIAMETER OF 89MM (AEGIS DRILL AND BLAST UNDERGROUND SOFTWARE, 2019)	108
APPENDIX 7.24: RING PATTERN ITERATION AND SIMULATION FOR S/B RATIO OF 1.0 WITH BURDEN AND SPACING OF 3M AND BLASTHOLE DIAMETER OF 89MM (AEGIS DRILL AND BLAST UNDERGROUND SOFTWARE, 2019)	109

LIST OF FIGURES

Figure	Page
Figure 1.1: South Deep Mine locality	3
Figure 1.2: South Deep Mine orebody showing six mining corridors and 16 reef horizons	4
Figure 1.3: A schematic of the development layout at South Deep Mine	5
Figure 1.4: A typical development and production layout at South Deep Mine	6
Figure 1.5: Cost as a function of increasing average particle size	7
Figure 2.1: Rock breakage mechanism by explosives	12
Figure 2.2: Schematic showing spacing in longhole drilling	17
Figure 2.3: Blastibility Index versus powder/energy factor	22
Figure 2.4: An underestimation of fines by the Rosin-Rammler fragment distribution compared with the sieved fragment size distribution	24
Figure 2.5: Comparison of Swebrec and Rosin-Rammler fits to coarse fraction data = 90mm and extrapolation to fines range.	30
Figure 2.6: Uniformity index versus burden curve for a two hole ring blast in a simulated hard competent rock	33
Figure 2.7: Unit charge length geometry	35
Figure 2.8: Attenuation curve	36
Figure 2.9: Stress distribution chart	37
Figure 2.10: Automatically delineated image of a muckpile	42
Figure 2.11: Display of a typical cumulative size distribution curve for the rock fragments	43
Figure 3.1: Image of an LHD scoop loaded with ore for fragmentation analysis.	45
Figure 4.1: South Deep Mine drill and blast planning process	50
Figure 4.2: Drill return from underground after drilling at South Deep Mine	50
Figure 4.3: Various strength classifications for intact rock	54
Figure 4.4: Strength - Modulus classification system proposed by Deere and Miller (1966)	55
Figure 4.5: Blastibility Index versus powder factor and energy factor	56
Figure 4.6: Longhole stope mining sequence at South Deep Mine	57
Figure 4.7: Fragmentation size distribution for five longhole stopes at South Deep Mine for; (a) 20% fragmentation size passing; (b) Mean (50%) fragmentation size passing and (c) 80% fragmentation size passing.	59

Figure 4.8: Top 20% of the fragmentation size distribution	60
Figure 4.9: Fragmentation size uniformity index	61
Figure 4.10: Inferred fragmentation size distribution for South Deep Mine	62
Figure 4.11: Ring pattern showing varying spacing between blastholes	64
Figure 4.12: Break overlap for 100 4W Cut04 LHS 7EMB stope for a toe spacing of 2m	65
Figure 4.13: Break overlap for 100 4W Cut04 LHS 7EMB stope for a toe spacing of 5m	66
Figure 4.14: Break Overlap for 100 4W Cut04 LHS 7EMB stope for a toe spacing of 7.5m	66
Figure 4.15: Pattern extent break radius	67
Figure 4.16: The stress distribution model	68
Figure 4.17: Drill and blast pattern evaluation	69
Figure 4.18: Suggested 2m by 2m drill pattern showing 2.6% overlap	71
Figure 4.19: Evaluation table for the suggested drill and blast pattern	71

LIST OF TABLES

Table	Page
Table 2.1: A comparison of the Rosin-Rammler uniformity index number for various fragmentation size distribution (School of Mining Engineering, 2019)	27
Table 3.1: Ring design simulation parameters	47
Table 4.1: Rock mass properties test results	52
Table 4.2: Summary of rock mass characteristics and properties at South Deep Mine	53
Table 4.3: AEL UG101S pumpable emulsion performance characteristics (AEL World, 2020)	57
Table 4.4: Summary of current and proposed ring design	75

LIST OF ABBREVIATIONS AND SYMBOLS

Run of Mine	ROM
Main Access Drive	MAD
Stope Access Drive	SAD
R	South African Rand
Ventersdorp Contact Reef	VCR
Blastibility Index	BI
Young's Modulus	E
Uniaxial Compressive Strength	UCS
Velocity of Detonation	VOD
Sublevel Caving	SLC
Julius Kruttschnitt Mineral Research Centre	JKMRC
Crush Zone Model	CZM
Uniaxial Tensile Strength	UTS
Poisson's Ratio	μ
Spacing to Burden ratio	S/B
Kuznetsov-Cunningham-Ouchterlony	KCO
Scientific Approach to Breaking Rock with Explosives	SABREX
Primary Wave	P-wave
Secondary Wave	S-wave
Two Dimension	2D
Three Dimension	3D
Load, Haul, Dump	LHD
International Society for Rock Mechanics	ISRM
Quality Assurance/Quality Control	QA/QC
Rock Quality Designation	RQD
Peak Particle Velocity	PPV

SAG

Semi Autogenous Grinding

1. INTRODUCTION

1.1 Chapter Overview

The purpose of this chapter is to provide an overview of the research. As a result, the research context and background, the problem statement and the research limitations are explained, including the significance of this research to the mine and communities surrounding the operation. The aim and objectives of the report are also described.

1.2 Research Background and Context

The mining of gold in the Witwatersrand goldfields in South Africa began over a century ago. The shallow high-grade gold deposits are depleted and as a result, mines now exploit lower grades at deep to ultra-deep mines (Neingo and Tholana, 2016). In the South African context, shallow mines are at depths of 1 000m, deep mines between 1 000m and 3 500m and ultra-deep mines at depths greater than 3 500m (Jager and Ryder, 1999). By virtue of mining at great depth, operational costs are high due to (CPM Group, 2012):

- The need for more skilled labour (to deal with increased complexities associated with such mining),
- Intricate infrastructure,
- Increased electricity costs (for cooling deep underground shafts); and
- Overall increase in overhead and maintenance costs.

This means that mining processes should be efficient and continuously optimised in order to derive optimal value from the remaining low-grade and deep-lying deposits (Musingwini, 2014). According to Shelswell and Labrecque (2014), “a fundamental aspect of an efficient mining operation is the steady movement of material throughout the mine system; particularly the flow of fragmented rock from the upstream excavation point to the downstream processing or stockpile site(s)”. Therefore, fragmentation achieved should be of a size suitable for all equipment and downstream processes.

This research emanates because Gold Fields’ South Deep Mine management wants to achieve an efficient oreflow system from upstream down to the Run of Mine (ROM)

stockpile. In order to achieve this, rock fragmentation from the stopes must be of an optimal size.

Optimising fragmentation is an important cost saving activity in every mining operation. Multiple studies including those by Marton and Cookes (2000), Strelec *et al.*, (2011), Afum and Temeng (2015) and Ninepence *et al.*, (2016) have been conducted on the optimisation of fragmentation for surface mines and a few including that of Cebrian *et al.*, (2017) and Preston (2019) have been done for underground mines that use sublevel stoping methods.

Cebrian *et al.* (2017) conducted an underground ring blasting optimisation study at Matsa Mine, an underground Cu-Pb-Zn mine in Spain. The mine was achieving coarser fragmentation than required. In order to optimise fragmentation, finer fragments were required. To do this, the powder factor and energy factor were increased by about 20% by adjusting the burden, spacing and explosive loads. Powder factor is the ratio of the weight of explosives used per unit of rock while the energy factor is the total explosive theoretical energy applied to a rock (ISEE, 2011). As a result, the mine experienced a 26% size reduction in the 80% passing size distribution range and a 38% reduction in ore loss with expected cost savings of about 660 000€/annum (Approximately R10.7 million) in crushing and grinding processes, and in addition toes were eliminated (Cebrian *et al.*, 2017).

At Eleonore Mine in Northern Quebec, Preston (2019) optimised the fragmentation profile for ring blasting to be 100% passing less than 400mm and reduce dilution to 10%. The mine does not have an underground crusher and therefore it was important that the fragmentation achieved by blasting is optimal to ensure an efficient ore flow.

These studies highlight the importance of achieving the correct fragmentation profile in terms of efficiency and saving costs. It is therefore imperative that the fragmentation size and ring designs at South Deep Mine should be evaluated and a simulation is conducted in order to achieve the optimal fragmentation size.

1.2.1 Mine Locality

Gold Fields' South Deep Mine is located in Westonia approximately 60km south – west of Johannesburg in South Africa as shown in Figure 1.1. It is an underground deep - level

gold mine that exploits the Ventersdorp Contact Reef (VCR) and the Upper Elsberg Reef in the Witwatersrand basin.

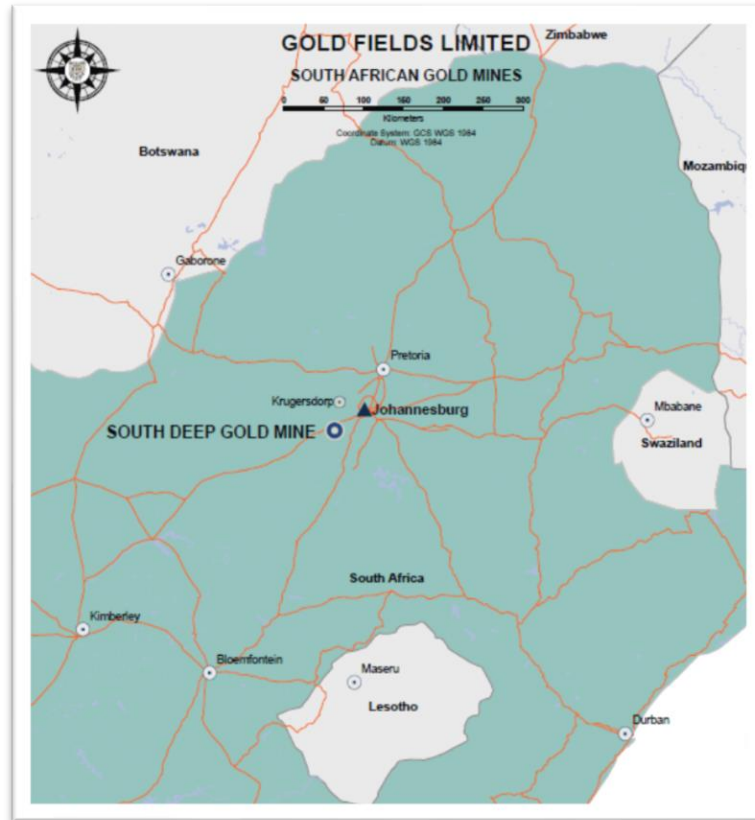


Figure 1.1: South Deep Mine locality (Gold Fields, 2017a).

The Witwatersrand basin is currently the largest underexploited orebody in the world known to man (Boshoff, 2016). It contains mineral resources of approximately 76.2Moz and mineral reserves of approximately 38.2Moz, with mining gold grades of between 5g/t and 6g/t (Holland *et al.*, 2015). The primary reef exploited at South Deep Mine is the Stacked Upper Elsberg reef that constitutes approximately 99% of the reserves with the remaining 1% being the Ventersdorp Contact Reef (VCR) (Gold Fields, 2018).

Figure 1.2 shows 16 reef horizons that make up the Upper Elsberg reef. The horizons sub-crop and form a wedge with the VCR.

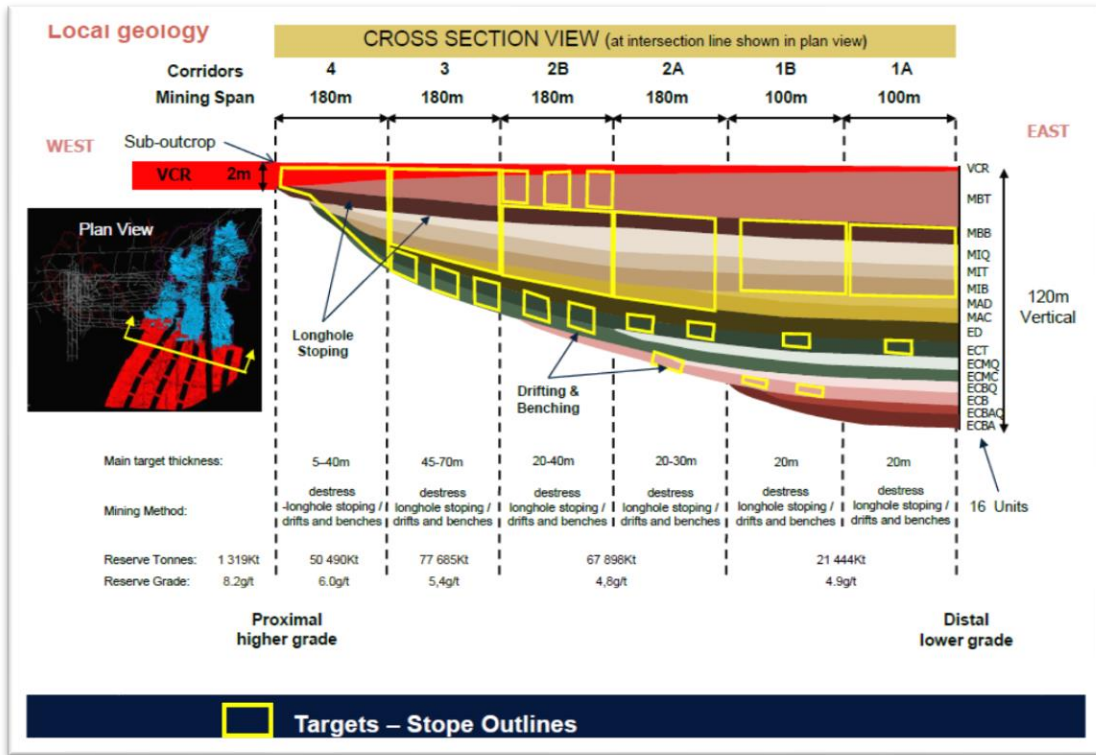


Figure 1.2: South Deep Mine orebody showing six mining corridors and 16 reef horizons (Gold Fields, 2017a)

Each of the 16 reef horizons vary with grade and has a thickness that ranges from 2m to 120m. The reef dips at an angle between 12 and 14 degrees (Gold Fields, 2017a).

The gold grades at South Deep Mine are low but the orebody can be suitably mined using massive mining methods. Hence, the company embarked on an extensive project to develop and mine the remainder of the VCR, and the Upper Elsburg reef orebody using mainly the longhole stopping mining method. Much of the VCR was exploited using conventional mining methods which ceased in 2008 when the longhole open stopping mining method was introduced. The drifting and benching mining method is also used but in thin areas that are beneath and above the destress cuts (Holland *et al.*, 2015).

Access to target areas/stopes is through the Main Access Drive (MAD) which leads the development advance. Stope Access Drives (SADs) breakaway from the MAD and extend up to the regional pillars at the limit of the orebody. In order to exploit the massive orebody and achieve production targets safely and economically while controlling the behaviour of

the rock mass, a series of individual longhole stopes are excavated in sequence using the checker board technique (Villaescusa, 2003). Primary stopes (Initial stopes) are extracted within a chosen area of an orebody and filled with consolidated backfill. Once the backfill cures, secondary stopes (stopes adjacent to the previously backfilled primary stopes) are extracted on retreat and backfilled (Villaescusa, 2003). Figure 1.3 shows a schematic of the development layout showing amongst others the longhole stoping, and the drifting and benching sections.

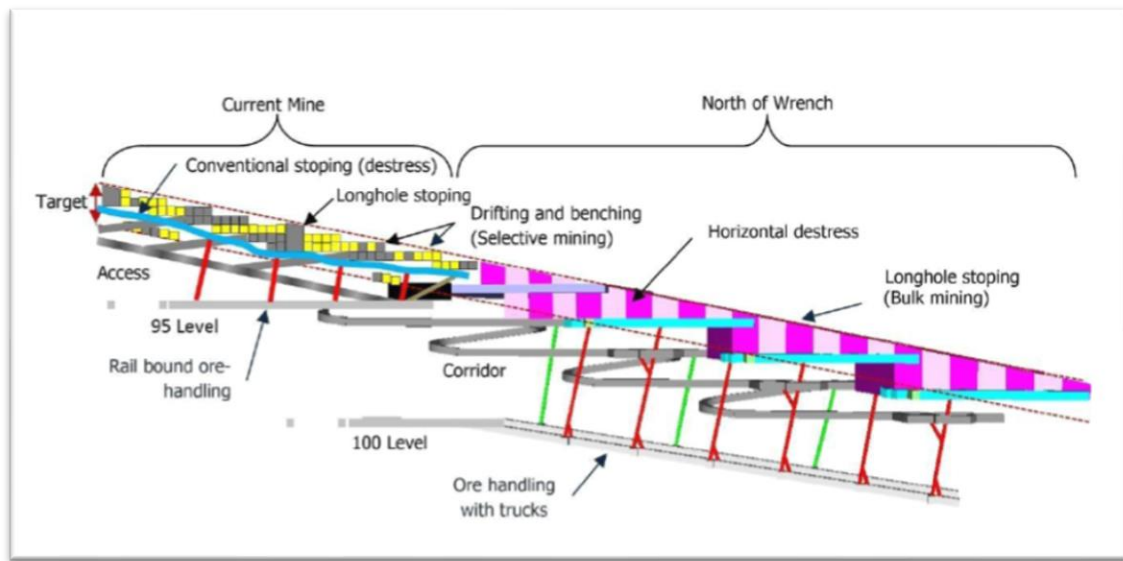


Figure 1.3: A schematic of the development layout at South Deep Mine (Gold Fields, 2019)

Rock fragmentation at South Deep Mine is achieved by drilling and blasting which is the most economical method of fragmenting hard and competent rock (Rai *et al.*, 2016; Tamrock Corporation, 1997). Production begins with the drilling and blasting of a slot raise to create a free face/void into which subsequent holes blast into. Multiple rows of longholes are drilled radially in retreat from the drill rig's pivot point in the SAD. This type of drilling is called ring drilling, and it is comparatively challenging considering that it requires blastholes to be drilled in a drive usually of a small cross-sectional area compared to the size of the stope block/longhole stope which can be as high as 20m and 13m wide (Gold Fields, 2019). As a result, the spacing between blastholes in a ring varies substantially from

the collar to the toe region. A scheme showing drilling in production stopes and development is shown in Figure 1.4.

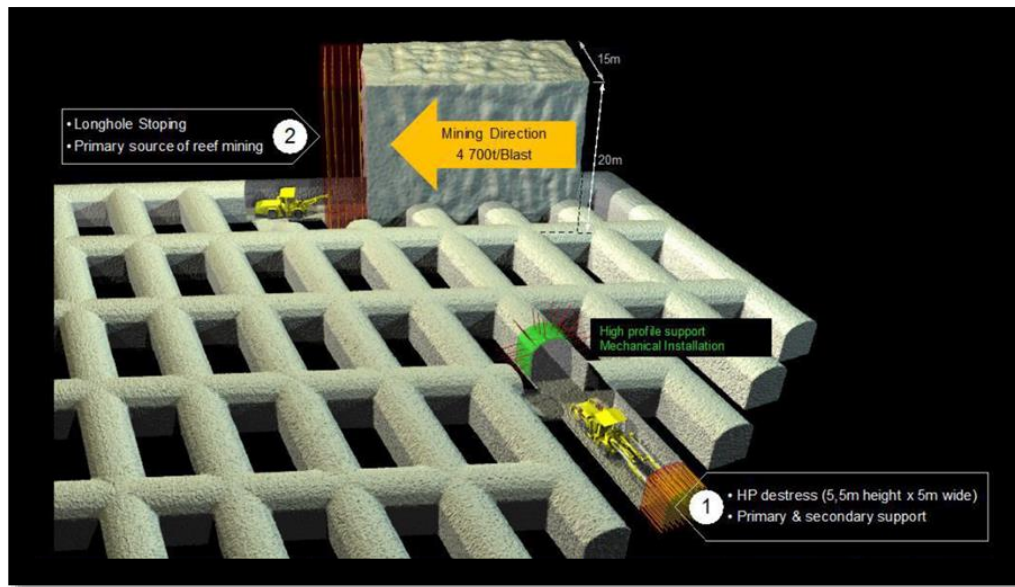


Figure 1.4: A typical development and production layout at South Deep Mine (Gold Fields, 2019)

Due to the non rectilinear geometry of the blastholes in a ring, a lack of measuring equipment during charging and non-adherence to charge plans result in the collar region being overcharged. This introduces high probabilities of inconsistent explosives energy distribution in the blasthole where the explosive energy is highly concentrated at the collar region. The opposite is true for the explosive's energy at the toe of the blastholes. Consequently, the collar region will produce fine fragmentation and the toe region will produce coarser material. It is therefore imperative that the drill and blast patterns are suitable to ensure a consistent distribution of explosive energy to generate an optimal fragmentation size. In addition, an adequate implementation control system is required to ensure that the planned blast pattern and charge plans matches implementation.

Based on studies conducted by Roy *et al.*, (2016), Marton and Crookes (2000), achieving good fragmentation improves the oreflow process and lowers the overall operational costs due to the reduction in power consumption and maintenance costs. Figure 1.5 shows the relationship between cost and fragmentation size.

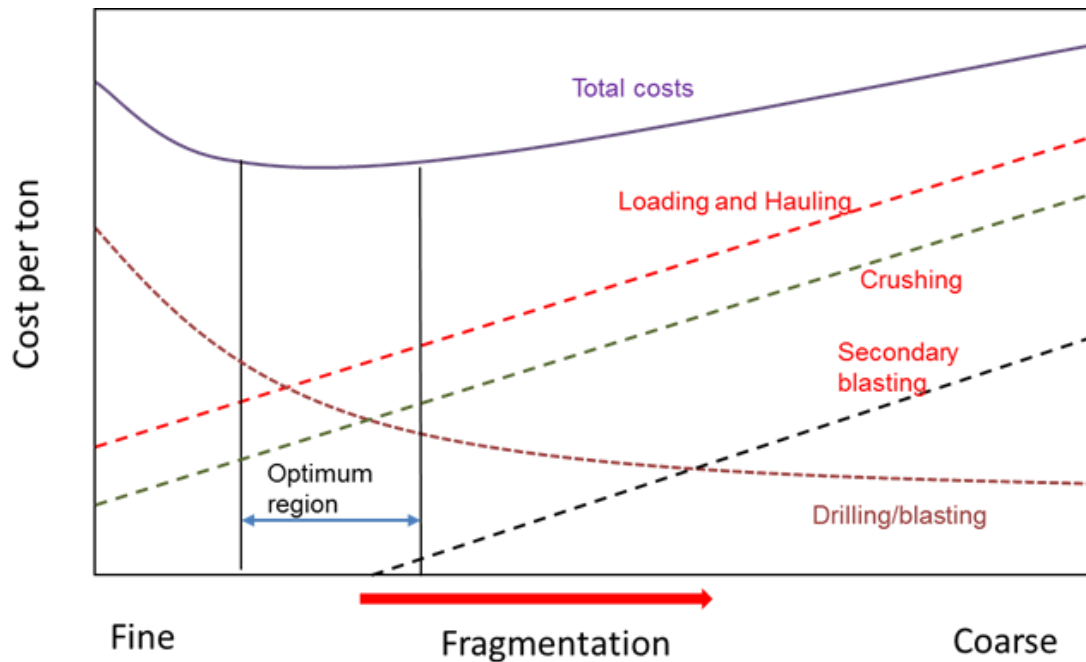


Figure 1.5: Cost as a function of increasing average particle size. (School of Mining Engineering, 2018)

The aim is to operate in the optimum region where the total costs are lower. Although drilling and blasting costs increase with fine fragmentation; crushing, loading and hauling costs are minimised, and the frequency of secondary blasting is reduced. As a result, the overall total costs are also reduced. It is also important to note that too fine fragmentation may result in increased gold losses in stopes yielding a lower Mine Call Factor (MCF).

Although the confined underground working environment and the geometry of ring blasts is complex, achieving suitable fragmentation distribution size ensures that the mine operates optimally in terms of costs and oreflow efficiency.

1.3 Problem Statement

Gold Fields has invested more than R32 billion (South African Rands) in South Deep Mine since acquisition in the year 2006. To date the company has been unable to recoup this investment with a loss of approximately R100 million a month (Gold Fields, 2018). In a bid to reduce losses and improve efficiencies, the company introduced strategies to counter-act this problem. As a low grade and high volume mechanised mine, it is essential that the oreflow system is continuous in order to improve the mine's throughput.

Rock fragmented in the longhole stopes is often coarse and inconsistent and therefore unable to pass through 300mm by 300mm grizzlies. Sometimes secondary blasting or impact breaking in the stopes and at the grizzly has to be done. This results in production delays. Due to the angle at which the rock lands, sometimes large rock fragments manage to pass through the grizzly blocking it, which leads to stoppages in the production cycle while it is being unblocked. Consequently, LHDs and trucks tram the ore to a distant orepass which negatively affect production targets.

The metallurgical plant is reporting Run-of Mine (ROM) feed that is too fine for the Semi-Autogenous Grinding (SAG) mill. As a result, the SAG mill operates inefficiently and results in gold losses reducing MCF (Mogoai, 2019). Therefore, every effort should be made to ensure that the fragmentation size is neither coarse nor too fine.

Achieving the correct fragmentation size upstream in the stopes has been found to have a major influence on the ore recovery, overall efficiency of the oreflow and crusher performance. Hence, South Deep Mine requested the author to review the drill and blast designs and analyse the current fragmentation size achieved in the stopes to evaluate if whether the stopes are the source of fine fragments. This will be achieved using available specialised software.

1.4 Research Aim and Objectives

The aim of the research is to optimise ring designs to yield satisfactory fragmentation size distribution. The primary objectives of this research are therefore to:

- Understand the mechanism of rock breakage and parameters that influence rock fragmentation.
- Characterise rock and rock mass properties.
- Determine and analyse the current fragmentation size using available fragmentation models and software.
- Conduct software simulations to determine the correct drill and blast patterns.

1.5 Significance of the Research

The optimisation of fragmentation has a direct impact on oreflow efficiencies. When the fragmentation size is optimal for all infrastructure and transportation equipment, orepass blockages are reduced and oreflow efficiencies improve. Dislodging an orepasses is a dangerous activity which when avoided can drastically improve safety and minimise stoppages. Avoiding blockages can improve the probability of achieving production targets and simultaneously reduce operating losses. The research findings will thus assist the company achieve its 2022 steady state production target of 254kt/month (Gold Fields, 2018).

A profitable mining company improves the socio-economic status of the society and communities around which the mine operates by bringing in community development and job creation. Therefore, the South African community also stands to benefit. This research also seeks to improve the knowledge base in the optimisation of fragmentation for underground mines that use ring blasting.

1.6 Research Contents

This research report is divided into seven chapters.

- Chapter one presents an introduction of the research topic, the research objectives and the value-add of the research. It further presents a brief research background and context.
- Chapter two presents a literature research on rock fragmentation dealing specifically with; the mechanism of rock breakage, factors that affect rock fragmentation, and the prediction and analysis of fragmentation.
- Chapter three presents the methodology followed to collect and analyse data.
- Chapter four details the results of the study such as South Deep Mine's drill and blast processes, rock characteristics and fragmentation size distribution.
- Chapter five uses information from the preceding chapters to design optimal drill and blast parameters for the efficient flow of ore.
- A summary of the pertinent points in the report and the benefit of additional research on this topic are presented as conclusions and recommendations in Chapter six.

- The report's reference list is presented in Chapter seven of the report.
- Supporting information is also included at the end of the report as Appendices.

1.7 Scope of the Research

In accordance with the project's requirements as outlined by South Deep Mine, this research is limited to the analysis and evaluation of fragmentation from the production longhole stopes to the grizzly although the discussion will also touch on crusher and plant requirements.

2. ROCK FRAGMENTATION

2.1 Chapter Overview

Having introduced the problem that this research aims to address and giving a background and context of the research in chapter one, this chapter presents a literature research on the mechanism of rock fragmentation and the factors that affect the way rock breaks. Further, the various methods of modelling and predicting fragmentation size distribution are discussed followed by evaluation methods.

2.2 Mechanism of Rock Breakage

Studies on the mechanism of rock breakage grew in popularity in the 1970's. This was in order to improve the knowledge and understanding of the general mechanism of rock breakage fundamental in drill and blast designs to yield optimal fragmentation size and solving mine geotechnical problems (Schmidt and Rossmanith, 1983).

Drilling and blasting remain the major technique of breaking rock in hard rock mines. Although rock breakage is mainly attributed to blasting, drilling also plays a role in rock breakage. When a drill bit is in contact with a rock surface, energy is transmitted from the drill bit to the rock in the immediate vicinity of the drill bit. As the drill rotates and advances into the rock material, it penetrates the rock with an increase in force initiating micro cracks as the strength of the rock is exceeded (Jimeno *et al.*, 1995; Rossmanith *et al.*, 1997). These micro cracks may extend radially and join pre-existing cracks occupying a layer of about 2 mm in thickness (Rossmanith *et al.*, 1997).

When drilling is complete, blastholes are charged with emulsion explosives and ignited. The ignition results in the detonation of the explosive which releases large amounts of energy per kilogram of reactants that can be greater than 3.5MJ/kg (Lownds, 1978).

Figure 2.1 illustrates the mechanism of rock breakage between two blastholes due to an explosive reaction in five phases (Jimeno *et al.*, 1995).

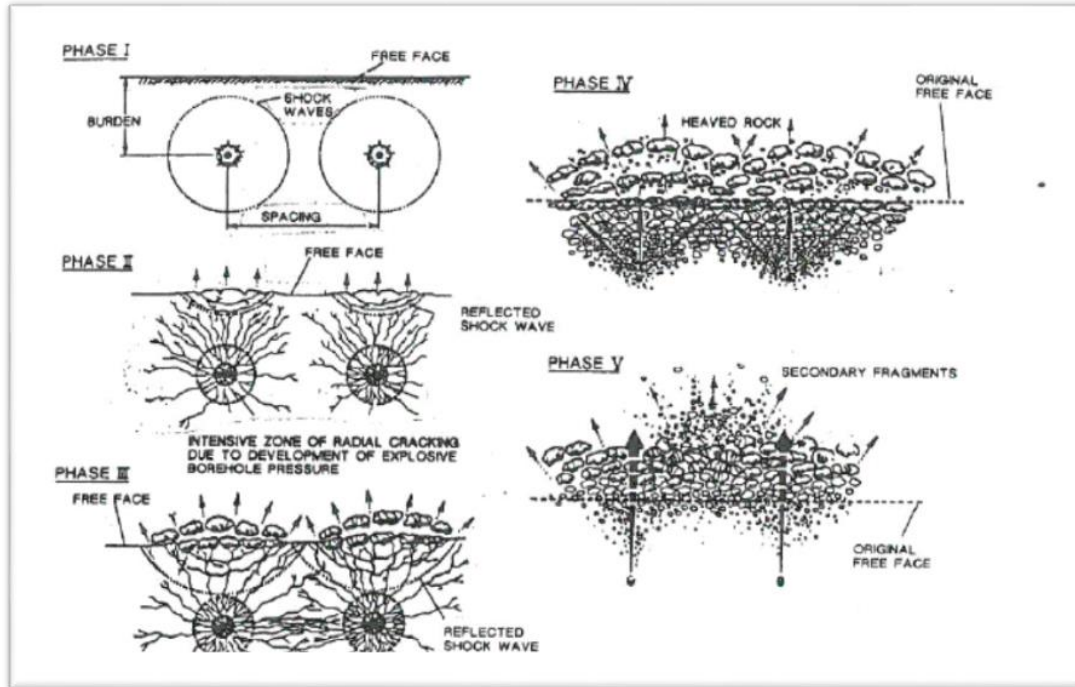


Figure 2.1: Rock breakage mechanism by explosives (Jimeno *et al.*, 1995)

Following the detonation of an explosive a transition from micro cracking to macro cracking and fracturing of the rock is observed. A compressive shockwave is generated due to an increase in pressure and gases in the blasthole. The compressive shockwave is forced radially outward from the blasthole exerting an intense compressive stress on the surrounding rock mass while inducing tensile stress in the tangential plane of the shock front (Zolezzi, 1961; Jimeno *et al.*, 1995). High-pressure gases from the explosive reaction then penetrate and expand pre-existing cracks in the rockmass including those that originate from drilling although minute. As the shock wave and high-pressure gases propagate through the rock mass, a bulk of new fractures are formed. Crushing of rock occurs in the immediate vicinity of the blasthole due to the shock front pressure exceeding the dynamic compressive strength of the rock mass (Zolezzi, 1961). A zone of intense radial cracks also forms around the crushed zone (Zolezzi, 1961 and Jimeno *et al.*, 1995). Macro fractures at discontinuities are formed when the compressive shockwave propagates through the rock towards a free face. During propagation, the intensity of the shockwave diminishes due to energy absorption and divergence. When the compressive shockwave

reaches a free face, it is reflected back as a tensile wave with an associated shear failure that grows the cracks resulting in rock fragmentation (Zolezzi, 1961).

In order to achieve production targets, single hole blasting is inadequate and therefore sequential multiple hole blasting is conducted. In sequential multiple hole blasting, blastholes are timed to detonate sequentially at varying times resulting in a time delay between blastholes. Following the detonation of blastholes the shockwaves and cracks generated from interact as collisions to develop damage zones. The zones result in rock fragmentation while the high-pressured gases from detonation cause rock displacement.

2.3 Factors Affecting Rock Fragmentation

Optimising rock fragmentation by explosives in ring blasting is a complex task due to its geometry and challenging geological and geotechnical conditions. In general, it requires an understanding of rock mechanics and geology, fracture mechanics and chemistry of detonation (Little, 2018) to develop blast designs that yield successful results. Research has shown that the quality and overall degree of fragmentation depends on explosives properties, rock properties, blast geometry and initiation sequence (Adebayo and Umeh, 2007; Roy et al., 2016; Little, 2018). Achieving optimal fragmentation requires the right combination of controllable and uncontrollable parameters. Controllable parameters such as the blast geometry and initiation sequence can be easily altered on site to yield required results whereas uncontrollable parameters such as rock properties cannot be neither altered nor manipulated due to their dependency on the materials that make up the rock mass.

2.3.1 Uncontrollable Rock Variables

Uncontrollable rock parameters are characterised by two main geological properties of rock namely; mechanical properties and physical properties. These properties of rock are important in determining how well the explosive interacts with the rock mass and achieves optimal fragmentation. This is estimated by determining a Blastability Index (BI) that is used to estimate the simplicity at which rock fragments. According to Nur Lyana *et al.*, (2016), mechanical properties are responsible for forming cracks that develop during blasting, and on the other hand structural properties influence the transmission of shock waves and high pressure gases from the explosive reaction. Mechanical properties of rock

include rock strength properties (Young's Modulus (E), Poisson's ratio (μ), Uniaxial Compressive Strength (UCS) and Uniaxial Tensile Strength (UTS)), rock density, hardness and porosity. Physical properties of rock include pre-existing fractures such as bedding planes and joints, the dip of the rock to be blasted and all physical properties of rock at a wider range. These properties are discussed below.

Rock Density and Rock Strength Properties

According to Jimeno *et al.*, (1995), there is a close correlation between the density of rock and the rock strength. Low-density rocks are usually weak, easily deformed and broken, while rocks with higher densities are usually strong and not easily broken. As a result, high density and high strength rocks require higher quantities of explosive energy for fragmentation and heave. The opposite is true for low-density rocks. It is therefore important to match the explosive energy to the strength and density of rock because if the intensity of the stress wave produced is much greater than the dynamic compressive strength of the rock, extreme crushing immediately around the blasthole results and the rock also scatter during heave.

Porosity

Porosity affects the physical properties of rock and is defined as “the ratio of the pore volume (e.g. pores, open cracks) to the volume of the whole rock” (Siegesmund and Dürrast, 2011). Two types of porosity exist in rocks; intergranular or formational (primary) and dissolution or post-formation (secondary) (Siegesmund and Dürrast, 2011). Intergranular or formational porosity is uniform in the rock and causes a reduction of the strain wave energy and the dynamic compressive strength in the rock. Therefore, highly porous rocks tend to absorb most of the available explosive energy released making desirable fragmentation and throw difficult. Hence, a rock with high porosity has an increased probability of crushing around the blasthole than a rock with low porosity (Jimeno *et al.*, 1995).

Structural Rock Mass Properties

Rock mass considers a wide range of rock material composed of both intact rock and any associated discontinuities. Lily (1986) learnt from surface mining field experience that the following rock mass properties significantly affect fragmentation:

- The structural nature of the rock mass – A blocky rock mass has more influence on the fragmentation size than a massive rock mass with fewer joints.
- Joint plane spacing - In situations where the spacing between joints is far apart, higher energies are required to fragment rock to the required size to avoid coarse fragmentation and boulders.
- Joint set orientation relative to the free face – This affects fragmentation size and the ease of mucking.
- Specific gravity and hardness – Heavy rocks require high explosive energies to break than lighter rock. Similarly, hard rock requires more explosive energy to break than softer rock.
- Filled, open or tight joints also affect the mechanical and physical properties of rock, reduce the strength of the rock, increase permeability and affect the explosive energy transmission in the rock (Jimeno *et al.*, 1995). Furthermore, filled discontinuities reflect and disperse the strain wave (Jimeno *et al.*, 1995) resulting in inconsistent rock fragmentation.

According to Maerz and Germain (1996), a combination of joint set orientation, joint set spacing and joint persistence delineates the rock mass into block sizes, and indicates the degree of fracturing. In addition, a combination of geological discontinuities consequently dictates the rock mass' behaviour during blasting. Such that in massive rock conditions (large block sizes), the pattern geometry greatly influences fragmentation than in small block sizes where average joint spacing is smaller than the nominal ring burden (Onederra, 2005). In this case, the block size influences the fragmentation achieved. Based on multiple studies and empirical evidence, block sizes greater than 1m are massive, those between 0.1 - 0.4m are fractured and those between 0.5 - 1.0m are less fractured. Joint persistence controls sliding, and refers to the length of the joint (Onederra, 2005)

Although challenging to quantify, there are several methods to determine the in-situ block size. According to Onederra (2005), the in-situ block size can be determined from advanced mapping techniques. However, this technique requires detailed geotechnical mapping information. As a result indices such as; the Rock Quality Designation (RQD), Volumetric Joint Count (J_v), Block Size Index (I_b) and direct in-situ block measurements from Joint

spacing and Joint frequency are preferred in industry due to the ease and simplicity with which rock can be classified (Maerz and Germain, 1996), however Stacey (2018) cautions against use these systems by inexperienced users .

2.3.2 Controllable Rock Variables

Jimeno *et al.*, (1995) classified controllable rock variables into three groups. The geometric group, the physicochemical group, and the time group. In underground ring blasting, geometric variables include amongst others the free face position, blasthole diameter, charge length, drilling pattern (burden and toe spacing) and blasthole inclination. The variables that fit in the physicochemical variables are explosive characteristics while time variables are concerned with delay timing and initiation sequence.

Geometric Variables

Free Face. Sometimes referred to as relief, a free face provides space into which the blasted rockmass moves. A lack of or inadequate free face results in the rock being immovable and choking, as a result the rock will either fragment unsatisfactorily or not break at all. Hence the practice of blasting and extending slots longhole stoping mining method in order to create a free face for the rings to move into.

Blasthole Size. For an operational mine, drilling and blasting costs, the properties of rock mass to be blasted, fragmentation size required, drilling depth, drilling equipment and equipment loading capacity dictate the size of the blasthole diameter, drilling pattern and blasthole inclination. These variables are dependent on each other. For example, provided other factors are kept constant, blasthole size influences burden and spacing. A small diameter blasthole generally result in reduced burden and spacing that increases the number of blast holes drilled. This in turn results in a more even distribution of explosives across the block being blasted which translate into an even fragmentation distribution size. This however increases drilling, priming and initiation costs (Sharma *et al.*, 1990).

According to Jimeno *et al.*, (1995) an optimum blasthole size is one that results in minimal drilling inaccuracies, is above the explosives critical diameter and produces a required fragmentation size. Generally, a larger blasthole size is more accurate than a small diameter

blast hole. However, depending on the design, large diameter blastholes are likely to result in large fragmentation size (Jimeno *et al.*, 1995).

Burden and Spacing. In longhole stoping, burden is the distance between rings, and spacing is the distance between blastholes in the same ring. Spacing is a function of the burden and the ratio of the blasthole length to the bench height (Myers *et al.*, 1990). In ring blasting terminology, spacing is referred to as toe spacing and it is the spacing between blastholes in the same ring as shown in Figure 2.2.

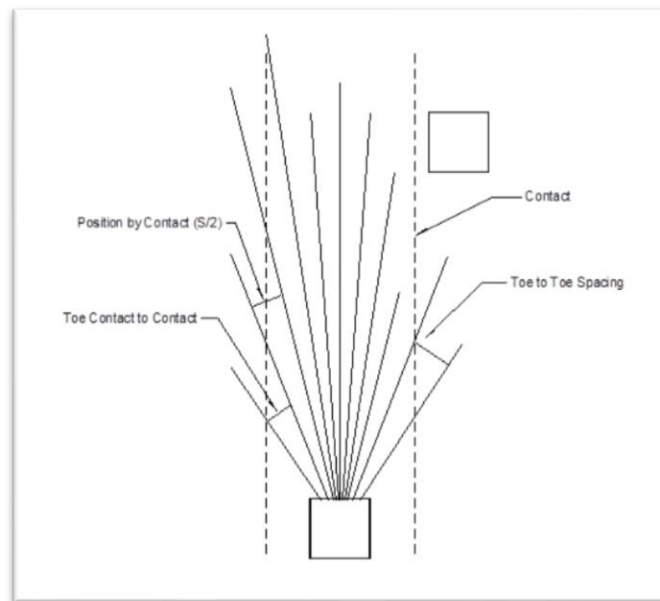


Figure 2.2: Schematic showing spacing in longhole drilling (iRing INC, 2018)

According to Myers *et al.*, (1990), burden is the most important parameter of a blast design owing to its influence on fragmentation and vibration in underground mines. It is therefore important to maintain a burden and spacing ratio that ensures an even distribution of energy and optimal fragmentation.

Onederra and Chitombo (2007) stated that the ring burden can range from 1.8m to 3.5m for common hole diameters, say 76mm, 89mm or 102mm used in practice to achieve optimal rock fragmentation. Sharma *et al.*, (1990) found that optimum burden resides in the range 20 – 25 times the blasthole diameter. Equation 2.1 and Equation 2.2 are empirical

formulas developed by Myers *et al.*, (1990) and Rustan *et al.*, (1990) cited in Onederra and Chitombo (2007) to estimate optimum burden respectfully.

$$B = 3.15d \left(\frac{SGe}{SGr} \right)^{\frac{1}{3}} \quad \text{Equation 2.1}$$

Where;

B - Optimal burden in feet (ft)

d - Blasthole diameter in inches

SGe - Specific gravity of the explosive, and

SGr - Specific gravity of the rock/ore being blasted

$$B = 11.8d^{0.63} \quad \text{Equation 2.2}$$

Where;

d - Blasthole diameter in inches

In order to determine spacing, rules of thumb have been empirically determined to calculate spacing to burden ratio (S/B). According to Onederra and Chitombo (2007) these include:

- i. S/B range of 1.1 - 1.4 for 76 – 115mm diameter holes after the Julius Kruttschnitt Mineral Research Centre.
- ii. S/B range of 1.5 – 2.0 after Rustan.
- iii. S/B range of 1.4 – 2.0 after Myers *et al.*
- iv. S/B range of 1.3 – 1.5 after Cunningham.

An S/B ratio in the ranges determined above yields satisfactory rock fragmentation results more so for strong or massive ore (Sharma *et al.*, 1990; iRing, 2018). However, Myers *et al.*, (1990) notes that S/B ratios determined from empirical equations may not be optimum for the best fragmentation and reduced costs, but provide a good starting point. Further, the best blast design might be determined after two or more blasts.

Drilling Accuracy. Accurate drilling is at the core of a successful blast. However, equipment manufacturing company Atlas Copco (2014) notes that 100% drilling

accuracies are impossible to achieve. Therefore, drilling must be quality driven and be as close to this accuracy as practicably possible to ensure quality results.

In the longhole mining method, up holes, particularly at South Deep Mine are drilled which are prone to deviation due to the long drilling lengths that can range from 10m to 25m. According to Atlas Copco (2014), the deviation in long hole drilling is attributed to “poor hole alignment, lack of guide tubes, too high feed, badly selected drill steel, poor collaring and deflections caused by various rock types or voids as bit attenuates to make its way through the orebody”. Holes deviating closer together at the toe of the hole result in finer fragments than planned while holes deviating apart at the toe result in coarser fragmentation.

Physicochemical Variables

Physicochemical variables pertain to both the physical and chemical properties of explosives. The choice of explosive to use is influenced by the rock mass properties, the degree of fragmentation, the displacement required (Sharma *et al.*, 1990) and whether up holes or down holes are drilled. Important explosives parameters amongst others are energy released, the velocity of detonation, critical diameter, borehole pressure, detonation pressure, explosive critical density, explosive density, explosive critical diameter, explosive diameter, water resistance and etc (Sharma *et al.*, 1990; ISEE, 2011). These factors must be catered for during blasting. The use of water-resistant explosives in wet holes circumvents explosives desensitisation. Increasing the density of an explosive leads to an increase in the velocity of detonation (VOD), leading to an increase in the detonation pressure which provides brisance resulting in maximum fragmentation (Sharma *et al.*, 1990). However, exceeding the explosive critical density may lead to desensitisation. Importantly, the critical diameter of the explosive must be exceeded to ensure the detonation process supports itself once initiated (ISEE, 2011). Critical diameter is the blasthole diameter below which an explosive will not reliably detonate. Therefore, a blasthole whose diameter is above the explosives’ critical diameter has the potential to reach the maximum VOD, and the explosive reaction is less likely to be affected by external conditions that may negatively affect the explosive reaction (Jimeno *et al.*, 1995).

Charging longholes require specialised type of equipment and explosives due to the blasthole orientation. Sticky emulsion is often used due to its ability to stay in the hole without falling out.

Time Variables

Initiating systems available in the market are electronic, non-electric (shock tubes) and electric detonators. These systems provide intra-row and inter-row time delay in a blast and assist in creating a free face onto which successive rows of blastholes blast into. The choice of an initiation system and time delay with a greater degree of accuracy is therefore important in achieving an adequate free face, heave and correspondingly a successful blast.

Electronic detonators are a recent invention in the market and, although costly are accurate with a 0.1ms timing delay error as compared to shock tubes and electric detonators (Cardu *et al.*, 2013). A study conducted by Cardu *et al.*, (2013) showed that electronic detonators result in consistent fragmentation, increase excavation productivity, saves costs and reduce ground vibrations amongst others. However, well-integrated geology, rock mass properties, explosive properties, blast design to the initiation accessories and timing is important in achieving a successful blast.

Based on many blast trials, Langerfors and Kihlstrom (1963) and Grant (1990) found that fragmentation is optimised with delay times of 3 to 5ms/m of burden for intra-row time delay. In addition, a generally accepted range for the inter-row delay is between 10ms/m and 30ms/m of burden for hard and soft rock respectively.

2.4 Blastibility Index

Blastibility Index (BI) is an empirical quantitative measure of the ease with which rock can be fragmented when subjected constraints such as the specified blast design, explosive characteristics and the block(s) being blasted (Lily, 1986; Dey and Sen, 2003; Chatziangelou and Christaras, 2015). A literature review by Dey and Sen (2003) suggests that research into rock BI has been the subject of interest for many researchers. According to Dey and Sen (2003), in the quest to determine the BI, some researchers correlated data from laboratory and field-testing of rock properties, some related the index with the rock and blast design parameters while others applied approaches based on the drilling rates and

blast performance in the field. To date, Lily (1986)'s BI approach is the most popular and applied in industry. According to Lilly (1986), this is due to its ability to incorporate significant rock mass parameters that affect blast performance and diggability.

Lily (1986) proposed a BI formula that incorporates rock mass description, joint spacing, joint orientation, specific gravity and hardness due to their effect on rock mass fragmentation. The formula proposed by Lily (1986) to calculate the BI is shown in Equation 2.3:

$$BI = 0.5 \times (RMD + JPS + JPO + SGI + H) \quad \text{Equation 2.3}$$

Where;

BI	- Blastibility Index
RMD (Rock mass Description)	- 10, for Powdery/Friable rock mass - 20, for Blocky rock mass - 50, for Totally Massive rock mass
JPS (Joint Plan Spacing)	- 10, for Closely Spacing (<0.1m) - 20, for Intermediate (0.1 – 1.0m) - 50, for Widely Spacing (>1.0m)
JPO (Joint Plane Orientation)	- 10, for Horizontal - 20, for Dip out of the Face - 30, for Strike Normal to Face - 40, for Dip into Face
SGI (Specific Gravity Influence) rock in t/m ³	- (25 x SG) – 50 where SG is Specific Gravity of
H (Hardness)	- (1 – 10) in Mohs Scale of hardness

Lily's (1986) BI numbers range from zero to 100 and are based on rock mass types at Australian iron ore mines. According to Lily (1986), a BI number of 100 is indicative of an "extremely hard, iron-rich cap rock, massive in nature having a specific gravity of 4t/m³" whereas a low BI indicates a soft rock that is relatively easy to blast or not suitable for

blasting with explosives. The BI can be used to characterise rock in order to get a sense of the amount of explosives and energy required to break rock in the early stages of a mining operation. Further, Lily (1986) determined the relationship between BI, powder factor and energy factor based on data from large-scale operations that use rope shovels. This relationship is shown in Figure 2.3

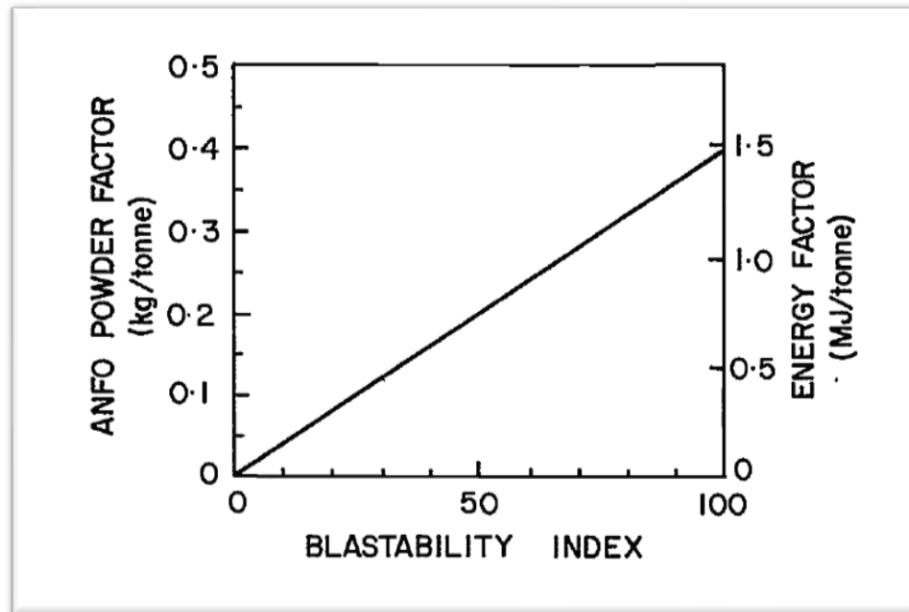


Figure 2.3: Blastability Index versus powder/energy factor (Lily, 1986)

The BI is directly proportional to both powder factor and energy factor. As shown in Figure 2.3, the higher the BI, the more energy factor and powder factor required to break the rock satisfactorily.

2.5 Fragmentation Prediction and Modelling

The prediction of rock fragmentation has been a major subject of importance for many years. It has become even more fundamental for mining companies to predict rock fragmentation size upfront during the mine design process for equipment selection, fleet size and capacity to optimise ore flow from the face to the mill.

SRK (2013) reported that modifying blasting practices to optimise fragmentation has the potential to improve mill throughput by 30%. Further, the increase in the drill and blast costs during modifications are outweighed by the reduction in the mill operating costs by approximately 7 to 10 times the drill and blast costs. In addition, an optimal fragmentation size has the potential to result in reduced specific energy consumption, which is the energy consumed when breaking the rock (Roy *et al.*, 2016).

The prediction of rock fragmentation size is popular for surface blasts and little is done for underground mines. As a result, models to predict fragmentation for surface mine are prevalent than those for underground ring blast applications. Although the prediction of fragmentation in mining is important, it should, however, be noted that it can be a costly and difficult task to perform (Sharma and Rai, 2017) especially if the trial and error approach is applied. The practice has been to use surface blast models for underground ring blasts as a start. With improvements in research and technological innovation, researchers have found ways to predict and analyse fragmentation using numerical, empirical and mechanistic models (Scott and Onederra, 2015). These models are embedded in software packages that make the process of predicting and analysing fragmentation size distribution for both surface mines and underground ring blasting applications in real time.

2.5.1 Empirical Models

Empirical fragmentation models are derived from structural geology, rock type, explosive properties and blast pattern to describe the influence of the rock on the blasting outcome (Scott and Onederra, 2015). Due to extensive research and continuous improvement, these models are now efficient to use due to their simplicity and ease of use (Strelec *et al.*, 2011; Afum and Temeng, 2015) and can be applied on a daily basis for blast designs (Cunningham, 2005). There exist a variety of empirical models but only the Kuz-Ram fragmentation model, Crush-Zone-Model (CZM) and the Kuznetsov-Cunningham-Ouchterlony (KCO) models are discussed in this study due to their popularity of use in the mining industry.

Empirical models were developed from historical data in bench blasting, and have been used to predict fragmentation for bench blasting. In some instances empirical models have been modified in order to predict fragmentation in simple underground blasting geometries (Onederra and Chitombo, 2015). Although helpful, empirical models do not consider the three-dimension (3D) distribution of explosives charges for complex underground geometries therefore yielding unreliable results. However, these models provide a good starting point for ring design.

Kuz-Ram fragmentation model

CVB Cunningham developed the Kuz-Ram fragmentation model in 1983. The model estimates size fragments from blasting. The model predicts fragmentation by combining the Kuznetsov equation, the Rosin-Rammler equation and the uniformity index (Oldfield *et al.*, 2009). Although popularly used in the industry the model's demise lies in its great dependency on the Rosin-Rammler equation that greatly underestimates the fines distribution (Oldfield *et al.*, 2009). This is shown in Figure 2.4.

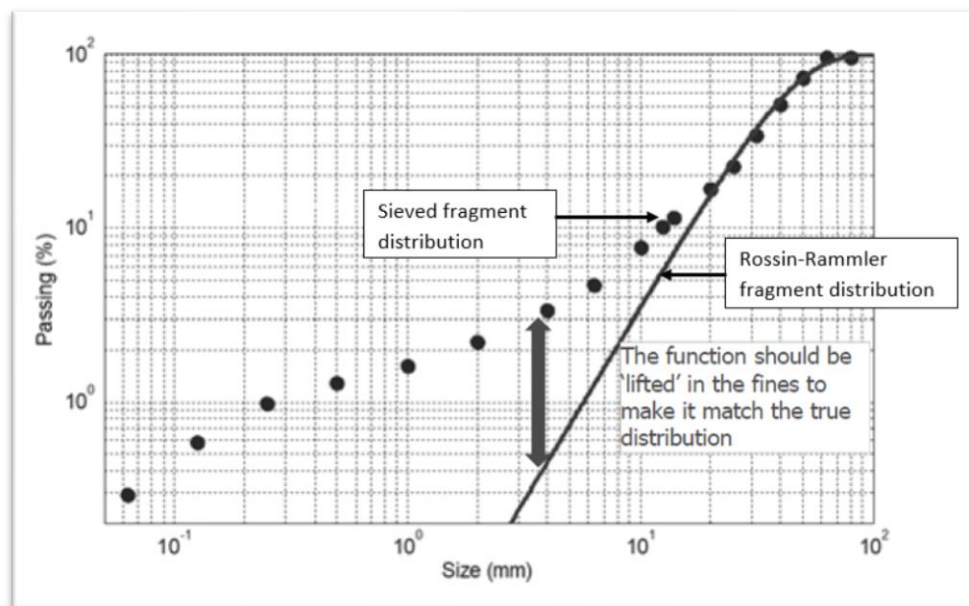


Figure 2.4: An underestimation of fines by the Rosin-Rammler fragment distribution compared with the sieved fragment size distribution (Sanchidrian, 2018).

Cunningham (2005) however argues that the model is “less about precision than about guidance”. Sieving is considered the most accurate method of evaluation fragmentation size distribution. As shown in Figure 2.4, rock fragments modelled by the Rosin-Rammler distribution differ considerably from sieved fragments. According to the figure, the Kuz-Ram model shows that the coarsest fragmentation size is $10^{0.5}$ which is not the case as seen from the sieved data function. Above 20mm, the Rosin-Rammler distribution follows a similar fit with the distribution from sieved data.

Cunningham (2005) later modified the Kuz-Ram fragmentation model in 2005 to factor in the effects of precision timing on mean fragmentation and uniformity. Although the modified model is an improvement, it does not however address the inaccuracies concerning the fines. Equations 2.4 to 2.6 show the modified Kuz-Ram fragmentation model (Cunningham, 2005).

Kuznetsov Equation:

$$X_{50} = A_T A \left(\frac{1}{q^{0.8}} \right) Q^{\frac{1}{6}} \left(\frac{115}{S_{ANFO}} \right)^{\frac{19}{30}} C(A) \quad \text{Equation 2.4}$$

Where:

X_{50} - The mean fragment size (cm)

q - Powder factor (kg/m^3)

S_{ANFO} - Relative weight strength of explosive to ANFO (ANFO=100 and TNT=115)

Q - Mass of explosive per hole (kg)

A - Rock factor constant

$C(A)$ - Correction factor for the Rock Factor (A)

A_T - Timing Factor

Rosin-Rammler Equation:

$$R = e^{-0.693 \left(\frac{X}{X_{50}} \right)^n} \quad \text{Equation 2.5}$$

Where:

- R - The proportion of material passing
- X - The diameter of rock fragment of interest (cm)
- X₅₀ - Mean fragmentation size (cm)
- n - Rosin-Rammler or uniformity index.

Uniformity Index:

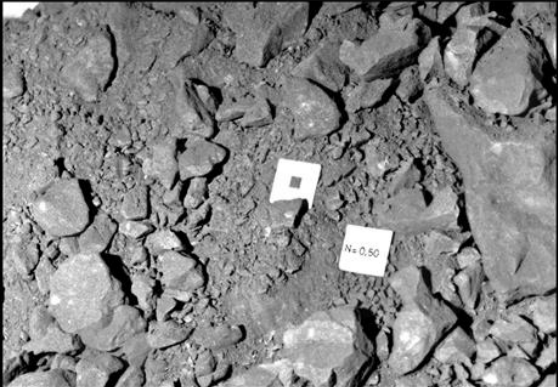
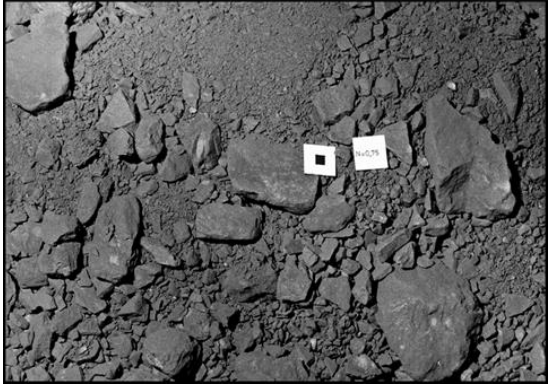
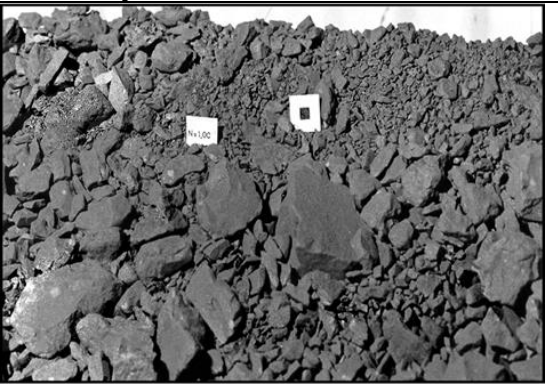
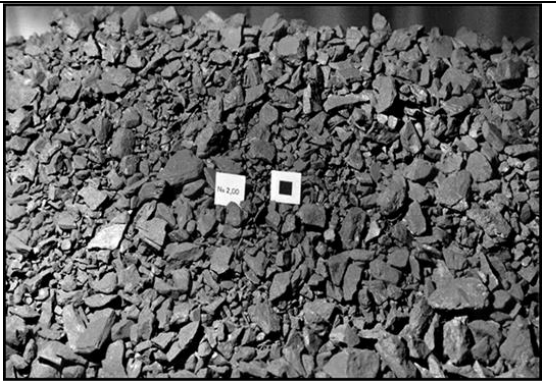
$$n = n_s \sqrt{\left(2 - \frac{30B}{d}\right)} \sqrt{\left(\frac{1+\frac{S}{B}}{2}\right)} \left(1 - \frac{W}{B}\right) \left(\frac{L}{H}\right)^{0.3} C(n) \quad \text{Equation 2.6}$$

Where:

- n - Uniformity exponent
- B - Burden, (m)
- W - Standard deviation of hole accuracy, (m)
- L - Charge length above grade, (m)
- H - Bench height, (m)
- S - Spacing, (m)
- n_s - Uniformity factor governed by the scatter ratio
- d - Blasthole diameter (mm)

The uniformity index gives an indication of how uniform or consistent the fragmentation distribution is between fine and coarse fragments. According to Onederra (2005), the uniformity constant varies from 0.6 to 2.2. Table 2.1 compares the different Rosin - Rammler uniformity index numbers with various fragmentation size distribution.

Table 2.1: A comparison of the Rosin-Rammler uniformity index number for various fragmentation size distribution (School of Mining Engineering, 2019)

	
<p>n = 0.5 fragmentation size of low uniformity</p>	<p>n = 0.75 fragmentation size of low uniformity</p>
	
<p>n = 1.0 fragmentation size of medium uniformity</p>	<p>n = 2 fragmentation size of high uniformity</p>

Smaller values of “n” depict a non-uniform fragment size distribution while higher values of “n” depict uniform fragmentation size distribution within the muckpile (Vesilind, 1980; Onederra, 2005; Wimmer et al., 2015; Singh *et al.*, 2016). In cases where “n” is less than 0.6, it was found that this was due to a combination of blasting and structural geology. The uniformity index range mentioned here is for surface mines however, investigations conducted at an underground sublevel caving mine confirmed that the range of uniformity index is also applicable to underground mines. This was determined by Onederra (2005) after implementing a simple three-dimensional PPV attenuation model that allowed the determination of breakage and fragmentation uniformity characteristics of underground mines.

Crush-Zone Model

The Crush-Zone Model (CZM) was developed by the Julius Kruttschnitt Mineral Research Centre (JKRMC) to address the problem of underestimating fines inherent in the Kuz-Ram fragmentation model. The model is in agreement with Zolezzi (1961) and considers that during breakage, the rock in the immediate vicinity of the borehole crushes due to compressive stress waves creating fine material, while that outside the crushed-zone breaks due to tensile fracturing resulting in coarse fragmentation (Ouchterlony, 2005). The model factors in crushing and fracturing in its calculations hence it is divided into two parts: the coarse distribution whose uniformity index is calculated from the Kuz-Ram model and the fines distribution whose uniformity index is determined by first calculating the percentage of blasted rock less than 1 mm (Kanchibotla *et al.*, 1999). The percentage of blasted rock less than 1mm is estimated from Equation 2.7. The rock size of 1mm is assumed to be the coarsest particle size that result from crushing during blasting (Valery et al., 2001).

$$\% -1\text{mm} = 100 \times \left(\frac{V_{\text{crush}}}{V_{\text{br}}} \right) \quad \text{Equation 2.7}$$

Where:

% -1mm - Percentage of blasted rock less than 1mm

V_{crush} - Volume of crushed rock around the blasthole

V_{br} - Total volume of blasted rock

The substitution of %-1mm as R in the Rosin-Rammler equation gives the uniformity exponent for the fines distribution (Kanchibotla, 1999; Ouchterlony, 2005). According to Ouchterlony (2005), the crush zone model yielded satisfactory results in fragmentation projects.

Kuznetsov-Cunningham-Ouchterlony Model

The Kuznetsov-Cunningham-Ouchterlony (KCO) model is a combination of the Kuz-Ram fragmentation model, the Swebrec function and the curve undulation factor shown in Equations 2.8 to 2.10 Ouchterlony (2005).

Kuznetsov Equation:

$$X_{50} = A \left(\frac{1}{q^{0.8}} \right) Q^{\frac{1}{6}} \left(\frac{115}{S_{ANFO}} \right)^{\frac{19}{30}} \quad \text{Equation 2.8}$$

Where:

- X_{50} - The mean fragment size (cm)
- q - Powder factor (kg/m^3)
- S_{ANFO} - Relative weight strength of explosive to ANFO (ANFO=100 and TNT=115)
- Q - Mass of explosive per hole (kg)
- A - Rock factor constant
- $C(A)$ - Correction factor for the rock factor (A)
- A_T - Timing Factor

Swabrec function:

$$P(x) = \frac{1}{\left\{ 1 + \left[\frac{\ln\left(\frac{X_{\max}}{X}\right)}{\ln\left(\frac{X_{\max}}{X_{50}}\right)} \right]^b \right\}} \quad \text{Equation 2.9}$$

Where:

- $P(x)$ - Percentage of material passing sieve size X (%)
- b - Curve undulation factor
- X_{\max} - Maximum in-situ block size (can be the spacing or burden)

Curve undulation factor:

$$b = \left[2. \ln 2. \ln \left(\frac{X_{\max}}{X_{50}} \right) \right] \cdot n \quad \text{Equation 2.10}$$

Where:

- X_{\max} - Maximum in-situ block size cm
- X_{50} - Mean fragmentation distribution size, cm
- n - Kuz-Ram model uniformity constant defined in Equation 2.6

According to Kansake et al., (2016), the KCO model is a modified version of the Kuz-Ram fragmentation model. It uses the original Kuznetsov equation to determine the mean fragment size. This is shown in Equation 2.8. In the KCO model, the Swebrec function in Equation 2.9 replaces the Rosin-Rammler function in Equation 2.5 and the curve undulation factor in Equation 2.10 replaces the uniformity index in Equation 2.6. The curve undulation function characterises the fragmentation distribution as opposed to the uniformity index in the Kuz-Ram model although it depends on the index.

Model testing at various sites proved the Swebrec function to be a best fit with sieved data especially for data ranging between 0.5 and 500mm (Ouchterlony, 2005; Ouchterlony *et al.*, 2017). This relationship is shown in Figure 2.5.

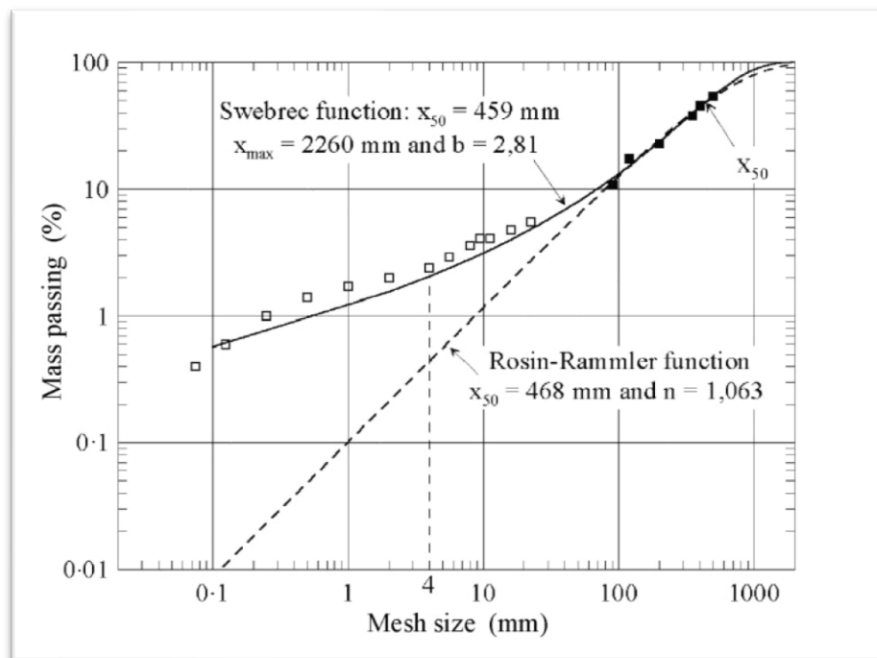


Figure 2.5: Comparison of Swebrec and Rosin-Rammler fits to coarse fraction data = 90mm and extrapolation to fines range. (Ouchterlony, 2005)

2.5.2 Numerical Models

Jager and Ryder (1999), define a numerical model as “any representation or abstraction of a system or process that include purpose, reference and is cost effective”. Performing actual experiments in mining is not always possible due to the inability to reproduce the mining

environment and stress conditions. Experiments tend to be costly and time consuming hence the development of numerical models to provide quick and reliable solutions for practical field application. Real life

The Hybrid Stress Blasting Model (HSBM) is one such a numerical model developed collaboratively by researchers from various mining and explosive companies, the University of Queensland and Itasca consulting group. HSBM combines numerical methods to model surface blast processes such as non-ideal detonation, fragmentation prediction and muckpile formation in laboratory scale experiments (Sellers *et al.*, 2011) for parallel holes (Onederra, 2004). Recently the HSBM algorithm was updated to simulate underground ring blasts for rock mass damage, fragmentation and burden displacement for Sublevel Caving (SLC). The simulation was validated against large scale experiments at Kiruna Iron Ore Mine and Ridgeway Gold and Copper Mine for a seven and eight hole ring pattern (Anglo American *et al.*, 2012).

2.5.3 Mechanistic Models

Mechanistic models combine empirical and constitutive approaches to solve problems (Kleine, 1991). They are generally sophisticated and require an understanding and description of the underlying physics of detonation, rock mass properties acquired from laboratory measurements, the action of explosive charge and energy transfer for the generation of realistic outcomes (Onederra, 2004; Cunningham 2005; Scott and Onederra, 2015). Obtaining and quantifying actual rock mass and explosives properties such as the velocity of detonation in the blasthole and characteristics of rock mass discontinuities is challenging. As a result, mechanistic models have been limited to simulation and analysis of small volumes and for research purposes only (Scott and Onederra, 2015). Similar to numerical models, mechanistic models seek to eliminate the trial and error approach for blast prediction and assessment.

To date, five mechanistic models have been developed for underground fragmentation modelling, and have been coded into FRAGNEW, SABREX, DynACAD-3D, FRAGMENTO and AEGIS software packages. Due to limited literature on DynACAD-3D, Only FRAGNEW, SABREX, FRAGMENTO and AEGIS are discussed in this study.

FRAGNEW

Kleine (1991) developed a mechanistic model that calculates fragmentation and damage from a blast. Although literature on FRAGNEW is limited, the model considers rock as a connected broken rock and a loose broken rock. Klein (1991)'s model is incorporated in the FRAGNEW model and has been applied in underground ring blasting (Riihioja, 2004, as cited in Onederra, 2004).

SABREX

The Scientific Approach to Breaking Rock with Explosives (SABREX) is a systematic and cost-effective design model that incorporates non-ideal detonation calculations and eliminates trial and error (Jorgenson and Chung, 1987). It combines three algorithms to calculate and predict fragmentation, muckpile movement, damage and cost (Kirby *et al.*, 1987).

The first algorithm is the Kuz-Ram that predicts the overall fragment size distribution using total explosive energy available and the volume of the rock to be blasted (Chung, 1994; Kirby *et al.*, 1987). The second is blast optimisation by Computer Analysis Technology (BOBCAT) that allows a three-dimensional view of the blast by incorporating stemming length, sub-drill, burden and spacing (Chung, 1994). The third algorithm is the CRACK that predicts fragmentation by generating a series of cracks around a series of blastholes in plan view (Jorgenson and Chung, 1987). According to Onederra (2004), the SABREX model is rarely accepted in the field due to its calibration requirements and also because the model is restricted to parallel hole patterns. Therefore, it cannot be applicable in an underground ring blasting environment.

FRAGMENTO

The JKMRC developed a modelling framework called FRAGMENTO. The model was developed specifically for underground production blasting applications. FRAGMENTO is a single ring deterministic model that extends into a stochastic model, and describes the response of rock masses to blasting by taking into consideration the extent of the near field and far field fractured zones to predict fragment size distributions (Onederra, 2004). In

addition, the stochastic component allows the simulation of the impact of blasthole deviation on fragmentation, dislocation and overall detonation performance” (Onederra, 2004). According to Onederra (2004), FRAGMENTO takes into consideration rock breakage by crushing and fracturing. As a result, the full range of the fragmentation size is modelled, a feature empirical models such as the Kuz-Ram fails to address.

With FRAGMENTO, the user is able to assess and evaluate the sensitivity of blast parameters on fragmentation, uniformity and costs (Onederra and Chitombo, 2013). Figure 2.6 is a plot of uniformity index versus burden for a two-ring blast simulated in hard competent rock.

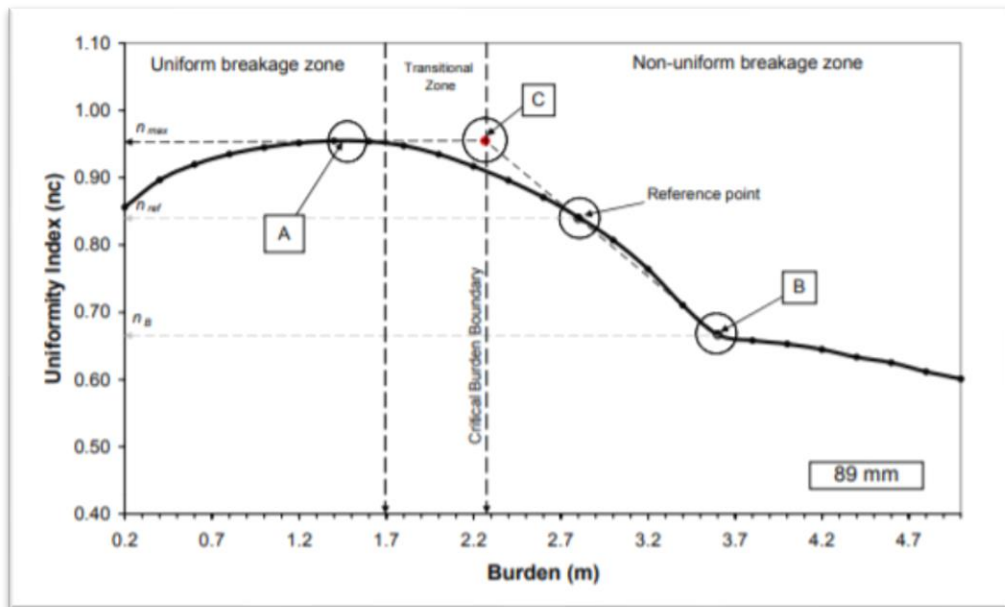


Figure 2.6: Uniformity index versus burden curve for a two hole ring blast in a simulated hard competent rock (Onederra, 2005)

From the graph, the blast engineer is able to evaluate the range of burden that will yield the best fragmentation uniformity and consistent breakage. The plot is separated into three zones, the uniform breakage zone, the transitional zone and the non-uniform breakage. The uniform breakage zone represents a range of burdens where efficient and fine fragmentation will result. In the transitional zone, good breakage is expected whereas the non-uniform breakage zone represents a range of burdens where poor breakage and

fragmentation is expected for a specific type of rock and blasting conditions (Onederra and Chitombo, 2013).

To enable field applications, FRAGMENTO is encoded in the JKSimBlast software package. The 2D Ring component of the software was developed specifically for ring blasts. Blast simulations with 2D Ring software offer a useful evaluation of energy distribution on each individual ring as well as interaction of several rings in 3D (Laredo and Chipana, 2017).

Unified Break Model

The Unified Break Model is a model recently developed by Preston (2019), a consulting engineer at iRing INC. It is a mechanistic model that takes into account the physics of detonation and mathematical models to predict adequate blasting patterns based on rock properties and shock wave characteristics for underground ring layouts. The Unified Break Model is based on four components; the unit charge, thermodynamic energy, stress reflection and radial break. These components take into account the local rock properties, explosive properties and shockwave attenuation characteristics linked with the mechanism of rock breakage during the propagation of the shock wave of explosive detonation as discussed in Section 2.2 of this research report. These components are discussed in detail below:

Unit Charge Model. The unit charge model is the “distance the explosive detonation head travels in time it takes the primary-wave (p-wave) to reach the free face” Preston (2019). According to Preston and Williams (2019), the unit charge model links rock properties, explosive properties and the blast pattern. When relating the VOD of the explosive with the p-wave velocity of the rock blasted, the unit charge length of the explosive column can be determined. The relationship between the properties as mentioned above allows the evaluation of different drill and blast patterns because the VOD, p-wave velocity and burden influences the length of the unit charge length. This in turn assists the drill and blast engineer analyse different combinations of patterns and explosives in the same rock.

The geometry illustrated in Figure 2.7 is used to determine the unit charge length of an explosive column. The blue line shows the charge length, P is the initiation point and the dashed lines represent the burden or the beginning of the free face.

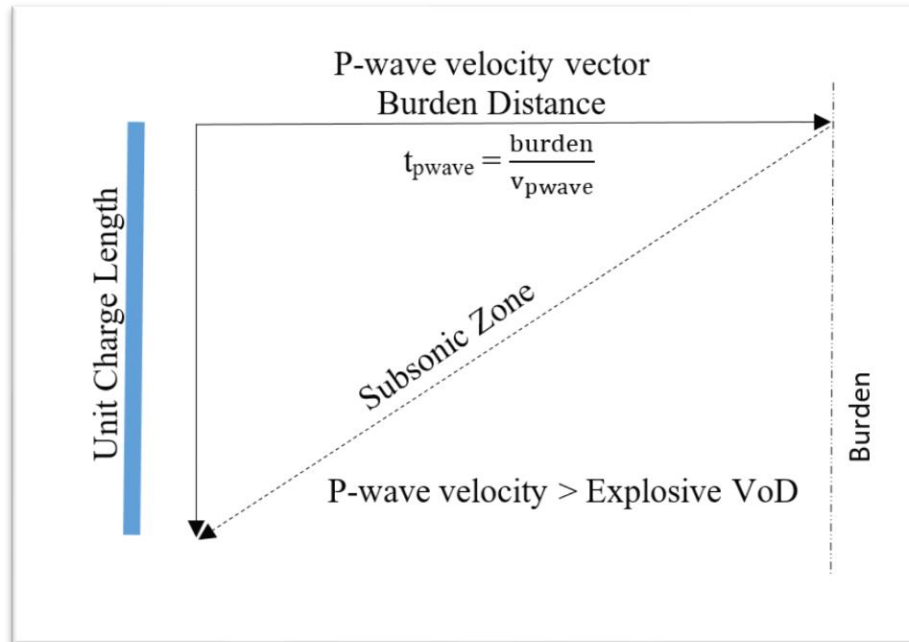


Figure 2.7: Unit charge length geometry (After Preston and Williams, 2019)

The following assumptions apply for the unit charge model (Preston, 2019):

- a) Ore/rock will break as a direct manifestation of the unit charge being in direct intimate contact with the ore/rock medium (no air gaps or portions of unloaded holes). No decoupling is allowed.
- b) The explosive is undergoing detonation for the full length of the unit charge. There are no inert gaps permitted, detonation velocity is assumed constant.

Thermodynamic/Heat Energy Model. Following the detonation of an explosive in a detonation column, rock breakage, and crack formation and extension result due to the compressive shock wave, high-pressure gases and explosive energy released. The thermodynamic model is used to calculate the energy available to break the rock at a charge

diameter (Preston and Williams, 2019). The following are the assumptions made for the thermodynamic model (Preston, 2019):

- a) The maximum energy generated by the detonation reaction will be at the ideal detonation velocity for any specific explosive that undergoes detonation at the ideal diameter of the explosive.
- b) The volumetric reaction extent is equal to the ratio of the critical velocity at the critical diameter of the explosive, divided by the detonation velocity measured in the ideal diameter of the explosive.

Stress Reflection Model. As discussed in Section 2.2, the compressive shock wave and high-pressure gases formed attenuate exponentially (Preston, 2019) as they radially propagate away from the borehole extending towards the free face. The propagation of the shockwave and high-pressure gases is dependent upon the properties of the rock. As the shock wave hits the free face, much of the shock wave is reflected back as a tensile wave due to the significant change in the propagation medium. The attenuation of the shock wave is modelled by the attenuation curve in Figure 2.8. The attenuation curves are determined from nearfield and/or far field seismic sensors in blasting operations.

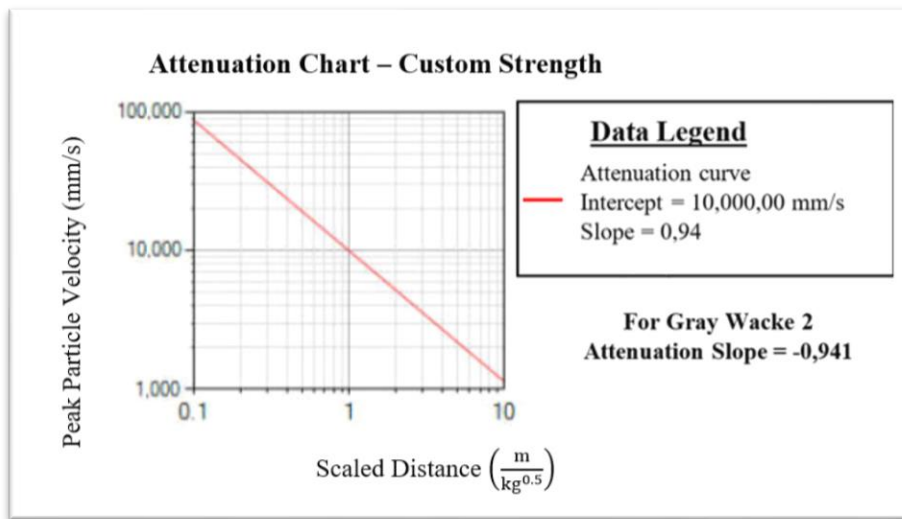


Figure 2.8: Attenuation curve (Preston and Williams, 2019)

Using Figure 2.8 and Equation 2.11, the stress at a particular radial distance from the borehole wall and the distance where the compressive stress falls below key material properties can be estimated (Preston and Williams, 2019).

$$\sigma = PPV \cdot \rho_{\text{rock}} \cdot V_p \quad \text{Equation 2.11}$$

Where:

- σ - Compressive stress
- PPV - Peak particle velocity
- ρ_{rock} - Rock density
- V_p - P-wave velocity.

From this, the relationship between the peak stress and the scaled distance can be determined as shown below.

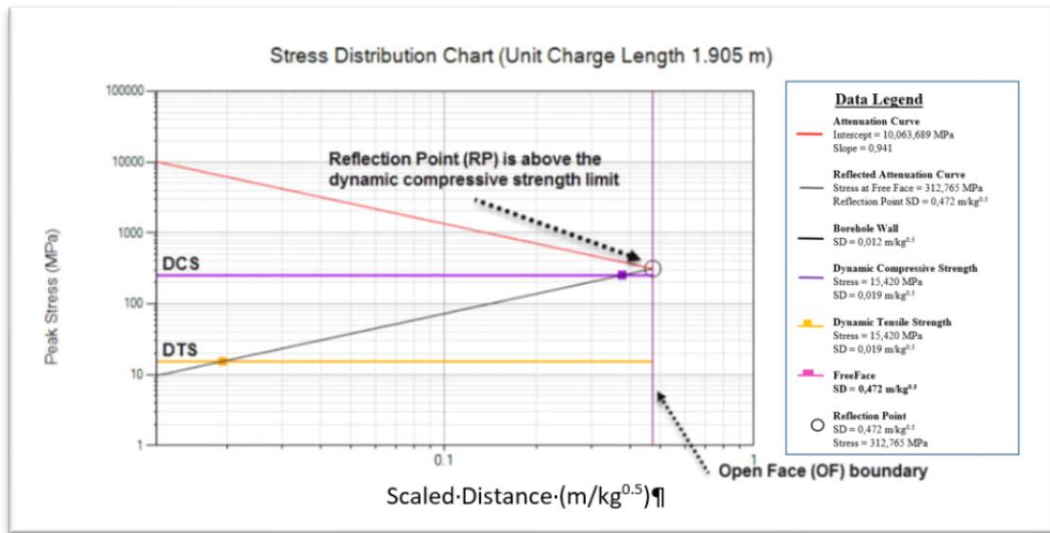


Figure 2.9: Stress distribution chart

Figure 2.9 illustrates the stress attenuation of a detonated blasthole. From the graph, the compressive stress at which the shock wave hits the reflection point at the wall of the free face should be between the dynamic compressive and tensile strength in order to get the required fragmentation and to minimise damage in the wall. When the stress is significantly greater than the compressive strength of the rock at the reflection point slabbing and scabbing

usually occurs resulting in coarse fragmentation. According to Williams (2019), this normally happens when mines try to remedy coarse fragmentation by increasing the powder factor, which results in a non-uniform muckpile that contains both coarse and fine fragmentation.

Radial Break Model. For the purpose of determining the break radius in the radial break model, the explosive charge is confined away from any free face. The determination of the break radius of the charge is based upon the following assumptions (Preston, 2019):

- a) The radial break from a detonating blasthole, break will expand outwards radially as an expanding cylinder or ellipse.
- b) It was determined that the rebounding stress waves are hyperbolic in nature, outbound as a compressive wave front and inbound changing mode to a tensile wave front after reflection from an open face.
- c) For the shock wave attenuation, it is assumed that the reflective tensile portion from the open face may produce tensile scabbing at the free face based on the value of the dynamic tensile strength of the rock/ore medium as well as its impulse value. The dynamic tensile strength of the rock is determined by inducing a dynamic load on the specimen by the Split Hopkinson Pressure Bar (SHPB) as suggested by the ISRM. The Shock magnitude is time dependent with maximum values at the borehole wall being steadily attenuated and stretched out traveling to the free face. The scabbing action will continue inward until the dynamic tensile stress in has decayed below the characteristic impulse value of dynamic tensile strength.

For the ring geometry, rectilinear methods of calculating the powder factor as a means of determining the energy distribution do not work. This is because different explosives (ANFO based or emulsion) do not have similar heat energies and VOD for the same weight (Preston, 2019).

The Unified Break Model is incorporated in the iRing INC AEGIS Underground Drill and Blast software and is part of the Analyser component of the software. It allows the designer to evaluate drill and blasts patterns in terms of stress distribution.

Due to the software's recent development, there has only been one account of its use. The software was applied successfully at Eleonore Mine in Canada to optimise the fragmentation to a size limited to 400mm. However, the software does not take into consideration the varying spacing between the collar and the toe and does not necessarily predict the fragmentation size.

An evaluation of the models presented in this section makes the FRAGMENTO model the best model because of its ability to simulate explosive detonation, show the explosive energy distribution and predict fragmentation. However, due to a lack of locally based service consultants and their inaccessibility within the limit period of the research, only the Unified break model encoded in the IRING INC – AEGIS Underground Ring Design Software was used.

2.6 Fragmentation Analysis

Subsequent to fragmentation prediction and the application of the blast design parameters in the field, the blasting engineer analyses the effectiveness of the design by evaluating fragmentation size distribution post blasting. This ensures continuous monitoring, and optimisation of the blasting operation. Franklin *et al.*, (1996) reviewed the evolution of fragmentation measuring systems. The methods of analysing fragmentation can be classified into two broad categories: direct and indirect methods. Sieving is an example of a direct method that is arduous and costly in nature particularly for large volumes of rock such as in production blasting, while indirect methods offer a more convenient and affordable means of analysing the fragmentation size distribution. Indirect methods are mostly empirical, observational and digital (Sereshki *et al.*, 2016). These methods are discussed briefly in the sections that follow.

2.6.1 Sieving

Sieving is the oldest method of accurately analysing fragment size distribution provided there are no errors. To perform this, a sample of rock collected from a muckpile is sieved through a series of screens of progressively smaller mesh size. The amount of rock retained on top of each screen of different size is weighed as a fraction of the total weight of the sample in order to calculate the percentage of material retained on the screen. The Rosin-Rammler equation provided in Equation 2.6 defines this relationship. By subtracting the percentage of material retained on screen from the whole size range (100%), the cumulative percentage passing versus size fraction graph can be drawn.

Although accurate, sieving is costly, time-consuming and inconvenient for full-scale production blasts where a large volume of rock is blasted. In addition, mining operations are interrupted during sieving (Sereshki *et al.*, 2016). To solve this, muckpile samples are often evaluated although not representative considering that, rocks do not perfectly mix (Ouchterlony, 2003). With the introduction and improvement of technology, rapid and convenient digital image analysis techniques for rock fragment size distribution have been introduced.

2.6.2 Visual Observations

Visual observations are a qualitative means of evaluating the rock size distribution. The drill and blast engineer inspects and judges the muckpile to determine if whether the blast is successful or not. Although quick, the visual observation evaluation method is very subjective and can lead to inaccurate results.

2.6.3 Digital Image Analysis Techniques

Aber *et al.*, (2010) define digital image processing and analysis techniques as “mathematical or statistical algorithms that change the visual appearance of geometric properties of an image and transforms it into another type of dataset.” In the context of blast fragmentation analysis, images of the exposed surface of the muckpile are captured in two dimension (2D) and an attempt is made to convert the images to three dimension (3D) using a fragmentation software in order to deliver a real measurement of the

fragmentation distribution (Noy, 1997). Many software packages currently available in the market were developed to process images to give a size distribution analysis. Split-desktop, Wipfrag, Fragscan and Gold Size are the most popular software in the market. These software packages are helpful especially from a design perspective where different blast designs and explosives types can be quickly and efficiently analysed to control and optimise fragmentation (Sereshki et al., 2016). To date, this technique is the only practical and quantitative method of analysing fragment size distribution in production blasts (Kansake *et al.*, 2016).

For this research, the digital image analysis technique is used to analyse the size distribution of fragmented rock. The Split-desktop was used because in addition to its affordability and continuous update, it offers locally based service consultants. Therefore, it is easily accessible within the limited period for the research. The application of the software is described in the next paragraph.

Muckpile images are first captured with a digital camera, however a D-SLR type of camera is recommended for an underground environment due to its light sensitivity and clearer images in dark areas (Wipware, 2013). When capturing images, an object of known size must be included for scaling and an attempt should be made to capture visible images over the entire exposed surface of the muckpile. The rock fragments must be distinct. The concept is, if the images are not clear to the human eye, neither can the software “see” and process the images. Images should not overlap in order to avoid repetition and hence flawed results. In addition, the technique for image capturing must be consistent. Split Engineering (2014) recommends capturing images of the same area for different muck piles for a valid comparison. For example if the surface of the muckpile is captured before mucking, this should be done for all muckpiles.

The processing and analysis of the image by the software is similar for all fragmentation software. For Split-desktop, the captured image is downloaded to the computer. The image is imported into the software for analysis. Bobo (2009) and Kansake *et al.*, (2016) describe the processes a user needs to follow post importing the image for analysis:

- The size of the scaling object is determined for each image.
- The image is delineated automatically. This is a process where algorithms in the software determine the edges of each rock.
- Depending on the visibility and quality of the delineation achieved, manual editing of fragments might be required especially for underground muckpiles where visibility is poor due to low lighting. A delineated image of a muckpile is shown in Figure 2.10.
- The software then calculates the size distribution based on the properties of the delineated fragments such as area and dimension.
- The results are displayed as either bar plots or cumulative plots (Figure 2.11) that show the various percentage of the size distribution retained or passing.

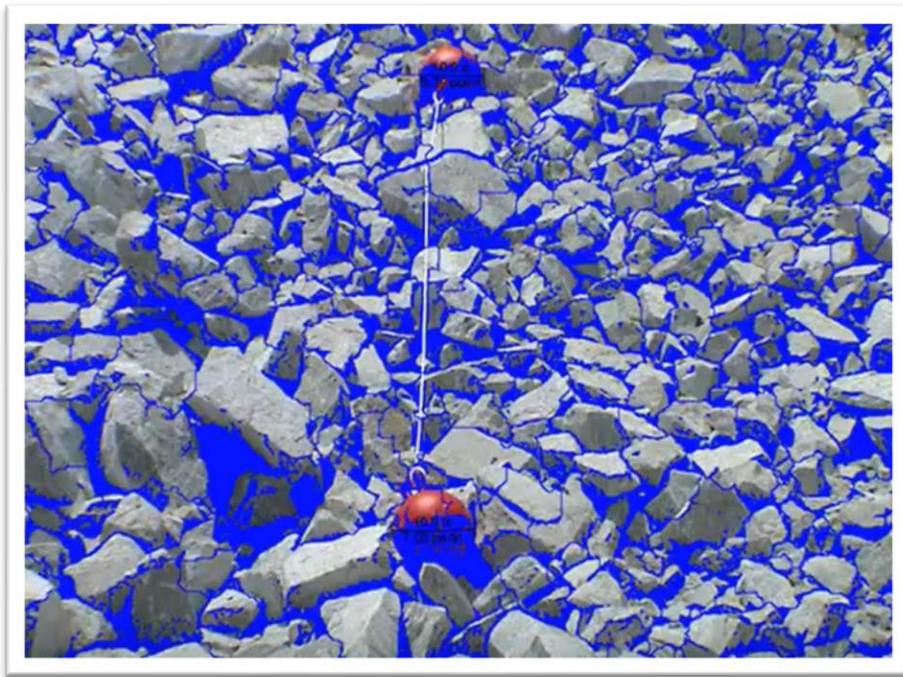


Figure 2.10: Automatically delineated image of a muckpile (Split Engineering, 2014)

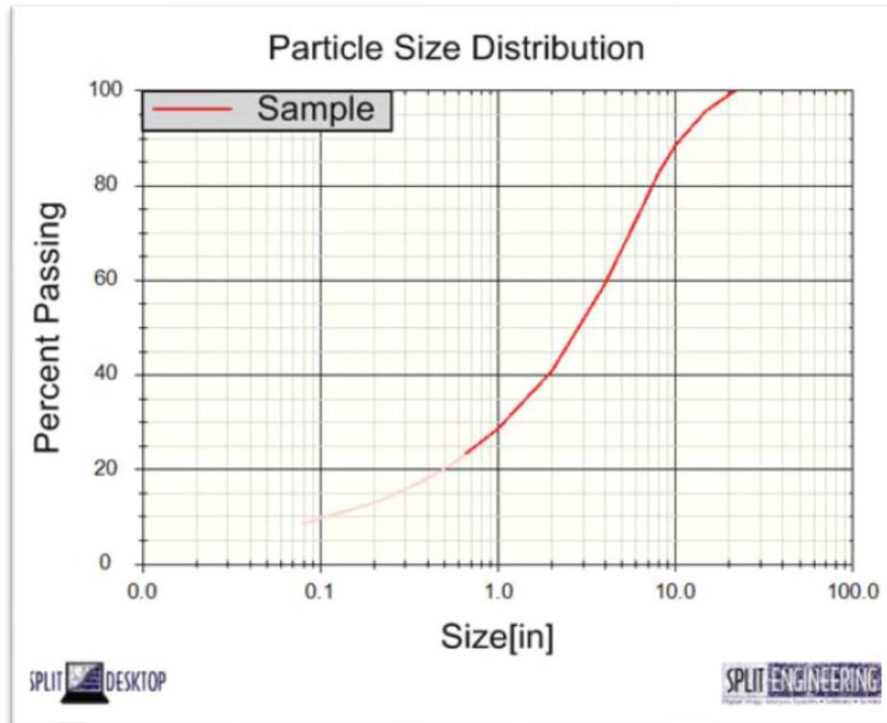


Figure 2.11: Display of a typical cumulative size distribution curve for the rock fragments (Split-Engineering, 2014)

2.7 Chapter Summary

The literature discussed has shown that in order to obtain the required fragmentation distribution size, an in depth understanding of the uncontrollable and controllable parameters affecting fragmentation and the interaction of these parameters with explosives is essential. Particularly the in-situ block size which has an influence on fragmentation depending on the block size.

Many fragmentation optimisation studies have been conducted with the focus mainly on surface mines and nothing much for ring blasts. Hence, throughout the years empirical models developed for surface operations are used to design drill and blast patterns for underground mines that conduct ring blasting. Although these methods are applicable for the determination of geological conditions, and provides a starting point, they cannot however be reliably used to design drill and blast patterns for ring blasts. This is mainly due to the geometry of ring blasts and the difficulties in achieving the correct energy

distribution. Hence, the need for the development of models and underground drill and blast software based on the physics of detonation, rock mass properties, the action of explosive charges and energy transfer for the generation of realistic outcomes specifically developed for designing ring patterns.

It has also been found from literature that for continuous optimisation of drill and blast patterns and as a result, fragmentation, digital image analysis techniques are essential for analysing and evaluating the results. However, the method is not accurate but gives an indication of what the fragmentation size could be.

3. METHODOLOGY

3.1 Chapter Overview

The purpose of this chapter is to describe the type of data collected and the methodology followed. The data collected include the mechanical properties of the host rock, explosives data, geometric blast designs and muckpile images to determine the size distribution of blasted rock.

3.2 Image Analysis and Fragmentation Size Distribution Determination

In order to determine the rock fragmentation size that the mine currently achieves, images of the muckpile were captured underground using the Ricoh WG-50 digital compact camera and analysed using the Split-desktop software. On average, ten images from ten (10) different Load-Haul-Dump (LHD) scoops of the same muckpile were captured. A total of fifty-five (55) images from five longhole stopes were analysed. Due to the poor lighting conditions underground and the small image sensors of the digital camera, a torch/light source was used to illuminate the muckpile. Medium sized soccer balls with a diameter of 15cm were placed and used as scaling objects in the muckpile as illustrated in Figure 3.1. The ball was subsequently removed after the image was captured and re-used for the next load.



Figure 3.1: Image of an LHD scoop loaded with ore for fragmentation analysis.

The images captured were analysed with the Split-desktop version 4.0 software. The procedure followed is outlined below after Bobo (2009) and Kansake (2016):

- i. Firstly, the images were imported/opened in the Split-desktop software.
- ii. The fines factor was kept at the default 50% because a site-specific calibration for the fines was not conducted. According to Split-Net (2014), calibrating the fines factor is possible for laboratory scale samples only.
- iii. The rock fragments in the images were then delineated automatically to determine the edges around them. Due to poor underground lighting conditions, the images were inadequately delineated with the automatic delineation function. Therefore, all pictures were subsequently manually delineated.
- iv. The scaling factor was set for the diameter of the soccer balls as 15cm.
- v. Following which the soccer balls were masked to exclude them from the size distribution calculations including areas that did not form part of the rock fragmentation.
- vi. Using the “fines fill” tool, material too small to be seen and delineated were classified as fines. The software measures the coarse size distribution to a certain point, below which an estimate of the percentage of fines is done.

3.3 Geometric Blast Design and Explosives Data

The geometric blast design parameters and explosives data was obtained from the issued drilling and charge plans from the Drill and Blast department. The explosives performance characteristics was obtained from the explosive manufacturer.

3.4 Mechanical Properties of Rock

The mechanical properties of rock are required in order to determine the strength and blastability of rock. This ensures the design of adequate drill and blast patterns and in turn the powder factor/energy required to break rock. Mechanical properties of rock and rock mass include amongst others Uniaxial Compressive Strength (UCS), Uniaxial Tensile Strength (UTS), Rock Quality Designation (RQD), Rock Quality Index (Q-rating), Rock Mass Rating (RMR) and deformation characteristics such as the Young’s Modulus (E) and

Poisson's ratio (μ). These properties are important in classifying rock as weak, moderate or strong, and as such crucial for the drill and blast design process.

In order to determine the intact rock properties, core samples were collected from the core yard at South Deep Mine. The samples were first prepared and tested according to the International Society for Rock Mechanics (ISRM) (2007) standards at the University of the Witwatersrand Gold Fields laboratory. The samples were assumed to be a representative of the entire complex rock mass strata on the basis that the rock has gone through a similar geological cycle (Bieniawski, 1974). The core samples were tested for UCS, UTS, density, primary and secondary wave velocities, Young's Modulus and Poisson's ratio. The RMR, RQD, Q-rating and other rock mass properties were sourced from a geotechnical study that SRK Consulting (2006) conducted at the mine.

3.5 Drill and Blast Design Simulation

The AEGIS underground Ring Design software was used to analyse the current ring designs to evaluate whether there are any shortfalls with the ring patterns. Through multiple iterations of the ring design parameters and simulation, the software was used to determine optimisation opportunities for acceptable energy distribution throughout the design for improving fragmentation and minimising overbreak. Table 3.1 shows the parameters that were varied for obtaining the optimal fragmentation. This was based on the spacing over burden parameter of between 1.0 and 1.5.

Table 3.1: Ring design simulation parameters

S/B Ratio	76mm blasthole diameter	89mm blasthole diameter
1	Burden = 2m, Toe spacing = 2m	Burden = 2m, Toe spacing = 2m
1	Burden = 1m, Toe spacing = 1m	Burden = 1m, Toe spacing = 1m
1	Burden = 3m, Toe spacing = 3m	Burden = 3m, Toe spacing = 3m
1.2	Burden = 2m, Toe spacing = 2.4m	Burden = 2m, Toe spacing = 2.4m
1.4	Burden = 2m, Toe spacing = 2.8m	Burden = 2m, Toe spacing = 2.8m
1.6	Burden = 2m, Toe spacing = 3.2m	Burden = 2m, Toe spacing = 3.2m
1.8	Burden = 2m, Toe spacing = 3.6m	Burden = 2m, Toe spacing = 3.6m
2.0	Burden = 2m, Toe spacing = 4m	Burden = 2m, Toe spacing = 4m

3.6 Chapter Summary

This chapter described the methodology and data collected during the study. The data include the mechanical and structural properties of rock, explosives information, muckpile images and blast designs. Mechanical and structural properties of rock information assist in classifying rock as either weak, medium strength or hard which in turn helps the Engineer design drill and blast patterns that yield the optimal fragmentation size as required by the downstream processes. It is important however that an adequate number of rock samples and areas are tested and observed for the determination of mechanical and structural properties in order to acquire a wide representation of the different rocks to be blasted. This ensures that the rock mass properties' results are representative of a wide area of the mine.

The ability to analyse fragmentation size distribution using image analysis techniques is advantageous in that it allows the Drill and Blast engineer to quickly evaluate and re-design drill and blast patterns accordingly. Therefore, the AEGIS underground drill and blast software becomes even more necessary and enables quick evaluation of energy distributions and optimisation of patterns to yield the required results.

4. RESULTS AND ANALYSIS

4.1 Introduction

The results from the data collected are presented and analysed in this chapter. The discussion covers drill and blast planning, the basic oreflow process from the stope to the stockpile, rock mass and rock strength classification, fragmentation analysis and prediction.

4.2 Blast Planning

The drill and blast planning process at South Deep Mine starts with the release of the long-term stope plan from the survey department. The Drill and Blast department then designs ring patterns based on the stope configuration. The drill and blast patterns are designed using the Deswik Underground Drill and Blast software. When the design is complete, the drill patterns are handed over to the drill rig operators whom upon completion hand back the drill patterns to the drill and blast engineer for tallying. These are referred to as drill returns.

Once drilling is complete, the lengths of the holes are measured to ascertain if whether the design matches actual drill lengths. Charge plans are then evaluated and redesigned to match the actual blasthole lengths. Once completed they are signed off and handed over to the charging crew and only then can the charging process begin. During the drilling and charging process, the Quality Assurance Quality Control (QA/QC) department conducts quality checks to ensure that the drilling and charging is done accordingly unless implementation is impossible due to stope size changes as a result of effects of the previous blast such as overbreak. In this case, the QA/QC department informs the drill and blast department to alter the charge plans accordingly.

Neither the drill plans nor the charge plans can be handed over by the drill and blast engineer unless all the preceding processes are completed, or discrepancies are modified.

Figure 4.1 illustrates the drill and blast planning process at South Deep Mine.

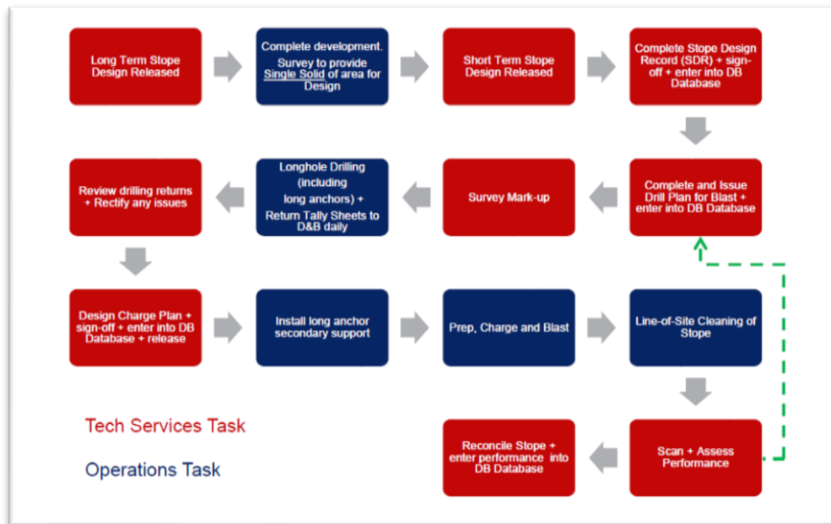


Figure 4.1: South Deep Mine drill and blast planning process (Gold Fields, nd)

During the study, it was observed that drill rig operators do not measure/inspect the lengths of holes drilled to ascertain their dimension for the drill and blast engineer to evaluate if whether the charge plans still match what is drilled. They tend to re-write dimensions as specified by the drill plan patterns without measuring the actual blasthole length. This is evident from the drill returns as shown in Figure 4.2.

095 01W CUT03 LHP 06B

RIG: SIMBA S7-D

RING: R2 TOTAL DRILL METRES: 124.6

DUMP: 0.00 LOOK DIRECTION: EAST

BURDEN: 6.951 : R1

HoleID	Dip	Length	Diã	Pivot Height	Offset	B/T	Drilld length	Driller	Date
H1	355.6	8.7	76 mm	1.8	L2.6	N	8.7	EWIS	
H2	359.3	8.1	76 mm	1.8	L1.5	N	8.1	EWIS	
H3	359.7	7.7	76 mm	1.7	R0.0	N	7.7	EWIS	
H4	7.8	7.2	76 mm	1.7	R0.1	N	7.2	EWIS	
H5	16.7	6.8	76 mm	1.8	L0.0	N	6.8	EWIS	
H6	24.7	7.7	76 mm	1.8	L0.0	N	7.7	EWIS	
H7	32.5	8.6	76 mm	1.8	L0.0	N	8.6	EWIS	
H8	39.9	9.8	76 mm	1.7	R0.0	N	9.8	EWIS	
H9	45.1	10.7	76 mm	1.8	L0.0	N	10.7	EWIS	
H10	53.1	10.1	76 mm	1.8	L0.0	N	10.1	EWIS	
H11	60.5	8.3	76 mm	1.8	L0.0	N	8.3	EWIS	
H12	70.0	7.5	76 mm	1.8	R0.1	N	7.5	EWIS	
H13	79.7	7.1	76 mm	1.8	R0.1	N	7.1	EWIS	
H14	90.6	6.7	76 mm	1.8	L0.0	N	6.7	EWIS	
H15	101.7	6.8	76 mm	1.8	L0.0	N	6.8	EWIS	
H16	111.8	2.9	76 mm	1.8	R0.1	N	2.9	EWIS	

Figure 4.2: Drill return from underground after drilling at South Deep Mine

As a result, the charge plans become inherently flawed in that the powder factor might be less or more than what is required to achieve the desired fragmentation size distribution.

The section that follows describes the flow of fragmented ore from the stopes to the stockpile including machinery and equipment used.

4.3 Oreflow System from the Stope to the Stockpile

Longholes are drilled radially to the limit of the target zone and charged with explosives for fragmenting the rock. Fragmented rock is loaded by Sandvik 514 Load-Haul-&-Dump (LHD) underground loaders with a volume and capacity of 14 tonnes and 5.4m³ respectively. The LHDs tip the fragmented rock from the stopes in the orepasses. To improve productivity and depending on availability, LHDs sometimes tip the ore into the Sandvik TH430 underground dump trucks with a 30-tonne capacity. On average, three LHD passes fill a dump truck but this is dependent on the quality of scooping and how skilled the operator is.

The dump trucks then transport the ore to the orepass. Trackbound locomotives with capacities of 14 tonnes tram the ore collected from the chutes in various sections to the main level station tip. The ore then goes through a series of tips to the shaft bottom. The bottom of the tip is equipped with a Metso C80 jaw crusher with a feed opening size of 800mm that has been designed to crush the rock down to between 0 and 185mm. The crushed rock is then fed to a conveyor belt that feeds a measuring flask which in turn feed the skips. Each skip has a capacity of 26 tonnes.

At the shaft headgear, the skips tip the rock into a series of conveyor belts that transport the rock to the ROM stockpile at the plant. From the ROM stockpile, ore is then fed into a SAG. Complexities of the oreflow experienced at the mine highlights the importance of achieving a suitable fragmentation size distribution. A schematic representation of the oreflow process at South Deep Mine is provided in Appendix 7.1.

Vander Westhuizen and Powell (2006) conducted an optimisation study at South Deep Mine to determine the optimal size requirement for the SAG mill. The study showed that the ROM feed size should be between 80mm and 90mm for the SAG mill to operate optimally.

In order to conduct an analysis of the fragmentation size distribution, the rock material properties and characteristics were determined. Hence, the section that follow seeks determine and describe the rock mass properties and characteristics at South Deep Mine.

4.4 Classification and Determination of Rock Mass Properties

According to Bieniawski (1989), Rock Mass Classifications systems are used to estimate and characterise the quality and strength of the rock mass in order to formulate an overall design rationale that is compatible with design objectives and site geology. In addition, an assessment of the rock quality assists in predicting the behaviour of rock exposed to compressive shockwaves during blasting (Hoseinie *et al.*, 2006) and the powder factor required.

In this research, the RQD, strength classification for intact rock using the UCS, UTS and Young’s Modulus, and the strength – strain classification system are used to classify the strength and quality of the rock in order to provide an adequate description of the rock mass. After gathering the relevant information, the rock properties’ information was used as an input in the AEGIS drill and blast software for the prediction and optimisation of fragmentation.

SRK Consulting (2006) and Joughin *et al.*, (2006) determined the rock mass properties at South Deep Mine. The results from the studies are compared with the laboratory rock test results that were conducted by the author. All tests were prepared and tested according to the International Society for Rock Mechanics (ISRM) (2007).

Table 4.1: Rock mass properties test results

	Joughin <i>et al.</i> , (2006) and SRK Consulting (2006)		Rock Mechanical test results		Average
	Mean Value	No. of tests	Mean Value	No. of tests	
UCS (MPa)	263.67	4	263.00	16	263.34
UTS (MPa)	14.85	4	12.60	17	13.73
Poisson’s ratio, μ	0.17	4	0.14	16	0.16
E (GPa)	68.67	4	86.89	16	77.78

An average of the rock mass properties' results obtained by the author, Joughin et al., (2006) and SRK Consulting (2006) was determined. A comprehensive table with all the compressive and Brazilian test results are provided in Appendix 7.7 and Appendix 7.8 respectively.

Laboratory tests were also conducted to determine the p-wave and secondary-wave (s-wave) velocities' propagation in the rock. However, it should be noted that the velocity of propagation in intact rock varies from that in the rock mass. The Holmberg-Persson constants (K and α) and the Peak Particle Velocity breakage threshold (PPV_{Breakage}) used in this study for analysis were taken from the look-up table compiled by Onederra (2005) for hard metalliferous environments. The results are summarised in Table 4.2.

Table 4.2: Summary of rock mass characteristics and properties at South Deep Mine

Rock test results by the author		Joughin <i>et al.</i> , (2006) and SRK Consulting (2006)		Onederra (2005)	
UCS (MPa)	263.34	Mean block size (X_{insitu}) (m)	Insitu >1.00 (Massive) -can be greater than 20 m ³	K (mm/s)	500.00
UTS (MPa)	13.72	RQD index (%)	82.70	α	0.90
Rock density (kg/m ³)	2 686.10	JPS	-0.87 -Rating= 20	PPV _{Breakage} (mm/s)	4 000 - 4 500
P-wave velocity (m/s)	5 900.00	JPO	-Dipping into the face -Rating = 40		
S-wave velocity (m/s)	3 750.00	H	7		
E (GPa)	77.78	RMD	-Massive -Rating = 50		
μ	0.16	RMR	-Faulted zones=76.5 -Unfaulted zones=92.3		

As shown in Table 4.2, the RQD index at South Deep Mine was found to be 82.70% (SRK Consulting, 2006). According to Deere (1968) cited in Bieniawski (1989), an

RQD index between 75 and 90 indicates a good quality rock. This implies that the rock mass at South Deep Mine is of good quality.

According to SRK Consulting (2006), the mean in-situ block size determined from naturally occurring discontinuities was found to be mostly massive at South Deep Mine and can be as large as 20m³ in other areas. This implies that the drill and blast patterns have more influence on the results of the fragmentation size achieved (Onederra, 2005). As a result, optimising fragmentation by varying drill and blast patterns such as burden, spacing blasthole diameter etc will yield the required results. The determination of the block size was done using photographic mapping techniques (SRK Consulting, 2006).

Bienwaski (1989) compared various intact rock mass classification systems available as shown in Figure 4.3. Using these strength classification systems, the rock mass at South Deep Mine can be classified.

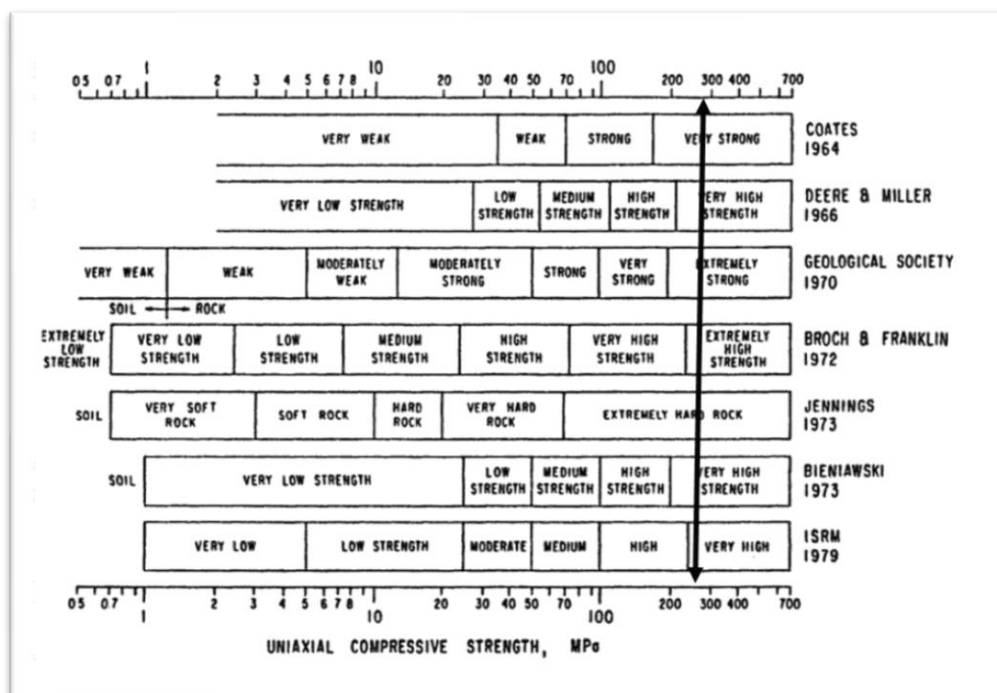


Figure 4.3: Various strength classifications for intact rock (Bienwaski, 1989)

Based on Figure 4.3 and using the intact rock strength of 263.34MPa determined from laboratory tests, the rock at South Deep Mine is found to be of very high strength.

The intact UCS – Modulus strength classification system illustrated in Figure 4.4 also suggests very high rock strength.

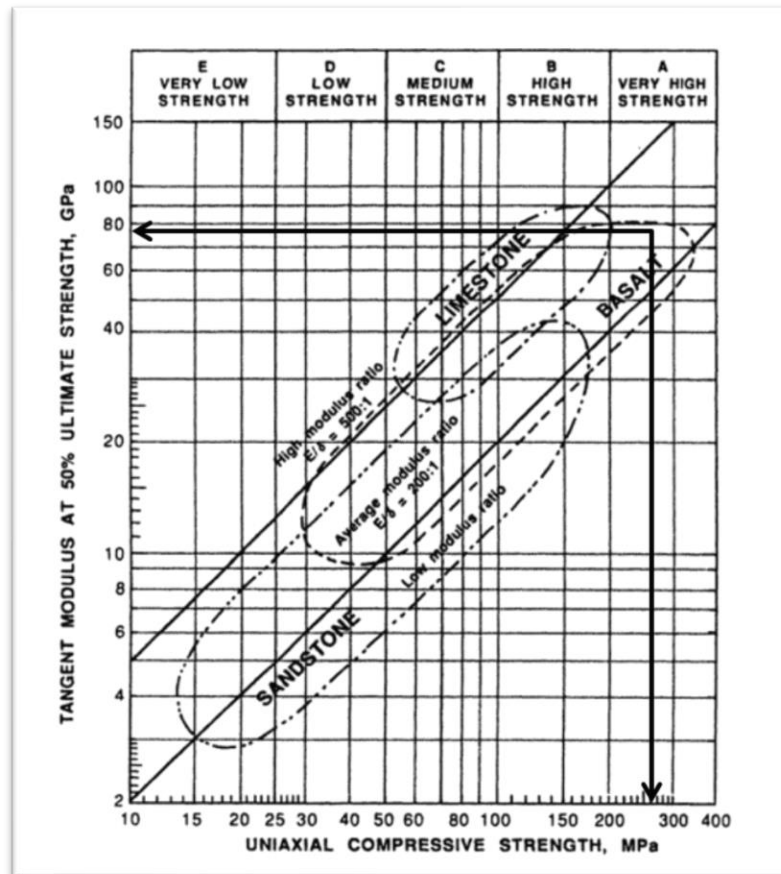


Figure 4.4: Strength - Modulus classification system proposed by Deere and Miller (1966)

4.5 Explosive Performance Characteristics

South Deep Mine uses the AEL UG101S pumpable emulsion usually referred to as “sticky” emulsion due to its ability to remain in the up hole after charging. The performance characteristics of the emulsion product are shown in Table 4.3.

Table 4.3: AEL UG101S pumpable emulsion performance characteristics (AEL World, 2020)

Minimum hole diameter	45 mm
Water resistance	Excellent
VOD (m/s)	4000 – 5500
Sensitised product density (g/cm ³)	1.00 – 1.10
Sensitiser	GS30
Pumping stages	4
Primer	150g booster
Ideal delivered energy (MJ/kg)	2.0 – 2.2
RWS @100MPa <small>(The Relative Weight and Bulk Strengths are relative to ANFO (=100 %) at a density of 0.80 g/cm³ determined using the VIXEN-i detonation code)</small>	88 - 92
RBS @100MPa <small>(The Relative Weight and Bulk Strengths are relative to ANFO (=100 %) at a density of 0.80 g/cm³ determined using the VIXEN-i detonation code)</small>	134 - 138
Application temperature	0°C - 55°C

4.6 Blastability Index

SRK Consulting (2006) also conducted an extensive underground geotechnical mapping exercise of the rock mass at South Deep Mine. The structural geological data gathered from this exercise as specified in Table 4.2 was used to determine the BI using equation 2.3. The BI was found to be 67. Parameters used to determine BI were gathered from SRK (2006)

A BI number of 100 is indicative of a strong rock with difficult blasting conditions whereas a low BI indicates a soft rock that is relatively easy to blast (Lily, 1986). Therefore, a BI of 67 indicates a strong rock with moderate to difficult blasting conditions. Figure 4.5 shows the Blastability Index versus powder factor and energy factor plot for the BI of 67.

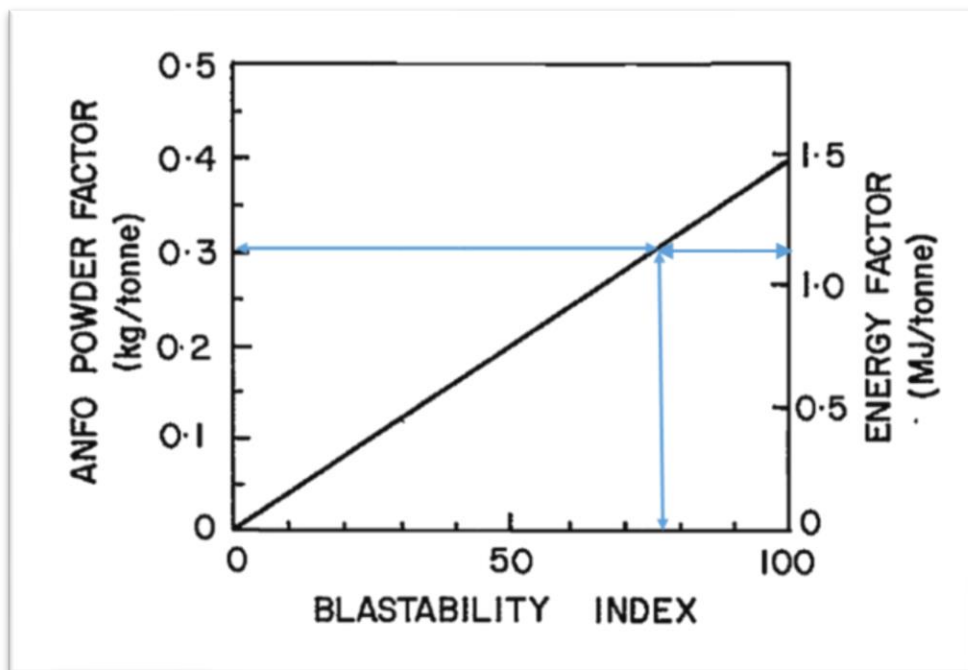


Figure 4.5: Blastability Index versus powder factor and energy factor (Lily, 1986)

The Figure shows that a BI of 76 gives an ANFO powder factor and energy factor of approximately 0.31kg/m^3 and 1.2MJ/tonne . The powder factor and energy factor magnitudes are however very low for an underground massive gold mine considering the strength of the rock mass and the confined blasting conditions. This is attributed to the fact that the relationship between BI, powder factor and energy factor in Figure 4.5 were specifically developed for large-scale surface iron ore mines that use ANFO as

the primary explosive (Lily, 1986). Further empirical evidence from Sasol Nitro (2014) and Dyno Nobel (2010) shows that a powder factor between 0.25kg/m^3 and 0.35kg/m^3 is suitable for soft rock hence 0.31kg/m^3 is not applicable for South Deep Mine. Prout (2019) recommends powder factors of between 0.9kg/m^3 and 1kg/m^3 for ring blasts as they have been successfully used at a South African diamond mine using a similar mining method.

Although the rock mass classification systems and the BI classify the rock mass at South Deep Mine to be high strength, the author suggests a more conservative rock mass strength for simulation purposes. This is based on a hypothesis of the potential reduction of the rock mass strength in secondary stopes due to fractures that may have been created by shock waves emanating from primary stopes. Figure 4.6 illustrates this phenomenon and the longhole stope mining sequence at South Deep Mine.

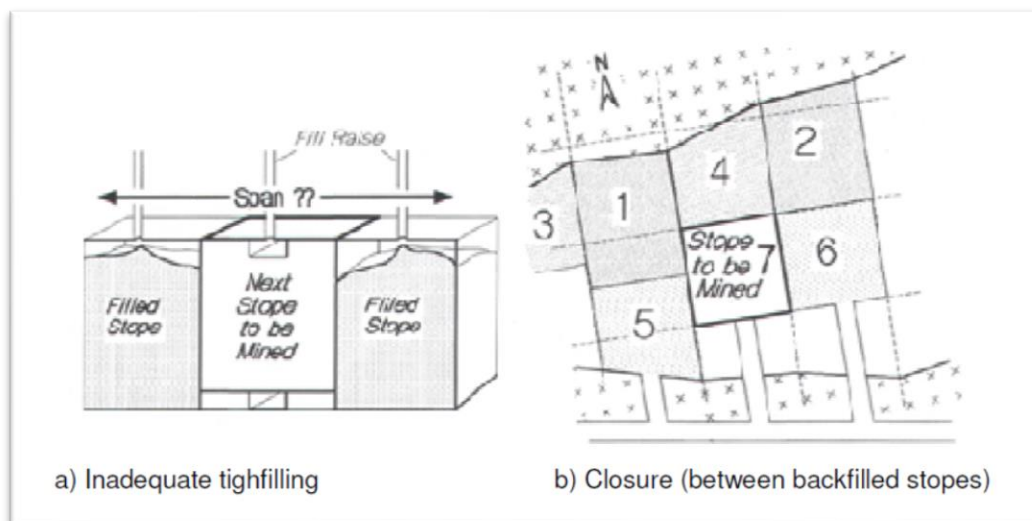


Figure 4.6: Longhole stope mining sequence at South Deep Mine (SRK Consulting, 2006)

As shown in Figure 4.6, stope 1 and 2 referred to as primary stopes are mined first subsequently back filled. After the back fill has cured, secondary stopes (stope 3 and 4) are then mined. It is possible that during the primary stope blasting, the shock waves may extend further from the limits of the stope creating and extending pre-existing fractures in the adjacent secondary stopes. This may result in highly fractured secondary stopes. In addition, the fractures will have an adverse effect on the propagation of shock waves and high-pressure gases during blasting of secondary stopes. Fractures serve as a free face where compressive shock waves are reflected and may result in coarse and

fine fragmentation depending on fracture orientation in the rock strata. Explosives also seep into these fractures during charging resulting in over-charging of the blastholes and the explosive energy may escape. This causes fine and coarse fragmentation.

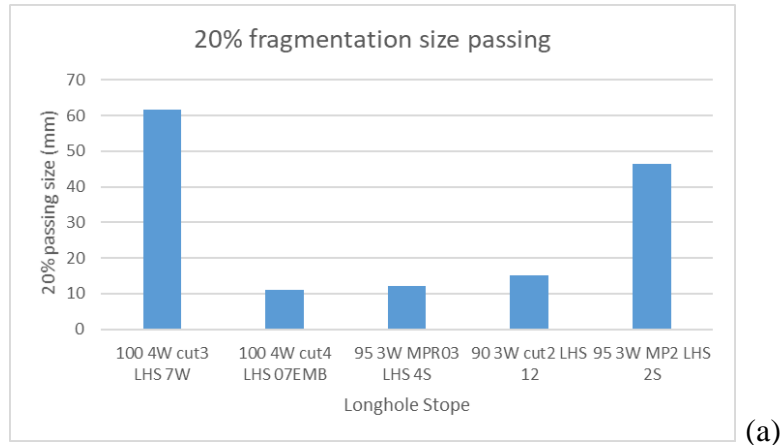
4.7 Analysis and Determination of the Current Fragmentation Size Distribution

For optimisation, the current fragmentation size distribution produced was quantified by analysing rock fragmentation in the longhole stopes using the Split-desktop software. In total five (5) longhole stopes were analysed. In each stope, an average of ten (10) images were captured from LHD buckets and subsequently analysed. This translates to an analysis of approximately 714 tonnes and a total LHD bucket area of 307.8m². The information from the analysis was used to infer the mean fragmentation size distribution of the entire mine although the true mean fragmentation size is unknown. This was done to get a sense of the fragmentation size distribution that the current blast designs were achieving.

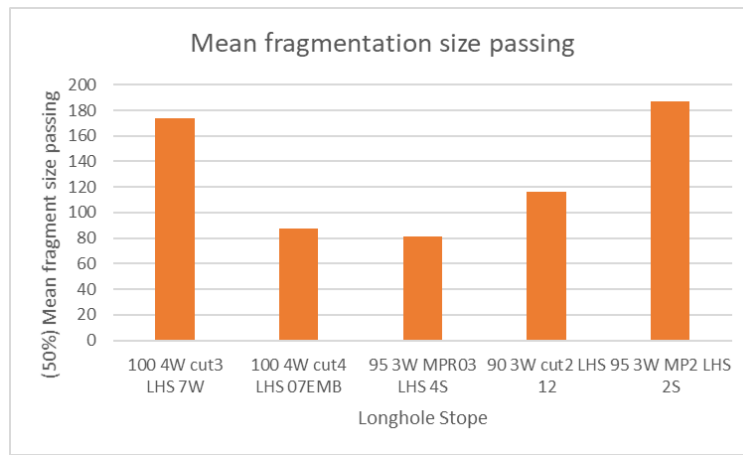
As mentioned in Section 4.3, the broken rock from the stopes is fed into orepasses. Rocks larger than the grizzly's opening are considered coarse and require secondary breaking. Although the maximum feed opening size of the jaw crusher is 800mm and reduces the product size to between 0mm and 185mm, the particle size fed to the crusher is limited to the grizzly's size of 300mm by 300mm.

With respect to the metallurgical plant's requirements, fragments smaller than 80mm are considered fine material. This is informed by the SAG mill's optimal operating ROM particle size requirements of between 80mm to 90mm. Therefore, the size of the rock fragmented in the stopes must be between 80mm and 300mm to satisfy the grizzly, crusher and plant requirements, which will in turn result in an efficient oreflow. Although it is not possible to entirely get rid of fine fragmentation, effort must be made to minimise their occurrence. Hence, blasts must be designed and executed in a manner that will yield the acceptable fragmentation size distribution.

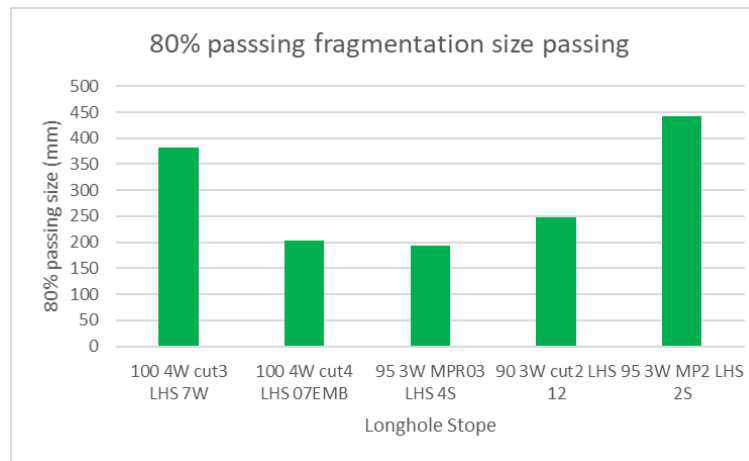
Figure 4.7 a – c shows a comparison of the 20% fragmentation size passing; mean (50%) fragmentation size passing and the 80% fragmentation size passing. In Appendix 7.2 to 7.6 detailed information of the fragmentation distribution size curves for these stopes is given.



(a)



(b)



(c)

Figure 4.7: Fragmentation size distribution for five longhole stopes at South Deep Mine for; (a) 20% fragmentation size passing; (b) Mean (50%) fragmentation size passing and (c) 80% fragmentation size passing.

From Figure 4.7, the F₂₀, F₅₀ and F₈₀ fragmentation sizes for the longhole stopes 100 4W cut4 LHS 07EMB, 95 3W MPR03 LHS 4S and 90 3W cut2 LHS 12 vary substantially with longhole stopes 100 4W cut4 LHS 07EMB and 90 3W MPR03 LHS 4S. This can be attributed to the exploitation of a similar reef horizon with generally similar rock characteristics (EC reef type) (Joughin *et al.*, 2006), drilling and charging practices and the stopes being drilled by different drill rig operators.

Although only 20% passing is between 10mm and 60mm, these fragmentation sizes are below the SAG mill requirements and at the same time might result in gold losses in the stopes affecting the MCF. The mean size (50%) passing varies between 80mm and 200mm, which is acceptable for the grizzly, crusher and the SAG mill. The 80% passing varies between 200mm and 450mm, which are reasonably acceptable. Size particles greater than 300mm can be reduced by the impact breaker at the grizzly.

A look at the upper 20% passing in Figure 4.8 shows that the distribution size in this range varies from approximately 500mm to 1 300mm.

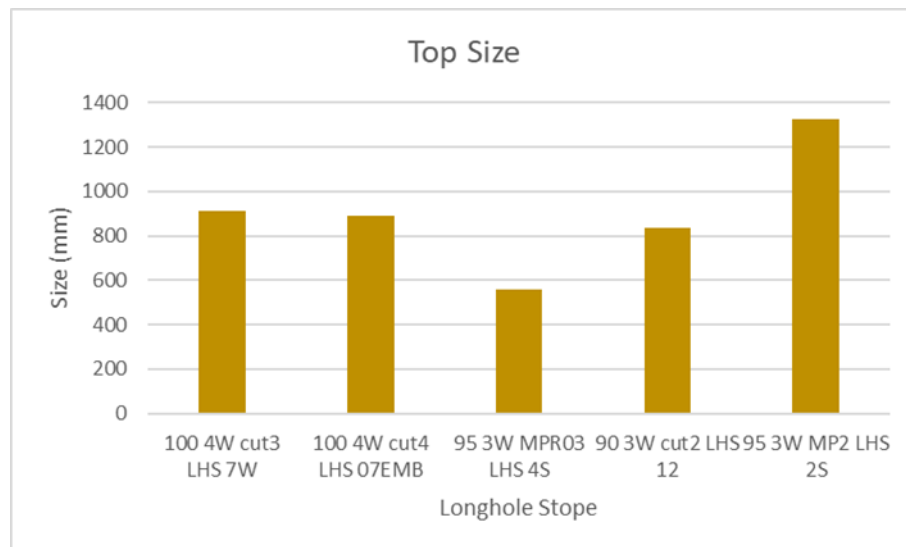


Figure 4.8: Top 20% of the fragmentation size distribution

These sizes are unacceptable especially those above 1 000mm because they sometimes block access for LHD mucking and thus require localised mobile impact breaking machine in the stope. This results in production delays.

Figure 4.9 shows the Rosin-Rammler uniformity index for the fragmentation size distribution of the longhole stopes

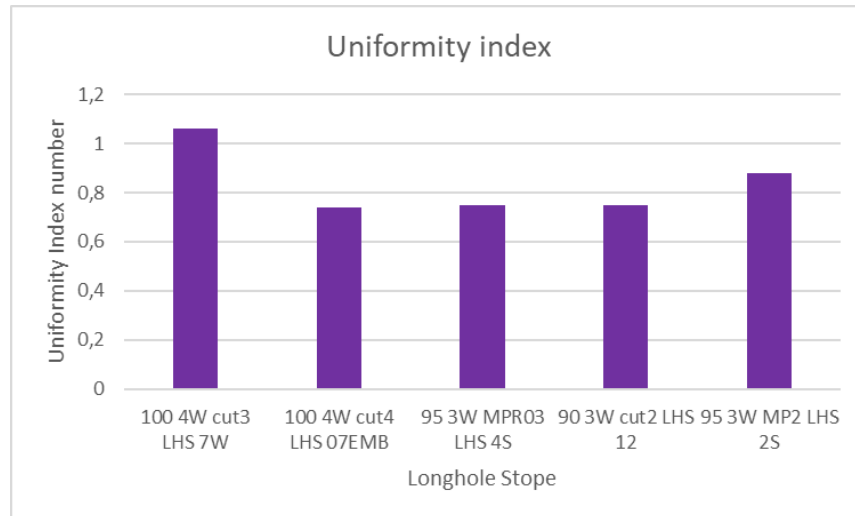


Figure 4.9: Fragmentation size uniformity index

As can be seen in Figure 4.9, the maximum uniformity index achieved for the stopes analysed is approximately 1.1. The uniformity index for stopes 100 4W cut4 LHS 07EMB, 95 3W MPR03 LHS 4S and 90 3W cut2 LHS 12 is between 0.6 and 0.8, and that for stopes 100 4W cut4 LHS 07EMB and 90 3W MPR03 LHS 4S is between 0.8 and 1.1. This implies a fragmentation distribution size of low to medium uniformity across stopes. With a uniformity index below 1, the mine produces both fine and coarse fragmentation. The coarse fragmentation introduces challenges during mucking, and the finer fragments may result in gold losses in the stopes. This also explains the fine fragments reporting at the plant.

The Split-desktop software allows users to conglomerate fragmentation size distribution of multiple stopes. To this effect, Figure 4.10 shows the overall fragmentation distribution curve for South Deep Mine.

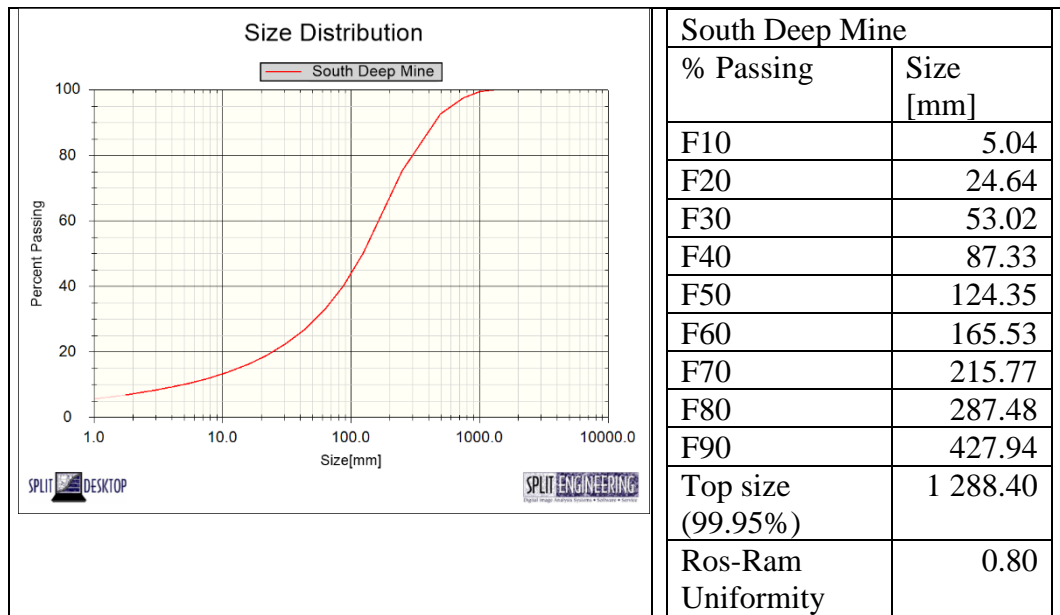


Figure 4.10: Inferred fragmentation size distribution for South Deep Mine

The results obtained agree with those obtained for individual stopes (Figure 4.7 to Figure 4.9). Figure 4.10 show that the overall F₂₀, F₅₀, F₈₀, the uniformity index “n” and the top size achieved are 24.64mm, 124.35mm, 287.48mm, 0.80 and 1 288.40mm respectfully. The mean fragmentation size (F₅₀) of 124.35mm deduces that 50% of the rock fragmented can pass through the grizzly without secondary breaking since the grizzly’s opening size is greater. In addition, an overall F₈₀ value of 287.48mm implies that a considerable percentage of the fragmented rock will also pass through the grizzly’s opening size. However, during data collection and physical observations, a great variation between coarse and fine fragments in longhole stopes was observed.

With 80% of the fragmentation size distribution being less than 300mm, this implies that the fragmentation size achieved is acceptable. However, the overall uniformity index is 0.80. This implies that the overall fragmentation size has a low-uniformity and varies greatly between fine and coarse material (Vesilind, 1980; Onederra, 2005; Singh *et al.*, 2016 and Wimmer *et al.*, 2015). In addition, the difference between the top size of 1 288.40mm and the lower 20% passing of 24.64mm support this observation. Achieved fragmentation size is highly inconsistent and lies within a wide size range. These observations explain why the plant reports fine ROM while a considerable amount of time is spent impact breaking large rocks in the longhole stopes and at the grizzly.

Using inferential statistics and bearing in mind that the true mean fragmentation size is unknown, the author is 95% confident that the average mean fragmentation size for South Deep Mine lies between 120.44mm and 128.26 mm with a 5% chance that the true population mean fragmentation size lies outside of this interval. These statistical values were obtained using Equation 4.1 with the degrees of freedom obtained from the “t-students table” (Curwin and Slater, 2002).

$$\mu = \pi \pm t \frac{S}{\sqrt{n}} \quad \text{Equation 4.1}$$

Where:

μ - confidence interval

π - Population mean

S - Standard deviation

n - Sample size

t - t-students' distribution degrees of freedom

Section 4.7 presents an analysis of the drill and blast patterns in order to get an insight into whether the designs are optimal.

4.8 Analysis of the Current Drill and Blast Patterns

The ring designs that yielded the fragmentation distribution size in Section 4.6 were analysed using the AEGIS analyser. The analysis was based on the availability of the explosives charge information in the format that the AEGIS drill and blast software supports.

A back analysis of the blast designs at South Deep Mine was done using the AEGIS drill and blast software. The analysis showed that the burden is kept at a constant 2m for all pattern designs while the toe spacing varies between 0.448m and 7.460m. The toe spacing is determined as the perpendicular distance from the top of a short blasthole to the next adjacent longest blasthole as stipulated by the JKRMC method of measuring toe spacing (Williams, 2019; Onederra and Chitombo, 2007). This is shown in Figure 4.11

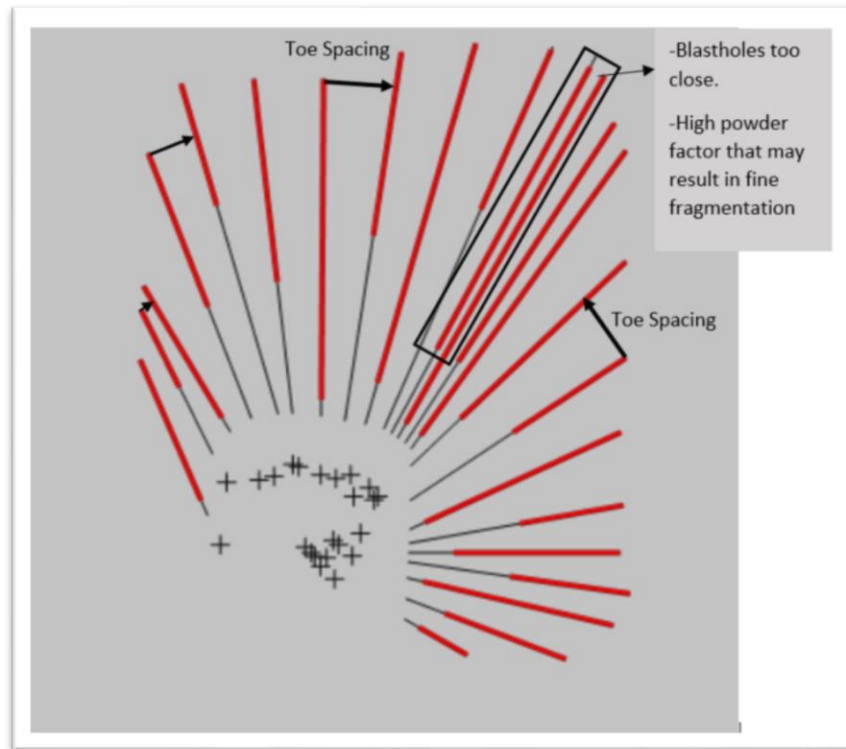


Figure 4.11: Ring pattern showing varying spacing between blastholes

According to the spacing to burden ratio rules of thumb discussed in section 2.3.2, for a burden of 2m, a toe spacing of between 2m and 3m is suitable. Toe spacing greater than 3m are unacceptable as is the case here. A toe spacing of 7.46m is extremely large. The author attributes this to the fact that there is no standard toe spacing for ring patterns at South Deep Mine and as a result, any toe spacing becomes acceptable to the designer. In addition, the large toe spacing can be exacerbated by:

- Drill rig operators not drilling according to the design, and missing some holes therefore creating large toe spacing.
- Inherent drilling inaccuracies in the machine.
- Hole deviations as a result of holes collared at wrong locations.

In order to understand the effect of the varying toe spacing, the AEGIS drill and blast analyser component of the software was used. The mine uses Simba S7-D drill rig to drill 76mm diameter blastholes. Based on empirical rules of thumb (section 2.3.2) for spacing to burden ratio, the AEGIS drill and blast software is calibrated and limited to only analyse drill patterns where the spacing to burden ratio is greater than one, otherwise an error in calculations is generated. Hence, the analysis is done for a toe

spacing of 2m, 5m and 7.5m where the spacing to burden ratio is 1, 2.5 and 3.75 respectively. In order to determine the attenuation parameters for the designs as required by the software, the rock strength was set at a conservative “medium high strength” to take fractures into consideration as described in section 3.4. The attenuation rate was set at “average”.

Figure 4.12 to Figure 4.14 shows the break overlap for toe spacing of 2m, 5m and 7.5m respectively using the radial break model embedded in the AEGIS analyser.

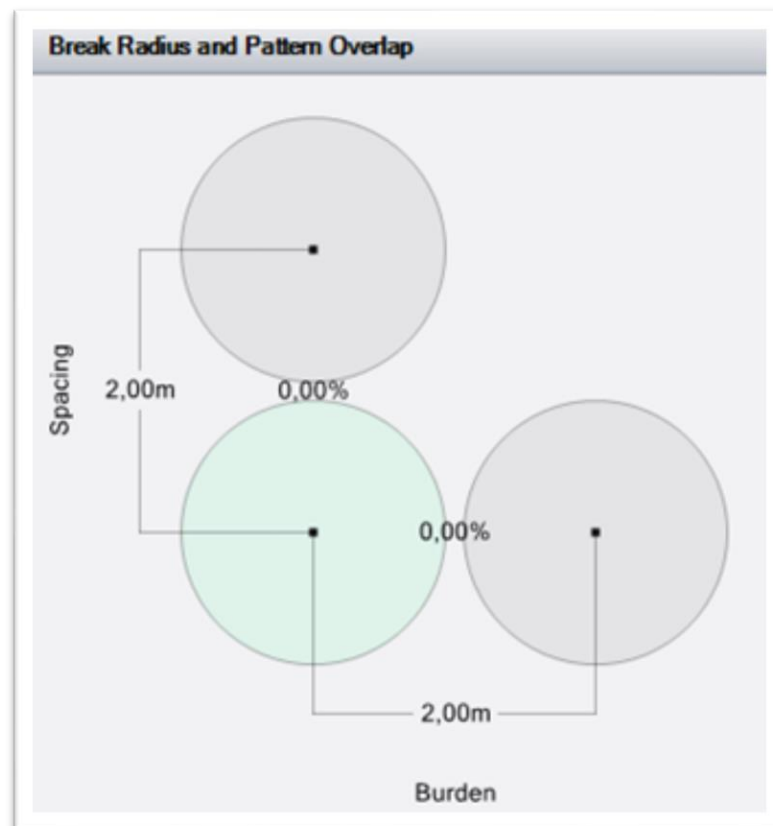


Figure 4.12: Break overlap for 100 4W Cut04 LHS 7EMB stope for a toe spacing of 2m

Figure 4.12 shows that there is a 0% overlap between blastholes in the same ring (toe spacing) and in different rings (burden) for a toe spacing of 2m. As a result, there is no interaction between the explosive energies and fractures of adjacent blastholes. According to Williams (2019), there might be some interaction of the explosive energy between these blastholes although there is no overlap because they (blastholes) are not very far from each other. This configuration with a toe spacing and burden of 2m will result in rock fragmentation although possibly not of an acceptable size distribution.

When the toe spacing is 5m and 7.5m, the area of no overlap is exacerbated as shown in Figure 4.13 and Figure 4.14.

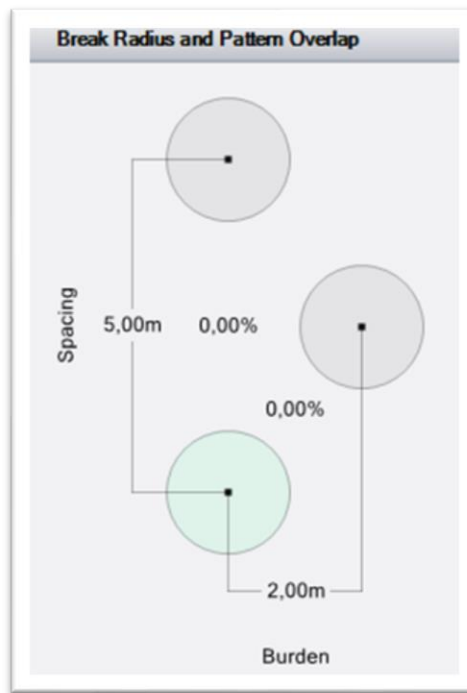


Figure 4.13: Break overlap for 100 4W Cut04 LHS 7EMB stope for a toe spacing of 5m

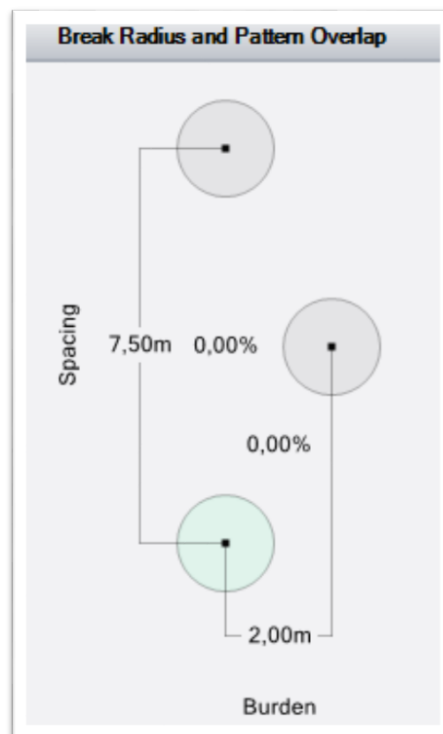


Figure 4.14: Break Overlap for 100 4W Cut04 LHS 7EMB stope for a toe spacing of 7.5m

With these toe spacing, there is no interaction between the explosive energies and fractures from adjacent blastholes. This increases the possibilities of the blast yielding coarse fragmentation and boulders. The boulders may emanate from the rock between blastholes in the same ring due to no overlap and interaction of explosive energies.

Figure 4.15 depicts an analysis of the pattern extend break radius for the 5m toe spacing. The figure shows that for the blasthole, the crack due to high-pressure gases extend for an average distance of 0.95m from each blasthole.

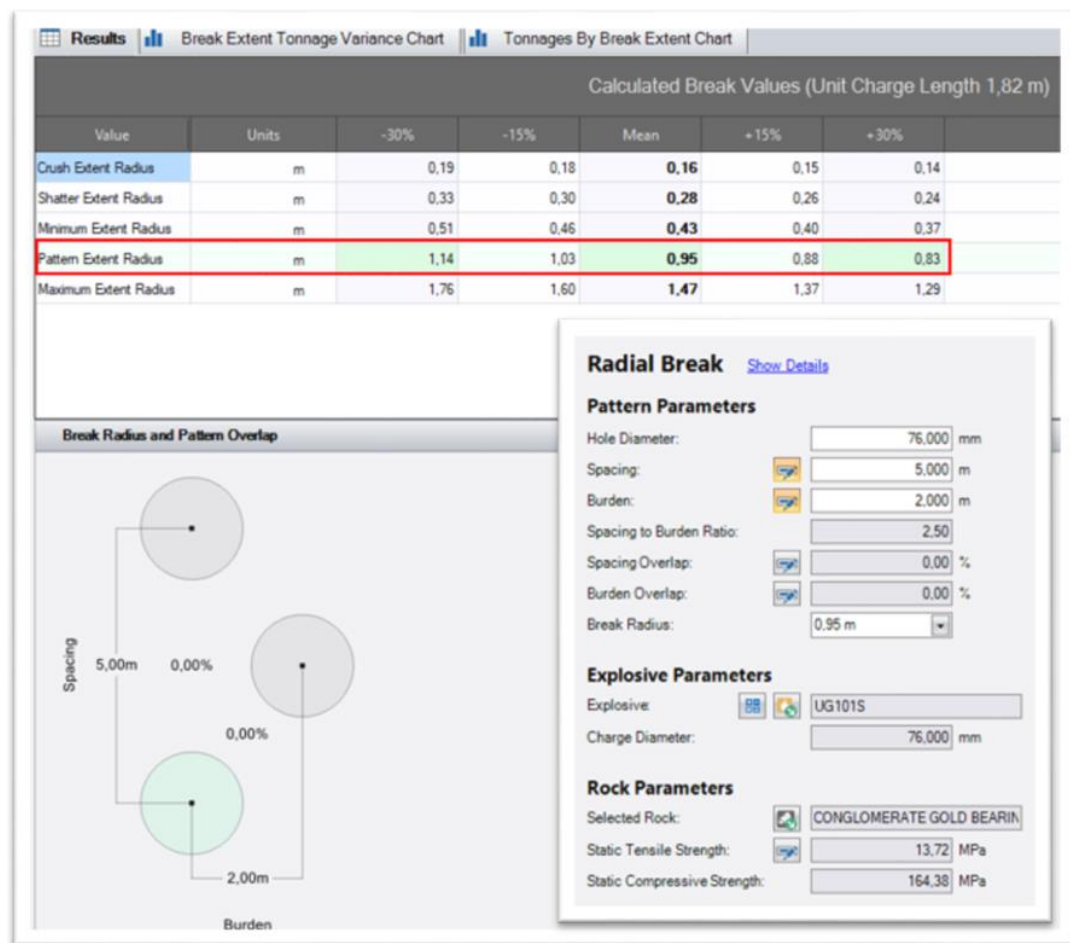


Figure 4.15: Pattern extent break radius

This implies that there may be interaction between cracks emanating from blastholes when the burden is 2m as alluded to in Figure 4.12. However, due to the variation in toe spacing, there will be no interaction between blastholes when the toe spacing is greater than 2m. As a result, a zone of no damage is created, the consequence of which is boulders and coarse fragmentation (Williams, 2019). This explains the boulders and coarse fragmentation observed during fragmentation distribution size analysis.

The radial break component of the model depicted in Figure 4.13 also shows the pattern overlap for various tensile strength values; -30%, -15%, 30% and 15%. Tensile strength is important because the rock fails in tension. According to Williams (2019), the pattern extend radius is highly dependent and sensitive to the rock's tensile strength. Hence, it is important to predict radial break for different strength rocks in case the tensile strength is not accurate. The model predicts that when the tensile strength of the rock is 15% and 30% weaker, the break radius will be 1.03m and 1.14m respectfully. This yields a break overlap of 0.3% and 2.5% respectfully. When the tensile strength of the rock is 15% and 30% stronger, there will be no overlap whatsoever. Based on the Brazilian tests conducted by SRK Consulting (2006) and Joughin *et al.*, (2006) matching and confirming those conducted by the author, there is improved confidence that the average UTS of 13.73MPa is accurate for South Deep Mine.

The second component of the AEGIS analyser is the stress distribution that explains the propagation and attenuation of the shock wave in the rock mass. This component of the model is highly dependent on the explosive's properties and the rock attenuation properties. The stress distribution for the ring design is illustrated in Figure 4.16.

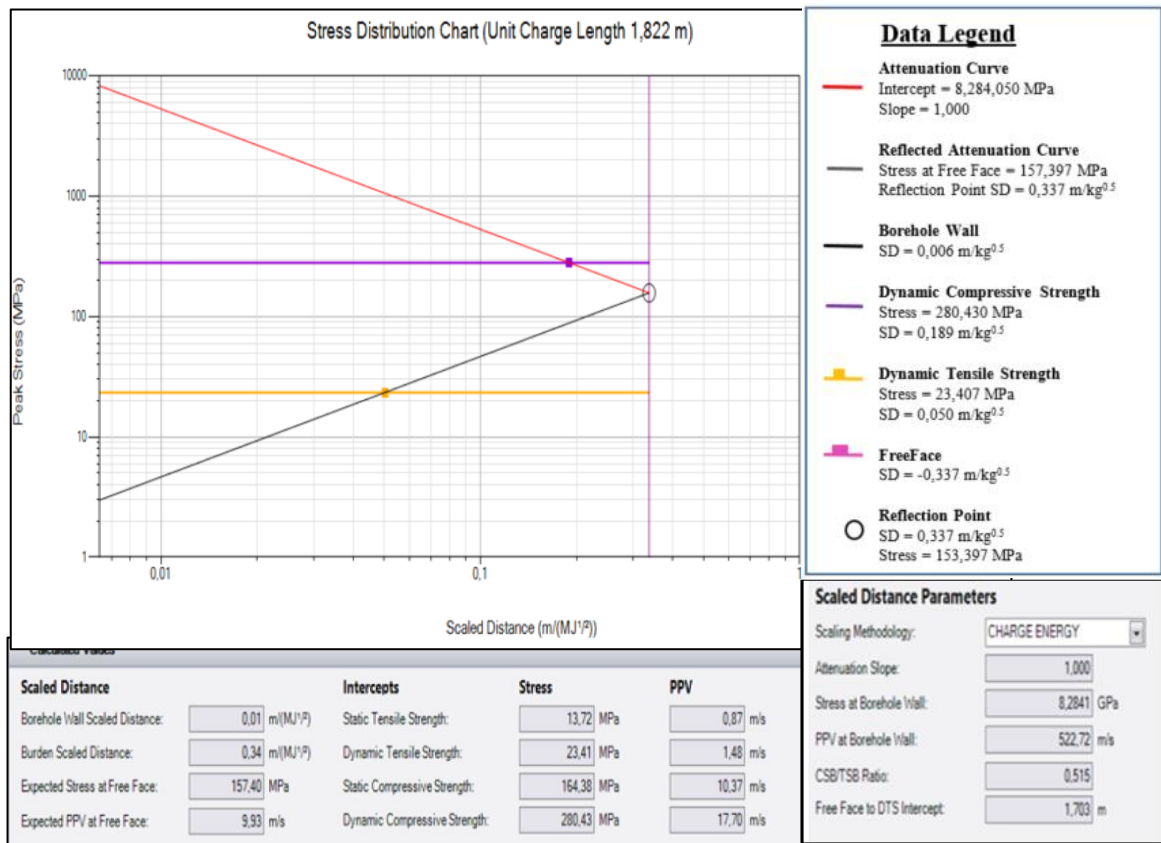


Figure 4.16: The stress distribution model

The model shows that after the explosive has detonated, the compressive shock wave radiates outward as its magnitude attenuates further from the blasthole. When the compressive shock wave hits the free face (air), the compressive shock wave is reflected towards the blasthole as a tensile wave because of different media (rock to air). According to Figure 4.16, the dynamic compressive shock wave hits the free face with a stress of magnitude 280.43 MPa, which is approximately twelve (12) times more than the dynamic tensile strength of the rock. According to Persson (1994), the enormous difference between the dynamic tensile and compressive stress results in multiple spalling and coarse fragmentation at the free face which is evidently the case at South Deep Mine.

Figure 4.17 shows the AEGIS drill and blast evaluation table used as a guide to determine the adequacy of a drill and blast pattern (Preston, 2019).

Statistics	Range	Value	Parameter Gauge	Result
Break Overlap Burden	2% - 12%	0,0%		✘
Break Overlap Spacing	2% - 12%	0,0%		✘
Reflection Point	23,42 MPa - 280,63 MPa	157,40 MPa		✔
Ratio of Radial Break t...	45% - 75%	47,45%		✔
Break Angle	80° - 90°	80,81°		✔
Powder Factor Mass	0.4 kg/tonne - 0.8 kg/tonne	0,59 kg/tonne		✔
Energy Factor Mass	1,52 MJ/tonne - 3,04 MJ/tonne	2,24 MJ/tonne		✔

Figure 4.17: Drill and blast pattern evaluation

According to the algorithms on which this table is based, parameters are in the correct range if they are within the green zone and out of range if they are in the red zone. Based on this table, the ring design pattern for the stopes is in the correct range for all parameters except for the burden and spacing break overlap. Thus, for optimisation, the

ring design must be altered until all the parameters are within the green range to yield acceptable fragmentation and minimise overbreak.

4.9 Proposed Drill and Blast Patterns

South Deep Mine is an already established mine and as a result, the optimisation is limited to a few controllable parameters. The explosive used at South Deep Mine is the UG101S sticky emulsion with a density of 1.12g/cm^3 . Currently, the burden for all drill patterns is kept at 2m with blastholes diameters of 76mm. The spacing varies for all rings and stopes as mentioned in the preceding section.

Following an earlier study conducted at the mine, Simba M6D drill rigs capable of drilling 89mm blasthole diameters were purchased and are currently on trial in some stopes. As a result, only the blasthole diameter, burden, toe spacing, and time delay are the controllable parameters for optimisation at this mine.

In order to determine the optimal ring design, the author conducted multiple simulations with the AEGIS analyser. The simulations were based on the spacing to burden ratio of between 1.0 to 1.5 and blasthole diameter of 76mm and 89mm as shown in Table 3.1.

The author found that a 2m by 2m ring pattern with blasthole diameters of 89mm for all blasts is a good starting point and has the potential to yield the required fragmentation size. All ring pattern simulations resulted in 0% overlap between the blastholes except with a toe spacing of 2m. Appendix 7.9 to Appendix 7.20 show the iterations and simulations for the spacing and blasthole diameter. The burden was kept at a constant 2m throughout the simulations.

Figure 4.18 and Figure 4.19 shows the pattern overlap and the evaluation table respectively for this ring design.

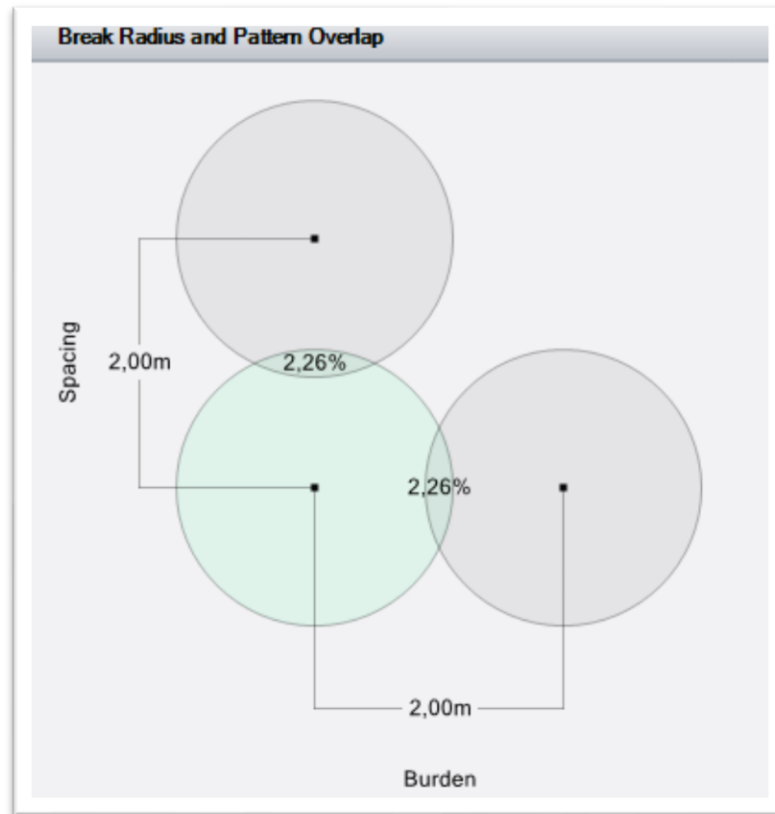


Figure 4.18: Suggested 2m by 2m drill pattern showing 2.6% overlap

Evaluation Table for – 100 4W Cut04 LHP 7EMB

Statistics	Range	Value	Parameter Gauge	Result
Break Overlap Burden	2% - 12%	2,3%		✓
Break Overlap Spacing	2% - 12%	2,3%		✓
Reflection Point	23,42 MPa - 280,63 MPa	187,62 MPa		✓
Ratio of Radial Break t...	45% - 75%	56,31%		✓
Break Angle	80° - 90°	82,38°		✓
Powder Factor Mass	0.4 kg/tonne - 0.8 kg/tonne	0,77 kg/tonne		✓
Energy Factor Mass	1,55 MJ/tonne - 3,09 MJ/tonne	3,00 MJ/tonne		✓

Figure 4.19: Evaluation table for the suggested drill and blast pattern

As illustrated in Figure 4.18 the ring pattern ensures a blasthole overlap and interaction of 2.26%. Figure 4.19 shows that 2.26% is within the acceptable range of between 2% and 12% for both burden and toe spacing and explosives. The powder factor ranges between 0.4kg/tonne and 0.8kg/tonne. Further, Figure 4.19 shows that the reflection point, ratio of radial break to burden distance, break angle, powder factor and energy factor are also within the acceptable range and has the potential to yield the required fragmentation results and minimise over break.

It is acceptable practice in many operations that when the blasthole diameter is increased (for example from 76mm to 89mm), the burden must also increase. The author however, advises against this approach for South Deep Mine. This is because the author is cognisant of the fact that drill rig operators are used to drilling a burden of 2m therefore did not want to modify many of their daily practices where possible.

The evaluation table in Appendix 7.23 shows that when the burden is increased to 3m, only the reflection point is within the acceptable range although the S/B ratio is one. Appendix 7.15 and Appendix 7.23 shows that when the burden is reduced to 1m with S/B ratio maintained at one for both 76mm and 89mm blastholes, the ring pattern will be over-designed.

To this effect, given the current available technology, the author, therefore proposes the 2m by 2m ring pattern with blasthole diameters of 89mm as a start. From there with continuous fragmentation distribution evaluation and analysis, the toe spacing must be increased, say by 0.5m until an acceptable fragmentation distribution size is achieved.

South Deep Mine recently introduced 4g electronic delay detonators that are accurate as discussed in Section 2.3.2. The mine currently uses 10ms intra-row delay timing and 30ms inter-row delay timing. Given the strength of the rock and the proposed drill pattern, the author suggests that the mine maintain these timings as they are within the limits as determined in accordance with Langerfors and Kihlstrom (1963) and Grant's (1990) findings.

Table 4.4 provides a summary of the current ring design and proposed ring design.

Table 4.4: Summary of current and proposed ring design

Parameter	Old design	Proposed design
Blasthole diameter	76mm	89mm
Explosive	“Sticky” Emulsion UG101S	“Sticky” Emulsion UG101S
Explosive density	1.12g/cm ³	1.12g/cm ³
Burden	2m	2m
Toe Spacing	0,5 – 7,5m	2m
Intra-row timing	30ms	30ms
Inter-row timing	10ms	10ms

4.10 Chapter Summary

South Deep Mine recently introduced the QA/QC department under the Drill and Blast Department to ensure compliance with the execution of drill and blast patterns. There has been some improvement since the introduction of the department but there is room for improvement. Achieving the correct fragmentation size while minimising overbreak is imperative for a low-grade high-volume deep level gold mine where costs are higher.

Multiple studies conducted have shown that optimising fragmentation upstream has the potential to improve efficiency downstream and reduce crushing costs. The Split-desktop overall fragmentation size analysis revealed that although the mean fragmentation size is less than the grizzly size, the uniformity constant is 0.8 implying a non-uniform fragmentation size distribution that consists of both fine and coarse fragmentation. This agreed with underground observations by the author. The software shows that F₂₀ is 24.64mm while the top size is 1 288.40mm.

The rock at South Deep Mine was found to be high strength following laboratory tests and the application of rock mass classification systems. Due to the influence and reduction of the rock strength in the secondary stopes by the stresses and fractures originating from blasting of primary stopes, the author proposes that a medium rock strength class should be considered for blast designs. This will account for the free faces formed at the fractures created by shock waves as a result of blasting in primary stopes.

The toe spacing between blastholes varies from about 0.5m to 7.5m. This was found to be the main source of both coarse and fine fragmentation. In areas where the spacing is

say less than 2m, fine fragmentation occurs and where toe spacing is greater coarse fragmentation ensues because of the greater zone of zero interaction between the blastholes. In addition, it has been found that the compressive shock wave hits the free face with a dynamic compressive stress of magnitude 280.43MPa, which is approximately twelve (12) fold more than the dynamic tensile strength of the rock which results in spalling and coarse fragmentation.

After multiple iterations between spacing, burden and blasthole diameter for drill and blast pattern optimisation to yield the required fragmentation, a drill pattern with 89mm blasthole diameter, a spacing and burden of 2m is proposed as a starting point for continuous optimisation of the blasting operation. The blasthole diameter of 89mm has the added benefit of reducing deviations.

5. CONCLUSIONS AND RECOMMENDATIONS

5.1 Chapter Overview

The purpose of this section is to provide a summary of the entire report. It details if whether the aim of this study was achieved and what the results are. Recommendations are also provided for future studies.

5.2 Conclusions

The optimisation of fragmentation is fundamental for an efficient ore flow through the mine system. More especially for a deep level underground mine where operational costs are high, gold grades are comparatively low and there is a dire need for increased throughput to ensure the mine's profitability.

The literature discussed has shown that in order to obtain the required fragmentation distribution size, an in depth understanding of the controllable and uncontrollable parameters affecting fragmentation and their interaction with explosives is essential. The uncontrollable parameters being rock mass strength and structural properties and the controlled parameters are the explosives and the blast pattern designs.

For an efficient ore flow system at South Deep Mine, the F_{80} (80% passing) must be 300mm or less which is the size of the grizzly. In this study, an analysis of the fragmentation distribution size using the Split-desktop software revealed that although the mean fragmentation size of 124.35mm and F_{80} of 287.48mm can pass through the 300mm grizzly, there is great variation between coarse and fine fragmentation size achieved in the longhole stopes. This is indicated by an overall uniformity index of 0.80 and the great variation between the F_{20} (20% passing) and the top size, which are 24.64mm and 1 288.40mm respectively.

The strength and structural properties of the rock mass at South Deep Mine were investigated and laboratory test work was done in order to do a back analysis of the drill and blast designs to optimise drill and blast patterns for future blast operations. The results from the photographic mapping study done by SRK Consulting (2006) and laboratory test work by the author showed that the block size is massive. This in turn implies that the blast designs will have more influence on the fragmentation size than the geology. With a 263.34MPa UCS, 13.72MPa UTS, 77.78GPa E and 0.16 μ

respectively, the strength of the rock mass at South Deep Mine is generally high. This was determined by using all the available rock mass classification systems (Bieniewski, 1989). However, due to the influence of blasting from primary stopes, additional fractures in secondary stopes are created reducing the block sizes and acting as free face for the compressive shock wave. As a result, the rock strength was input as “medium strength” to consider the fractures.

The drill and blast patterns at the mine consist of 76mm blastholes diameters, a burden of 2m and a toe spacing that vary from 0.5m to about 7.5m. The AEGIS analyser was used to analyse the blast designs and gain insights into what causes fragmentation distribution size with low uniformity index. It was found that there is no overlap for 2m toe spacing and the condition worsens as the toe spacing increases to 5m and 7.5m. As a result, zones of no damage are created between toe spacing resulting in coarse fragmentation. It was also found that due to the magnitude at which the compressive shock wave hits the free face being 12-fold greater than the tensile strength, multiple rock spalling occurs resulting in coarse fragmentation and boulders. In rings where the toe spacing is smaller than 2m, fine fragmentation will result. This explains the low uniformity index as observed in the stopes.

To curb this, several drill and blast pattern simulations were conducted using the AEGIS analyser. The author settled on a drill and blast pattern, which uses 89mm blasthole diameters, 2m burden and incremental toe spacing starting at 2m until acceptable results are achieved.

5.3 Recommendations

It is recommended that South Deep Mine should maintain a constant toe spacing for all rings and further, the mine should trial the proposed drill and blast pattern. This should be coupled with regular evaluations and analysis of the fragmentation size distribution or if any improvements in terms of productivity and/or profitability are realised to ensure a continuous optimisation of the drill and blast patterns and consequently fragmentation. This means that after every blast, muckpile images should be captured in the stopes for analysis to assist with identifying deviations. In addition, a fragmentation analysis system must be installed on underground belts and at the plant to get a better understanding of the size fragmentation distribution size achieved from the stopes to the SAG mill.

This should however not be limited to drill patterns but also charging plans which should be adhered to all the time to avoid over or under charging blastholes. The QA/QC team must regularly enforce compliance especially during drilling and charging of the blastholes.

The author only analysed fragmentation in the production stopes and nothing was done for the rock tipped at the orepass which is a mixture of rock fragmented in both the production stopes and development. Thus, it is recommended that the fragmentation distribution size from the development tunnels also be analysed in order to get a better understanding of the fragmentation size distribution of the entire mine (development and in production stopes).

6. REFERENCES

Aber, J.S., Marzloff, I and Ries, J.B. 2010. Small-Format Aerial Photography Principles, Techniques and Geoscience Applications. Amsterdam: Elsevier. [Online]. Available at: <https://doi.org/10.1016/B978-0-444-53260-2.10020-1> (Accessed:15.04.2019)

AEGIS drill and blast underground software. 2019.

AEL World, 2020. Underground bulk emulsions. [Online]. Available at: <https://www.aelworld.com/application/files/7415/4442/8864/ael-intelligent-blasting-differentiated-products-underground-bulk-emulsions.pdf> [Accessed 06 February 2020]

Adebayo, B. and Umeh, E.C. 2007. Influence of some rock properties on blasting performance – A case study. *Journal of Engineering and Applied Sciences*, 2(1); 41 -44.

Afum, B.O. and Temeng, V.A. 2015. Reducing Drill and Blast Cost through Blast Optimisation - A Case Study. *Ghana Mining Journal*, 15(2); 50–57.

AngloAmerican, Atlas Copco, BHP Billiton, Codelco, De Beers, LKAB, Newcrest, Orica, Sandvik, Xstrata. 2012. Mass Mining Technology Project II. Understanding the fundamentals of block, panel and sublevel caving: Sublevel caving blast dynamics. Presentation. [Online]. Available at: <https://www.slideserve.com/banyan/sublevel-caving-blast-dynamics> (Accessed 24.08.2019)

Atlas Copco. 2014. Underground Mining – A global review of methods and practices. Sweden. 94

Bieniawski, Z.T., 1974. Estimating the strength of rock materials. *International Journal of Rock Mechanics and Mining Sciences & Geomechanics Abstracts* 11, A160. [https://doi.org/10.1016/0148-9062\(74\)91782-3](https://doi.org/10.1016/0148-9062(74)91782-3)

Bieniawski, Z.T., 1989. *Engineering rock mass classifications: A complete manual for engineers and geologists in mining, civil and petroleum*. New York: Wiley

Bobo, T. 2009. What's new with the digital image analysis software split-desktop? *Mining and Blasting*, September 2009 [Online]. Available at:

https://miningandblasting.files.wordpress.com/2009/09/whats_new_with_split-desktop.pdf
(Accessed: 19.04.2019)

Boshof, J. 2016. Extending the economic life of the Witwatersrand ore bodies. The orebody dictates. Presentation. [Online]. Available at:
<https://www.harmony.co.za/invest/presentations/2016/send/107-2016/2114-the-orebody-dictates>
(Accessed 24.08.2019)

Cardu, M., Giraudi, A. and Oreste, P. 2013. A review of the benefits of electronic detonators. *Rem Revista Escola de Minas*, 66(3); 375–382. [Online]. DOI: <https://doi.org/10.1590/S0370-44672013000300016>

Cebrian, B., Laredo, R and Chipana, J. 2017. Ring blasting mine to mill optimization. *International Society of Explosives Engineers*.

Chatziangelou, M and Christaras, B. 2015. A geological classification of rock mass quality and blast ability for intermediate spaced formations. *International Journal of Engineering and Innovative Technology*, 4(9): 52 – 61.

Chung, S.H. 1994. Blast Modelling With Sabrex 3.5 And its Applications To Improve Mine Productivity. *Fifth Annual High-Tech Seminar - State-of-the-Art Blasting Technology Instrumentation and Explosives Applications – volume 2*. Toronto. International Society of Explosives Engineers.

CPM Group. 2012. Overview of Mining Costs. Presentation. [Online]. Available at:
<http://www.goldconvention.in/iigc2012/presentation/CPM%20Group%20Overview%20of%20Mining%20Costs%20RS.pdf> (Accessed: 16.07.2019)

Cunningham, C.V.B. 2005. The Kuz-Ram fragmentation model – 20 years on. Brighton Conference Proceedings. Brighton; 2005 European Federation of Explosives Engineers.

Curwin, J and Slater, R. 2002. Quantitative methods for business decisions. 5th ed. Tunbridge Wells: Gray Publishing

Dey, K and Sen, P. 2003. Concept of Blastibility – An update. *The Indian Mining and Engineering Journal*. 42(8 and 9). 24 – 31.

Dyno Nobel. 2010. Blasting and Explosives quick reference guide 2010. [Online]. Available at: https://www.leg.state.mn.us/docs/2015/other/150681/PFEISref_1/Dyno%20Nobel%202010.pdf (Accessed: 06.08.2019)

Franklin, J., Kemeny, J. and Girdner, K. 1996. Evolution of measuring systems: A review. *Fragblast-5 Workshop on Measurement of Blast Fragmentation*. Montreal, Canada.

Gold Fields. 2018. South Africa Region | Operations | Gold Fields. [Online]. Available at: <https://www.goldfields.com/south-africa-region.php> (Accessed 06.24.18).

Gold Fields. nd. South Deep – Longhole Stopping Standards. Unpublished

Gold Fields.2017a. 2017 Mineral Reserves and Resources Report. [Online]. Available at: <https://www.goldfields.com/reports/annual-report-2017/minerals/south-africa-overview.php>. (Accessed 07.12.2018)

Grant, John R. “Initiation Systems – What does the Future Hold?” Third International Symposium on Rock Fragmentation by Blasting. The Australasian Institute of Mining and Metallurgy. Brisbane, Queensland. 1990

Holland, N., Muller, N. and South Deep team. 2015. South Deep: Finding its Feet, South deep Site Visit. Presentation. Available at: <http://www.goldfields.com/pdf/investors/presentation/2015/south-deep-site-visit/presentation.pdf> (Accessed date: 06.12.2018)

Hoseinie, Seyed Hadi & Pourrahimian, Yashar & Fardin, Nader & Aghababaei, Hamid. (2006). Determination of blasting index (BI) to predict the fragmentation amount and blasting efficiency of Sungun copper mine using Rock Mass index (RMi). *8th International Conference on Rock Fragmentation by Blasting (Fragblast-8)*, Santiago, Chili

International Society of Explosives Engineers. 2011. *Blaster's Handbook*. 18th Edition. Ohio. International Society of Explosives Engineers. ISBN 9781892396198

International Society for Rock Mechanics, 2007. The Complete ISRM Suggested Methods for Rock Characterization, Testing and Monitoring: 1974-2006. Ankara, Turkey.

iRing INC. 2018. iRing INC Knowledgebase version 1.1. [Online]. Available at: [http://www.iring.ca/ Knowledgebase/module_5_4.html](http://www.iring.ca/Knowledgebase/module_5_4.html) (Accessed 13.03.2019)

Jager, A. J and Ryder, J.A. 1999. A handbook on Rock Engineering Practice for Tabular hard rock mines. Johannesburg. The safety in Mines Research Advisory Committee (SIMRAC)

Jimeno, C.L., Jimeno, E.L. and Carcedo, F.J.A. 1995. Drilling and blasting of rocks. Broomefield; A.A Balkema Publishers.

Jorgenson, G.K and Chung, S.H. 1987. Blast Simulation surface and underground with the SABREX model. First Annual High-Tech seminar. State of the Art Blasting Technology instrumentation and Applications CIM Bulletin. 80 (904)

Joughin, W.C., Armstrong, R., Petho, S.Z., SRK Consulting and South Deep. 2006. Assessment of the stability of Longhole Stope backs at South Deep. The 3rd Southern African rock engineering symposium. *The South African Institute of Mining and Metallurgy*.

Kanchibotla, S.S., Valery, W and Morell, S.1999. Modelling fines in blast fragmentation and impact on crushing and grinding. Julius Kruttschnitt Mineral Research Centre, The University of Queensland. Research gate

Kansake, B.A., Temeng, V.A., and Afum, V.A. 2016. Comparative analysis of rock fragmentation models: A case study. Researchgate. [Online]. DOI: 10.13140/RG.2.2.10655.82081 (Accessed: 19.04.2019)

Kirby, I.J., Harries, G.H and Tidman, J.P. 1987. ICI's Computer Blasting Model SABREX

Kleine, T. H. 1991. A mathematical model of rock breakage by blasting. 7th International Society for Rock Mechanics and Rock Engineering Congress. 16 – 20 September 1991. Aachen; International Society for Rock Mechanics and Rock Engineering.

Langerfors, U and Kihlstrom, B.1963. *The modern technique of rock blasting*. Detroit; Wiley

Laredo and Chipana, 2017 – Ring blasting mine to mill optimisation, International society of explosives engineers

- Lily, P.A. 1986. An empirical method of assessing rock mass Blastibility. Large open pit mining conference. October. The AusIMM/IE Aust Newman Combined Group
- Little, T.N. 2018. Blasting geology. Blasting Geomechanics Pty Ltd
- Lownds, C.M. 1978. Chemistry of explosives. In: Drilling, rock breaking and blasting techniques, vacation school. *The South African Institute of Mining and Metallurgy (SAIMM)*.
- Maerz, N. H., Germain, P., 1996. Block size determination around underground openings using simulations. Proceedings of the FRAGBLAST 5 Workshop on Measurement of Blast Fragmentation, Montreal, Quebec, Canada, 23-24 Aug., 1996, pp. 215-223.
- Marton, A and Crookes, R., 2000. A case study in optimising fragmentation. The AusIMM Proceedings. *The Australasian Institute of Mining and Metallurgy*.
- McMahon, D. 2018. Unit Manager: Drill and Blast at South Deep Mine. [Personal Communication]. July 2018
- Mogoai, K. 2019. Plant Metallurgist at South Deep Mine. [Personal Communication]. 27 May 2019.
- Musingwini, C. 2014. Introduction of specialization in Mine Planning and Optimisation within the Master's degree (MSc) programme at the University of Witwatersrand. *Proceedings of the 6th International Platinum Conference, 'Platinum – Metal for the Future'*, Sun City, South Africa, 20-22 October 2014. Symposium Series S81. Southern African institute of Mining and Metallurgy, Johannesburg. pp. 23-27.
- Myers, T.R., Lundquist, R and Konya, C. 1990. Computer aided design of ring blasts. International Society of Explosives Engineers. 1990 General Proceedings. 43 - 52
- Neingo, P.N., & Tholana, T. (2016). Trends in productivity in the South African gold mining industry. *Journal of the Southern African Institute of Mining and Metallurgy*, 116(3), 283-290. <https://dx.doi.org/10.17159/2411-9717/2016/v116n3a10>
- Ninepence, J. B., Appianing, E.J., Kansake, B.A., and Amoako, R. 2016. Optimisation of drill and blast parameters using empirical fragmentation modelling, 4th UMat Biennial International Mining and Mineral Conference.

- Noy, M. 1997. 2D versus 3D fragmentation analysis: preliminary findings. *Proceedings 13th Annual symposium on Explosives and Blasting research*. 2 – 5 February. Las Vegas. 181 - 190
- Nur Lyana, K., Hareyani, Z., Kamar Shah, A., Mohd and Hazizan, M. 2016. Effect of Geological Condition on Degree of Fragmentation in a Simpang Pulai Marble Quarry. *Procedia Chemistry*. 19: 694-701. [Online]. DOI: <https://doi.org/10.1016/j.proche.2016.03.072> (Accessed 06.12.2018)
- Oldfield, N., Dight, P., Cameron, A and Pal, A. 2009. Evaluation of the Hybrid Stress Blasting Model (HSBM). *CEED Seminar Proceedings*.
- Onederra, I. 2004. Breakage and fragmentation modelling for underground production blasting applications. IRR Drilling and Blasting Conference, Perth.
- Onederra, I. 2005. A fragmentation model for underground production blasting. Doctor of Philosophy degree. The University of Queensland.
- Onederra, I. and Chitombo, G. 2007. Design methodology for underground ring blasting. *Mining Technology* 116(4), 180–195. DOI: <https://doi.org/10.1179/174328607X282244> (Accessed 06.12.2018)
- Ouchterlony, F. 2003. Influence of blasting on the size distribution and properties of muckpile fragments, a state-of-the-art review. MinFo Project P2000-10: Energy optimisation in comminution. [Online] <https://www.diva-portal.org/smash/get/diva2:995258/FULLTEXT01.pdf> (10.04.2019)
- Ouchterlony, F. 2005. The Swebrec function: linking fragmentation by blasting and crushing. *Mining Technology (Trans. Inst.Min. Metall.A)*, 114: 29 – 44. DOI: 10.1179/037178405X44539 [Accessed: 08.04.2019]
- Ouchterlony, F., Sanchidrian, J.A, and Moser, P. 2017. Percentile fragment size distributions predictions for blasted rock and the fragmentation – Energy fan. *Rock Mech Rock Eng* (2017) 50:751–779. [Online]. DOI 10.1007/s00603-016-1094-x [Accessed: 08.04.2019]
- Persson, P., Holmberg, R and Lee, J. 1994. *Rock Blasting and explosives Engineering*. New York: CRC Press

Preston C, J. 2019. Transforming underground blasting operations into primary crushing operations. iRing INC

Preston, C.J and Williams, T. 2019. Advanced fragmentation prediction to eliminate underground crushers. iRing INC

Prout, B.2019. Retired drill and blast engineer and senior lecturer at University of the Witwatersrand. [Personal Communication]. 04 October 2019.

Rai, P., Schunnesson, H., Lindqvist, P.A. and Kumar, U. 2016. Measurement-while-drilling technique and its scope in design and prediction of rock blasting. *International Journal of Mining Science and Technology*. 26, 711–719. DOI: <https://doi.org/10.1016/j.ijmst.2016.05.025> (Accessed 06.12.2018)

Rossmannith, H.P., Daehnke, A., Knasmillner, N., Kouzniak, M., Ohtsu, M and Uenishi, K. 1997. Fracture mechanics applications to drilling and blasting. *Fatigue and fracture of engineering materials and structures Ltd*. 20(11). 1617-1636.

Roy, M., Paswan, R., Kumar, S., Jha, R. and Singh, P. 2016. Rock fragmentation by blasting - A review. *Journal of Mines, Metals and Fuels*. 64(9), 424–431.

Sanchidrian, J.A. 2018. Fragmentation by Blasting models – A review. Detonation and Rock Fragmentation short course. Fragblast 12. Unpublished.

Sasol Nitro. 2014. Explosives Engineers surface field guide.

Schmidt R.A., Rossmannith H.P. (1983) Basics of Rock Fracture Mechanics. In: Rossmannith H.P. (eds) *Rock Fracture Mechanics. International Centre for Mechanical Sciences (Courses and Lectures)*, vol 275. Springer, Vienna DOI https://doi.org/10.1007/978-3-7091-2750-6_1

School of Mining Engineering. 2018. Module 10: Fragmentation due to blasting [Excavation Engineering notes]. University of the Witwatersrand. Unpublished

Scott, A. and Onederra, I., 2015. Characterising Rock Mass Properties for Fragmentation Modelling. 11th International Symposium on rock fragmentation by blasting. Sydney. *The Australasian Institute of Mining and Metallurgy*.

Sellers, E., Furtney, J., Onederra, F and Chitombo, G. 2011. Improved understanding of explosive–rock interactions using the hybrid stress-blasting model. *The South African institute of Mining and Metallurgy*, 112(8); 721 – 728.

Sereshki, F., Hoseini, S.M and Ataei, M. 2016. Blast fragmentation analysis using image processing. *International Journal of Mining and Geo-Engineering*. 50 (2); 211-218

Sharma, D., Pandey, A., Srivastava, A. and Das, A. 1990. A Performance Prediction Model for Optimized Drilling and Blasting Costs. Fragblast'90. 26-31 August. Brisbane. *The Australasian Institute of Mining and Metallurgy*.

Sharma, K.S. and Rai, P. 2017. Establishment of blasting design parameters influencing mean fragment size using state-of-art statistical tools and techniques. *Measurement*, 96; 34-51.

Shelswell, K. and Labrecque, P. 2014. Discrete Simulations Quantifying the Effects of Material Handling Conveyors in Series or Parallel Oreflow Streams. *2014 SME Annual Meeting & Exhibit (SME 2014)*. 23-26 February. Salt Lake City, Utah, USA. Available at: http://www.labt.ca/wp-content/uploads/2015/01/2014_SME_Salt_Lake_City_ver03.pdf (Accessed 06.12.2018)

Siegesmund, S. and Dürrast, H. 2011. Physical and mechanical properties of rocks. Heidelberg; Springer. https://doi.org/10.1007/978-3-642-14475-2_3

Singh, P.K., Roy, M.P., Paswan, R.K., Sarim, M.D., Kumar, S and Jha, R.R. 2016. Rock Fragmentation control in opencast blasting. *Journal of Rock Mechanics and Geotechnical Engineering*. 8, 225 - 237

Split Engineering. 2014. Split-Net Service instruction Manual. [Online]. Available at: <https://www.spliteng.com/dloads/> (Accessed: 19.04.2019)

Split-Net. 2014. Service Instruction manual. [Online]. Available at: <https://www.spliteng.com/downloads/Split-Net%20Manual.pdf> Accessed (26.04.2019)

SRK Consulting. 2006. Evaluation of the critical mining span based on the hydraulic radius concept and evaluation of the mining sequence for 95 1W longhole stopes. Unpublished

Strelec, S., Gazdek, M., Mesec, J., 2011. Blasting Design for Obtaining Desired Fragmentation. *Tehniki vjesnik*.18 (1). 79–86.

Tamrock Corporation. 1997. *Underground drilling and loading handbook*. Tampere.

U. Langefors and B. Kihlstrom. 1963. The modern technique of rock blasting. Stockholm: Jone Wiley & Sons, Inc.

Valery, W., Morell, S., Kojovic, T, and Kanchibotla, S.S. 2001. Modelling and Simulation techniques applied for optimization of mine to mill operations and case studies. *Research gate*.

[Online]. Available at:

https://www.researchgate.net/publication/43463182_Modelling_and_simulation_techniques_applied_for_optimisation_of_mine_to_mill_operations_and_case_studies [Accessed: 08.04.2019]

Van der Westhuizen, A and Powell, M., 2006. South deep Milling circuit testwork, model fitting, and simulations. Internal South Deep Mine Report. Unpublished.

Vesilind, P, A. 1980. The Rosin-Rammler Particle size distribution. *Resource Recovery and Conservation*. Elsevier Scientific publishing company, Amsterdam. (275-277)

Villasescusa, E. 2003. Global extraction sequences in sublevel stoping. *MPES 2003 conference*. April 2003. Kalgoorlie.

Williams, T. Vice President Software Development at iRing INC. [Personal Communication]. 1 June – 19 August 2019

Wimmer, M., Nordqvist, A., Righetti, E., Petropoulos, N and Thurley, M.J. 2015. Analysis of rock fragmentation and its effect on gravity flow at the Kiruna Sublevel Caving Mine. *11th International Symposium on rock fragmentation by blasting*. 24 -25 August 2015. Sydney.

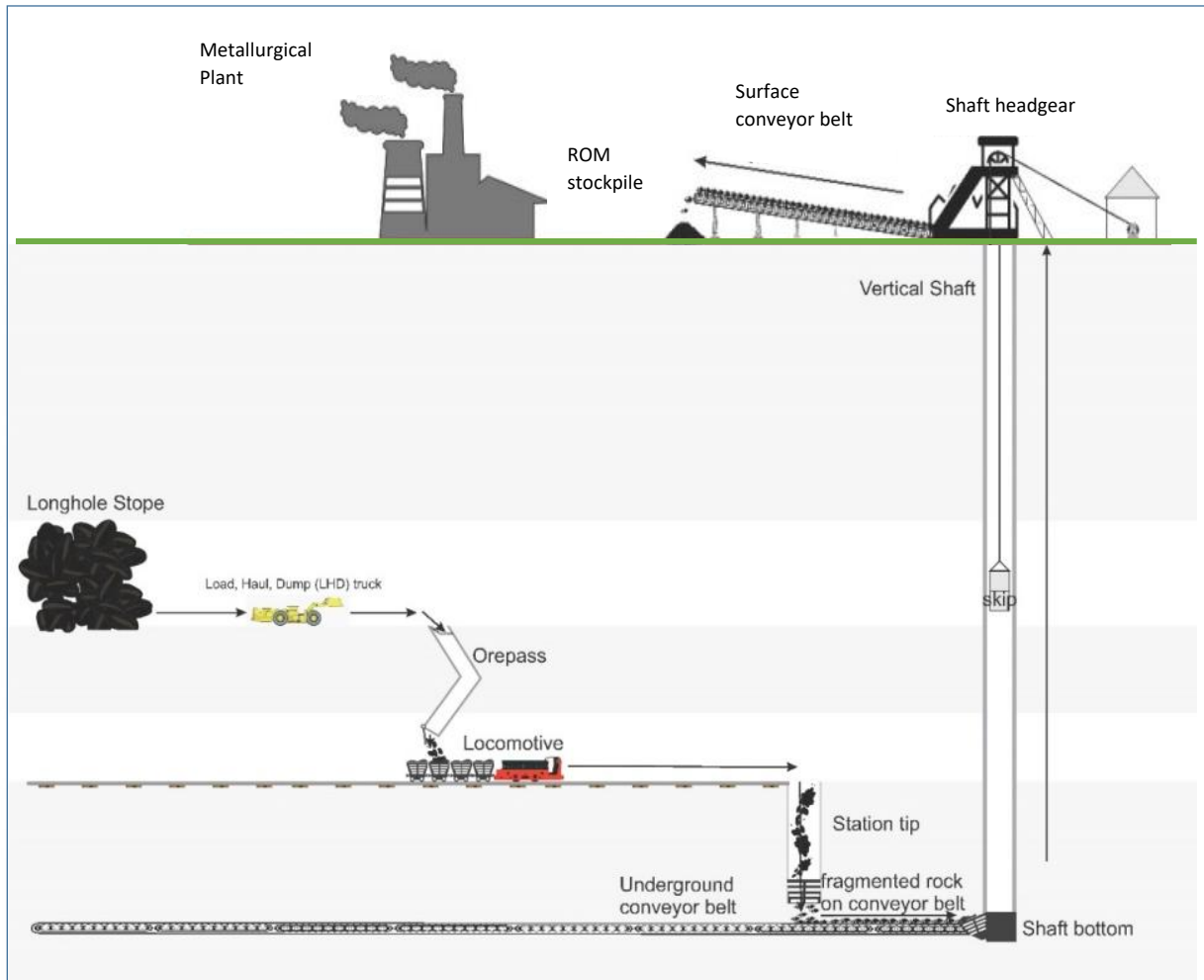
Wipware. 2013. Sampling and analysis guide – version 1. [Online]. Available at:

<http://wipware.com/wp-content/uploads/2018/01/Sampling-and-Analysis-Guide.pdf> Accessed (Accessed: 23.04.2019)

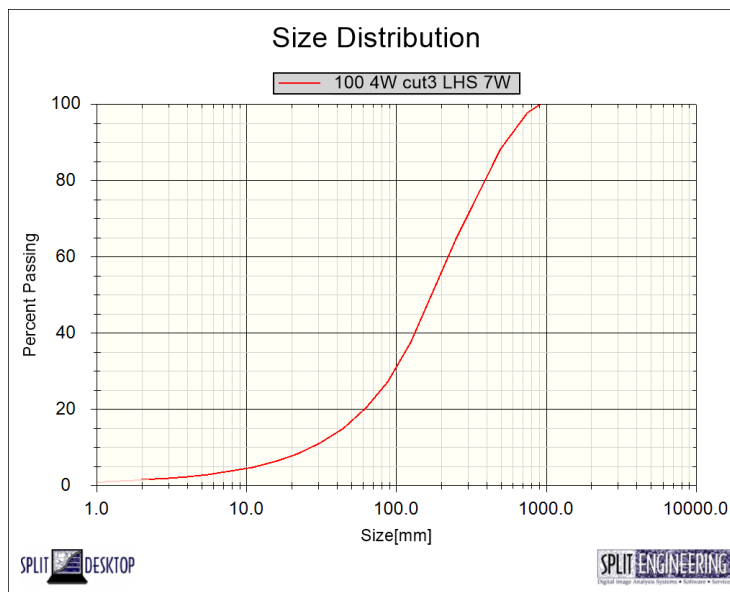
Zolezzi, N. 1961. Breaking ground with explosives: a review of the theory and practice and an experimental study of blasting parameters based on single-hole blasts. *MSc thesis*. University of the Witwatersrand.

7. APPENDICES

APPENDIX 7.1: A SCHEMATIC FLOW OF BROKEN ROCK FROM THE STOPE TO THE STOCKPILE AT THE METALLURGICAL PLANT

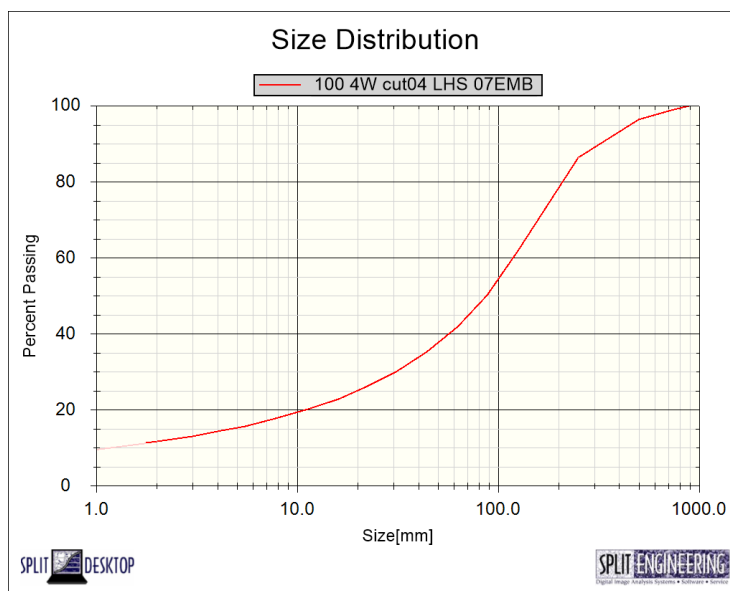


APPENDIX 7.2: FRAGMENTATION SIZE DISTRIBUTION FOR LONGHOLE STOPE 100 4W CUT3 LHS 7W (SPLIT-DESKTOP, 2019)



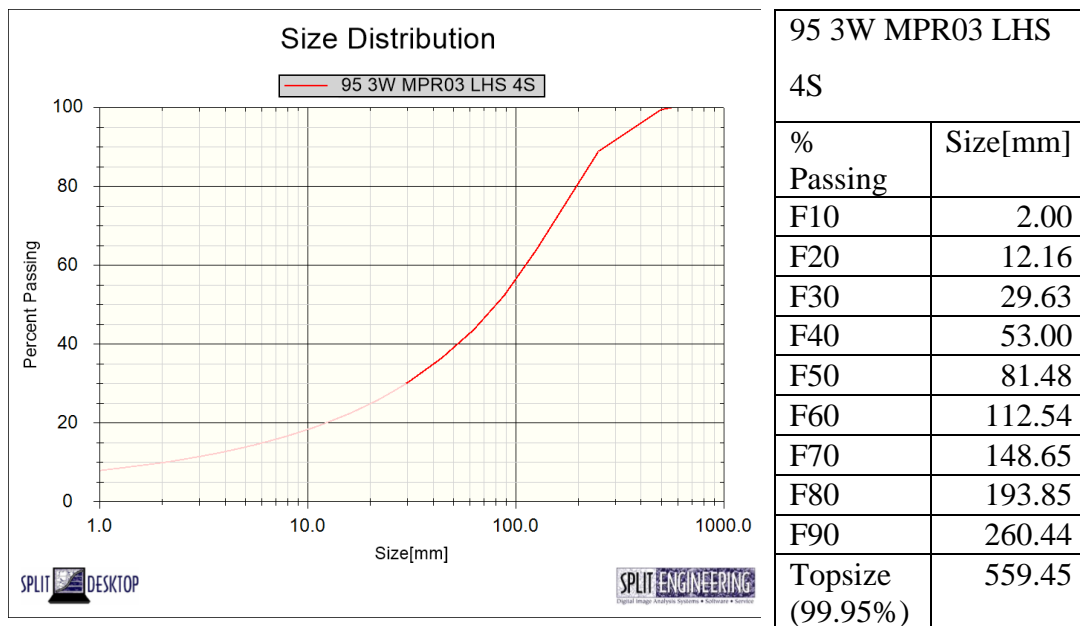
100 4W cut3 LHS 7W	
% Passing	Size[mm]
F10	27.56
F20	61.69
F30	98.11
F40	134.24
F50	174.06
F60	222.74
F70	286.97
F80	381.83
F90	533.60
Topsize (99.95%)	909.44

APPENDIX 7.3: FRAGMENTATION SIZE DISTRIBUTION FOR LONGHOLE STOPE 100 4W CUT4 LHS 07EMB (SPLIT-DESKTOP, 2019)

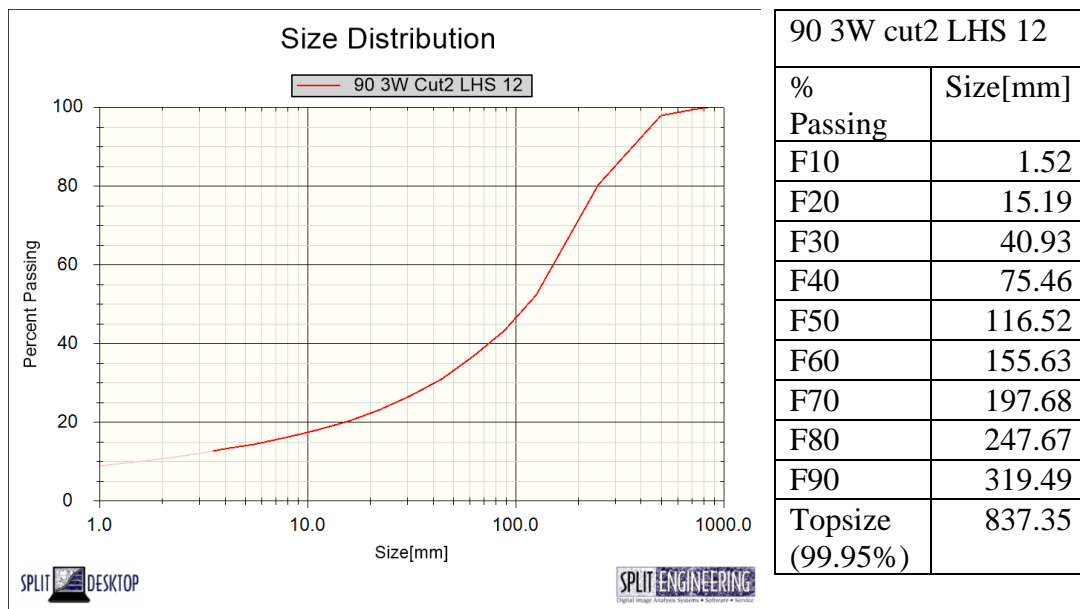


100 4W cut4 LHS 07EMB	
% Passing	Size[mm]
F10	1.15
F20	11.12
F30	30.91
F40	57.63
F50	87.68
F60	118.94
F70	154.51
F80	202.33
F90	297.05
Topsize (99.95%)	887.40

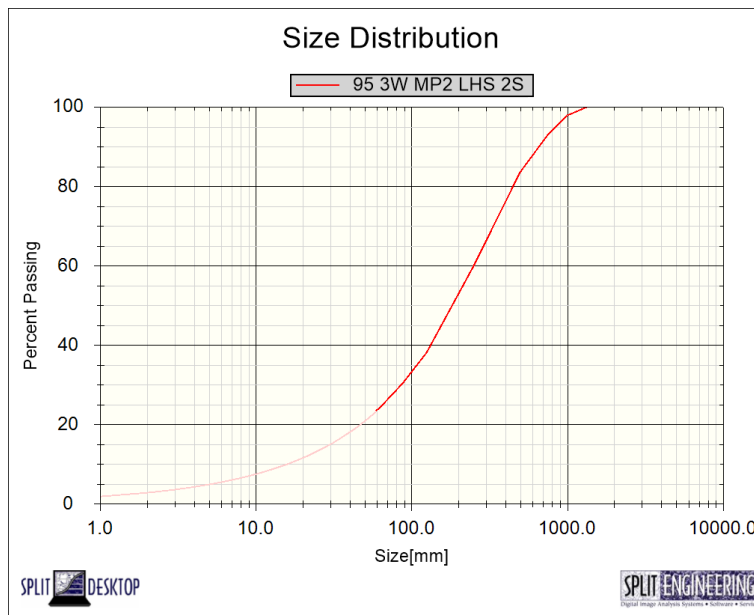
APPENDIX 7.4: FRAGMENTATION SIZE DISTRIBUTION FOR LONGHOLE STOPE 95 3W MPR03 LHS 4S (SPLIT-DESKTOP, 2019)



APPENDIX 7.5: FRAGMENTATION SIZE DISTRIBUTION FOR LONGHOLE STOPE 90 3W CUT2 LHS 12 (SPLIT-DESKTOP, 2019)



APPENDIX 7.6: FRAGMENTATION SIZE DISTRIBUTION FOR LONGHOLE STOPE
 95 3W MP2 LHS 2S (SPLIT-DESKTOP, 2019)



95 3W MP2 LHS 2S	
% Passing	Size[mm]
F10	15.55
F20	46.47
F30	86.69
F40	134.12
F50	187.21
F60	249.63
F70	327.88
F80	442.67
F90	644.16
Topsize (99.95%)	1 326.35

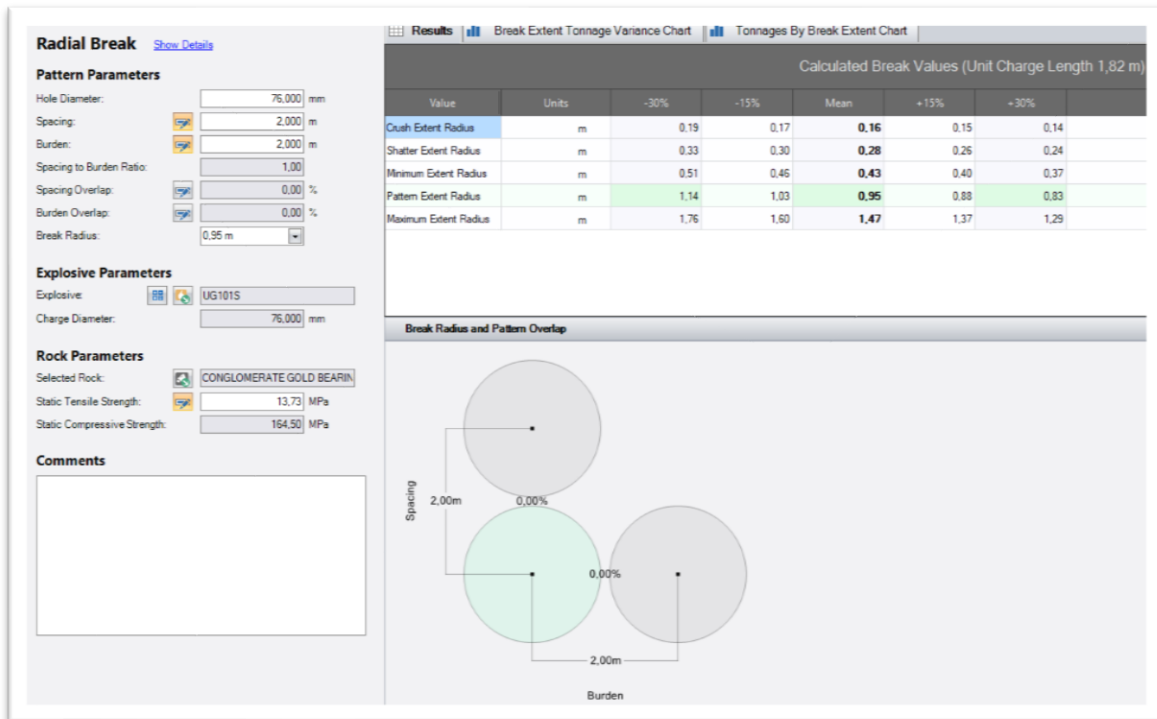
APPENDIX 7.7: UNIAXIAL COMPRESSIVE TEST RESULTS FOR DETERMINING UCS, YOUNG'S MODULUS AND POISSON'S RATIO

Test :		Uniaxial Compressive Strength Test						
Date:		25 June 2019						
Test Location:		Gold Fields Laboratory, Wits University						
Rock Description:		Conglomerate medium grains						
Laboratory Temperature:		Room Temperature approx. 23°C						
Moisture Content:		Dry						
Machine Certificate:		UHQ-57892						
Serial Number:		76/51						
Loading Rate:		1kN/s						
Specimen No.	Length (mm)	Diameter (mm)	Mass (g)	Density (kg/m ³)	Load at Failure (kN)	UCS (MPa)	Young's Modulus, E (GPa)	Poisson's ratio (γ)
UCM 1	103.20	42.00	391.30	2 736.79	336.60	242.96	88.73	0.13
UCM 2	103.20	42.00	395.30	2 764.77	338.45	244.29	89.09	0.14
UCM 3	103.30	42.00	378.50	2 644.70	250.71	180.96	86.65	0.08
UCM 4	103.30	42.00	385.10	2 690.82	401.44	289.76	87.87	0.13
UCM 5	104.40	41.00	392.90	2 729.38	395.40	286.76	86.10	0.14
UCM 6	104.40	41.70	386.30	2 709.33	346.15	253.46	84.91	0.24
UCM 7	104.50	42.00	385.90	2 665.45	299.75	216.36	88.36	0.13
UCM 8	104.30	42.00	380.80	2 635.26	432.89	312.46	84.37	0.12
UCM 9	104.60	42.00	408.30	2 817.47	357.32	257.91	92.52	0.16
UCM 10	105.00	42.20	395.80	2 695.08	335.40	239.80	93.66	0.11
UCM 11	104.70	42.00	381.90	2 632.78	254.39	183.62	83.67	0.06
UCM 12	105.00	42.00	386.80	2 658.94	428.76	309.48	83.92	0.15
UCM 13	104.80	41.90	393.20	2 721.04	398.39	288.93	89.23	0.10
UCM 14	104.60	42.20	396.80	2 712.22	222.01	158.73	62.37	0.05
UCM 15	104.60	42.20	393.70	2 691.03	174.22	124.56	80.23	0.16
UCM 16	104.40	42.30	393.30	2 680.73	316.43	225.17	82.73	0.15
UCM 17	105.00	42.00	392.90	2 700.87	358.90	259.05	83.61	0.16
UCM 18	105.20	41.90	386.70	2 665.88	402.74	292.08	87.18	0.16
UCM 19	104.30	42.00	384.60	2 661.56	296.71	214.16	83.25	0.15
UCM 20	105.00	42.00	393.70	2 706.37	256.29	185.00	85.58	0.12
UCM 21	105.10	42.00	385.80	2 649.54	163.49	118.01	79.90	0.03
UCM 22	104.60	42.10	388.20	2 666.06	383.42	275.44	84.71	0.10
Average Young's Modulus (GPa)							86.89	
Average Poisson's Ratio							0.14	
Average UCS (MPa)							263.00	
Average Density (kg/m ³)							2 686.09	

APPENDIX 7.8: BRAZILIAN TEST RESULTS

Test :	Brazilian Test			
Date:	24 June 2019			
Test Location:	Gold Fields Laboratory, Wits University			
Rock Description:	Conglomerate medium grains			
Laboratory Temperature:	Room Temperature approx. 23°C			
Moisture Content:	Dry			
Loading Rate:	1.5mm/min			
Specimen No.	Thickness(mm)	Diameter (mm)	Load at Failure (kN)	Tensile Strength (MPa)
UTB-BRAZ 12	22.00	42.00	17 069.70	11.80
UTB-BRAZ 13	21.70	42.00	14 263.70	10.00
UTB-BRAZ 14	21.80	42.00	13 975.00	9.70
UTB-BRAZ 15	22.00	42.00	13 856.40	9.50
UTB-BRAZ 16	22.00	42.00	21 383.90	14.70
UTB-BRAZ 17	21.90	42.00	16 935.30	11.70
UTB-BRAZ 18	21.80	42.00	20 677.80	14.40
UTB-BRAZ 19	22.00	42.00	13 784.90	9.50
UTB-BRAZ 20	22.00	42.00	12 344.60	8.50
UTB-BRAZ 21	21.60	42.00	24 900.30	17.50
UTB-BRAZ 22	22.00	42.00	30 789.90	21.20
UTB-BRAZ 23	21.60	42.00	22 149.70	15.50
UTB-BRAZ 24	21.70	42.00	15 141.70	10.60
UTB-BRAZ 25	22.00	42.00	20 300.80	14.00
UTB-BRAZ 26	21.70	42.00	18 440.70	12.90
UTB-BRAZ 27	21.80	42.00	16 076.00	11.20
UTB-BRAZ 28	22.00	42.0	17 043.90	11.70

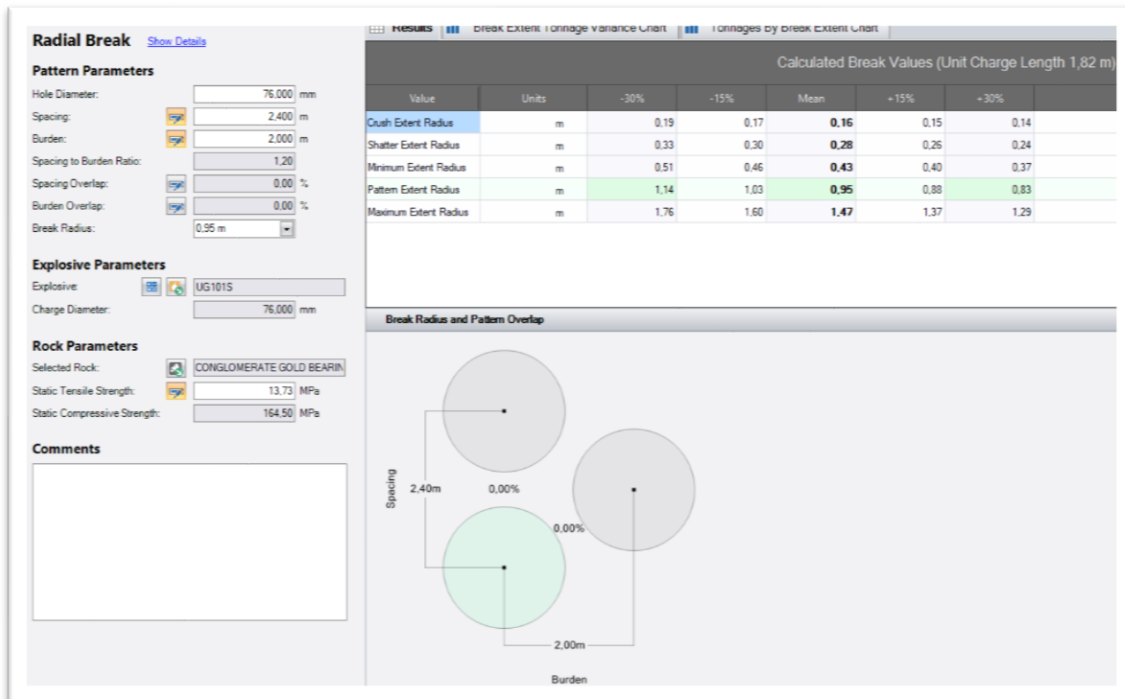
APPENDIX 7.9: RING PATTERN ITERATION AND SIMULATION FOR S/B RATIO OF 1 AND BLASTHOLE DIAMETER OF 76MM (AEGIS DRILL AND BLAST UNDERGROUND SOFTWARE, 2019)



Evaluation Table for – 100 4W Cut04 LHP 7EMB

Statistics	Range	Value	Parameter Gauge	Result
Break Overlap Burden	2% - 12%	0,0%		✘
Break Overlap Spacing	2% - 12%	0,0%		✘
Reflection Point	23,42 MPa - 280,63 MPa	157,40 MPa		✔
Ratio of Radial Break t...	45% - 75%	47,45%		✔
Break Angle	80° - 90°	80,81°		✔
Powder Factor Mass	0,4 kg/tonne - 0,8 kg/tonne	0,59 kg/tonne		✔
Energy Factor Mass	1,52 MJ/tonne - 3,04 MJ/tonne	2,24 MJ/tonne		✔

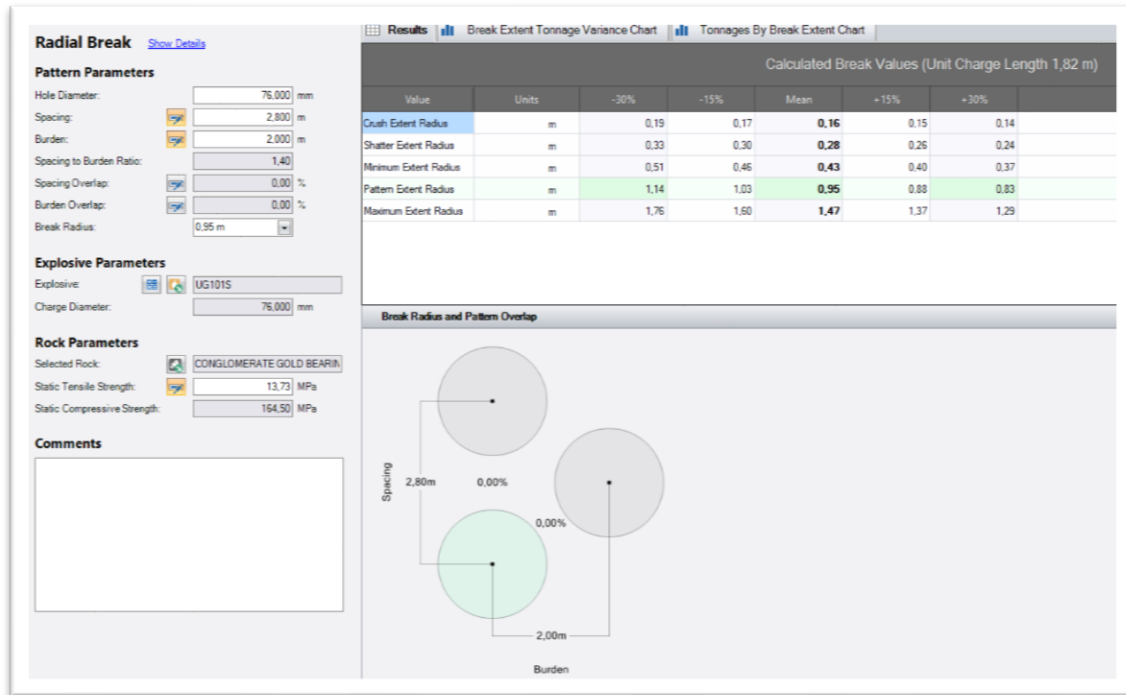
APPENDIX 7.10: RING PATTERN ITERATION AND SIMULATION FOR S/B RATIO OF 1.2 AND BLASTHOLE DIAMETER OF 76MM (AEGIS DRILL AND BLAST UNDERGROUND SOFTWARE, 2019)



Evaluation Table for - 100 4W Cut04 LHP 7EMB

Statistics	Range	Value	Parameter Gauge	Result
Break Overlap Burden	2% - 12%	0,0%		✘
Break Overlap Spacing	2% - 12%	0,0%		✘
Reflection Point	23,42 MPa - 280,63 MPa	157,40 MPa		✔
Ratio of Radial Break t...	45% - 75%	47,45%		✔
Break Angle	80° - 90°	80,81°		✔
Powder Factor Mass	0.4 kg/tonne - 0.8 kg/tonne	0,59 kg/tonne		✔
Energy Factor Mass	1,52 MJ/tonne - 3,04 MJ/tonne	2,24 MJ/tonne		✔

APPENDIX 7.11: RING PATTERN ITERATION AND SIMULATION FOR S/B RATIO OF 1.4 AND BLASTHOLE DIAMETER OF 76MM (AEGIS DRILL AND BLAST UNDERGROUND SOFTWARE, 2019)



Evaluation Table for - 100 4W Cut04 LHP 7EMB

Statistics	Range	Value	Parameter Gauge	Result
Break Overlap Burden	2% - 12%	0.0%		✘
Break Overlap Spacing	2% - 12%	0.0%		✘
Reflection Point	23,42 MPa - 280,63 MPa	157,40 MPa		✔
Ratio of Radial Break t...	45% - 75%	47,45%		✔
Break Angle	80° - 90°	80,81°		✔
Powder Factor Mass	0.4 kg/tonne - 0.8 kg/tonne	0,59 kg/tonne		✔
Energy Factor Mass	1,52 MJ/tonne - 3,04 MJ/tonne	2,24 MJ/tonne		✔

APPENDIX 7.12: RING PATTERN ITERATION AND SIMULATION FOR S/B RATIO OF 1.6 AND BLASTHOLE DIAMETER OF 76MM (AEGIS DRILL AND BLAST UNDERGROUND SOFTWARE, 2019)

Radial Break [Show Details](#)

Pattern Parameters

Hole Diameter: 76,000 mm

Spacing: 3,200 m

Burden: 2,000 m

Spacing to Burden Ratio: 1.60

Spacing Overlap: 0.00 %

Burden Overlap: 0.00 %

Break Radius: 0.95 m

Explosive Parameters

Explosive: UG101S

Charge Diameter: 76,000 mm

Rock Parameters

Selected Rock: CONGLOMERATE GOLD BEARIN

Static Tensile Strength: 13.73 MPa

Static Compressive Strength: 154.50 MPa

Comments

Results | Break Extent | Tonnage Variance Chart | Tonnes by Break Extent Chart

Calculated Break Values (Unit Charge Length 1.82 m)

Value	Units	-30%	-15%	Mean	+15%	+30%
Crush Extent Radius	m	0.19	0.17	0.16	0.15	0.14
Shatter Extent Radius	m	0.33	0.30	0.28	0.26	0.24
Minimum Extent Radius	m	0.51	0.46	0.43	0.40	0.37
Pattern Extent Radius	m	1.14	1.03	0.95	0.88	0.83
Maximum Extent Radius	m	1.75	1.60	1.47	1.37	1.29

Break Radius and Pattern Overlap

Evaluation Table for - 100 4W Cut04 LHP 7EMB

Statistics	Range	Value	Parameter Gauge	Result
Break Overlap Burden	2% - 12%	0,0%		✘
Break Overlap Spacing	2% - 12%	0,0%		✘
Reflection Point	23,42 MPa - 280,63 MPa	157,40 MPa		✔
Ratio of Radial Break t...	45% - 75%	47,45%		✔
Break Angle	80° - 90°	80,81°		✔
Powder Factor Mass	0.4 kg/tonne - 0.8 kg/tonne	0,59 kg/tonne		✔
Energy Factor Mass	1,52 MJ/tonne - 3,04 MJ/tonne	2,24 MJ/tonne		✔

APPENDIX 7.13: RING PATTERN ITERATION AND SIMULATION FOR S/B RATIO OF 1.8 AND BLASTHOLE DIAMETER OF 76MM (AEGIS DRILL AND BLAST UNDERGROUND SOFTWARE, 2019)

Radial Break [Show Details](#)

Pattern Parameters

Hole Diameter: mm

Spacing: m

Burden: m

Spacing to Burden Ratio:

Spacing Overlap: %

Burden Overlap: %

Break Radius: m

Explosive Parameters

Explosive:

Charge Diameter: mm

Rock Parameters

Selected Rock:

Static Tensile Strength: MPa

Static Compressive Strength: MPa

Comments

Calculated Break Values (Unit Charge Length 1.82 m)

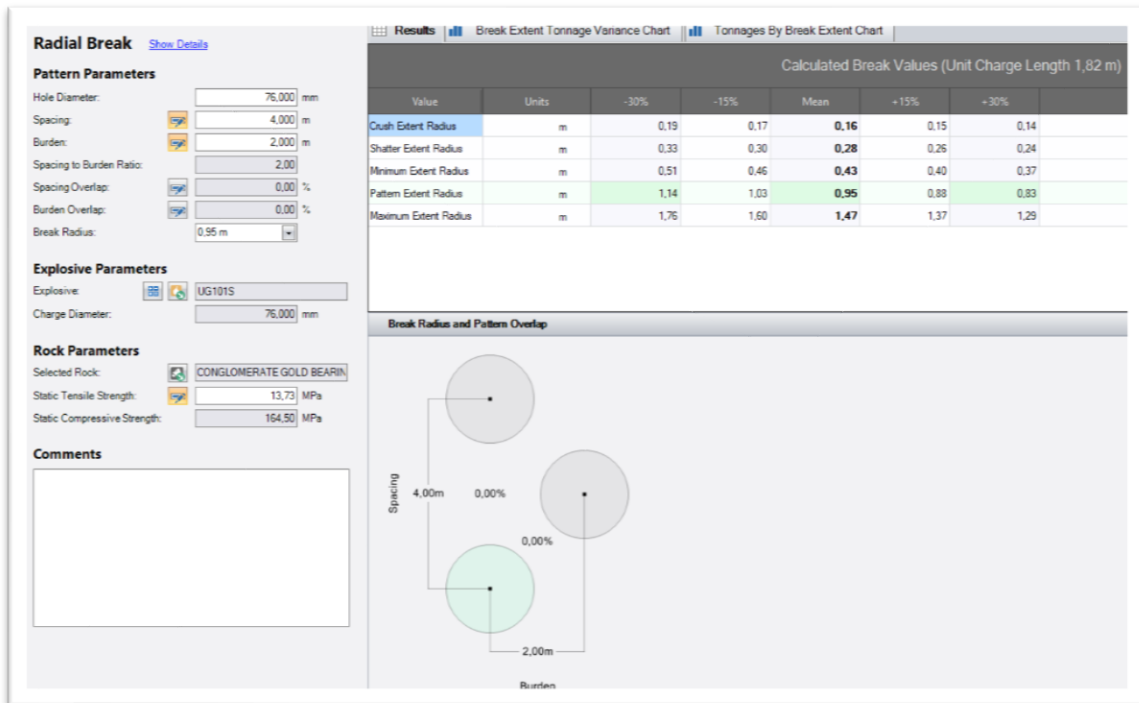
Value	Units	-30%	-15%	Mean	+15%	+30%
Crush Extent Radius	m	0.19	0.17	0.16	0.15	0.14
Shatter Extent Radius	m	0.33	0.30	0.28	0.26	0.24
Minimum Extent Radius	m	0.51	0.46	0.43	0.40	0.37
Pattern Extent Radius	m	1.14	1.03	0.95	0.88	0.83
Maximum Extent Radius	m	1.76	1.60	1.47	1.37	1.29

Break Radius and Pattern Overlap

Evaluation Table for - 100 4W Cut04 LHP 7EMB

Statistics	Range	Value	Parameter Gauge	Result
Break Overlap Burden	2% - 12%	0,0%		✘
Break Overlap Spacing	2% - 12%	0,0%		✘
Reflection Point	23,42 MPa - 280,63 MPa	157,40 MPa		✔
Ratio of Radial Break t...	45% - 75%	47,45%		✔
Break Angle	80° - 90°	80,81°		✔
Powder Factor Mass	0.4 kg/tonne - 0.8 kg/tonne	0,59 kg/tonne		✔
Energy Factor Mass	1,52 MJ/tonne - 3,04 MJ/tonne	2,24 MJ/tonne		✔

APPENDIX 7.14: RING PATTERN ITERATION AND SIMULATION FOR S/B RATIO OF 2.0 AND BLASTHOLE DIAMETER OF 76MM (AEGIS DRILL AND BLAST UNDERGROUND SOFTWARE, 2019)



Evaluation Table for - 100 4W Cut04 LHP 7EMB

Statistics	Range	Value	Parameter Gauge	Result
Break Overlap Burden	2% - 12%	0,0%		✘
Break Overlap Spacing	2% - 12%	0,0%		✘
Reflection Point	23,42 MPa - 280,63 MPa	157,40 MPa		✔
Ratio of Radial Break t...	45% - 75%	47,45%		✔
Break Angle	80° - 90°	80,81°		✔
Powder Factor Mass	0.4 kg/tonne - 0.8 kg/tonne	0,59 kg/tonne		✔
Energy Factor Mass	1,52 MJ/tonne - 3,04 MJ/tonne	2,24 MJ/tonne		✔

APPENDIX 7.15: RING PATTERN ITERATION AND SIMULATION FOR S/B RATIO OF 1.0 AND BLASTHOLE DIAMETER OF 76MM (AEGIS DRILL AND BLAST UNDERGROUND SOFTWARE, 2019)

Radial Break [Show Details](#)

Pattern Parameters

Hole Diameter: 76,000 mm

Spacing: 1,000 m

Burden: 1,000 m

Spacing to Burden Ratio: 1.00

Spacing Overlap: 22.07 %

Burden Overlap: 22.07 %

Break Radius: 0.95 m

Explosive Parameters

Explosive: UG101S

Charge Diameter: 76,000 mm

Rock Parameters

Selected Rock: CONGLOMERATE GOLD BEARIN

Static Tensile Strength: 13.73 MPa

Static Compressive Strength: 164.50 MPa

Comments

Results | Break Extent | Tonnage Variance Chart | Tonnages by Break Extent Chart

Calculated Break Values (Unit Charge Length 0.91 m)

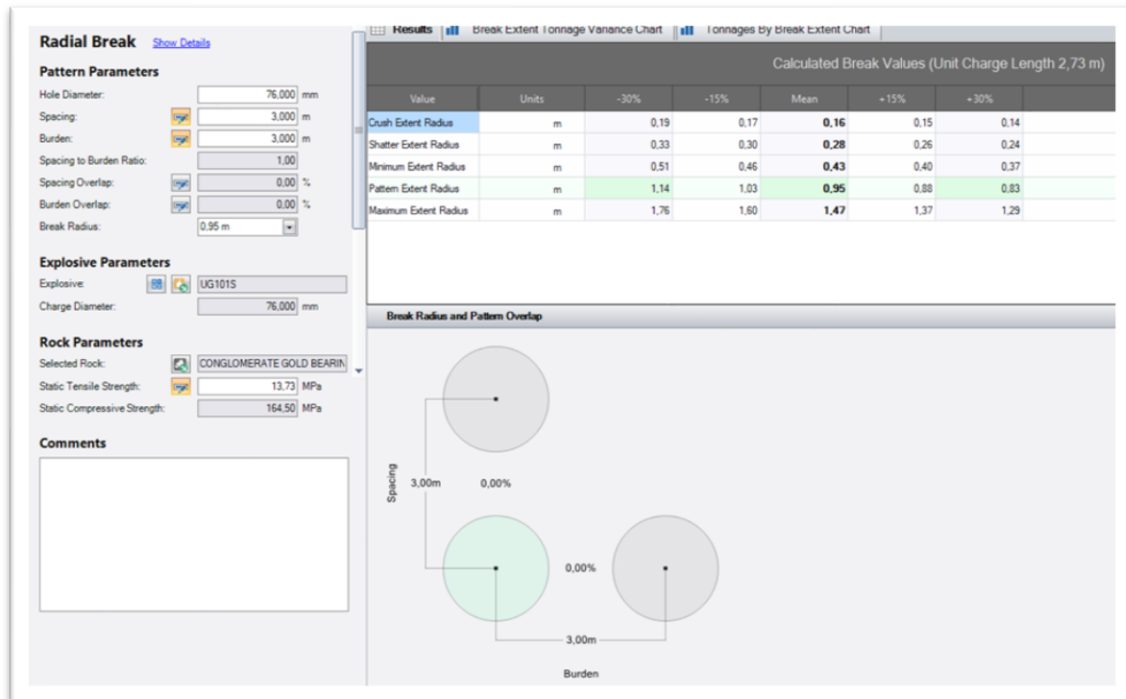
Value	Units	-30%	-15%	Mean	+15%	+30%
Crush Extent Radius	m	0.19	0.17	0.16	0.15	0.14
Shatter Extent Radius	m	0.33	0.30	0.28	0.26	0.24
Minimum Extent Radius	m	0.51	0.46	0.43	0.40	0.37
Pattern Extent Radius	m	1.14	1.03	0.95	0.88	0.83
Maximum Extent Radius	m	1.76	1.60	1.47	1.37	1.29

Break Radius and Pattern Overlap

Evaluation Table for - 100 4W Cut04 LHP 7EMB

Statistics	Range	Value	Parameter Gauge	Result
Break Overlap Burden	2% - 12%	22,1%		✘
Break Overlap Spacing	2% - 12%	22,1%		✘
Reflection Point	23,42 MPa - 280,63 MPa	314,79 MPa		✘
Ratio of Radial Break t...	45% - 75%	94,89%		✘
Break Angle	80° - 90°	85,57°		✔
Powder Factor Mass	0.4 kg/tonne - 0.8 kg/tonne	2,08 kg/tonne		✘
Energy Factor Mass	1,52 MJ/tonne - 3,04 MJ/tonne	7,91 MJ/tonne		✘

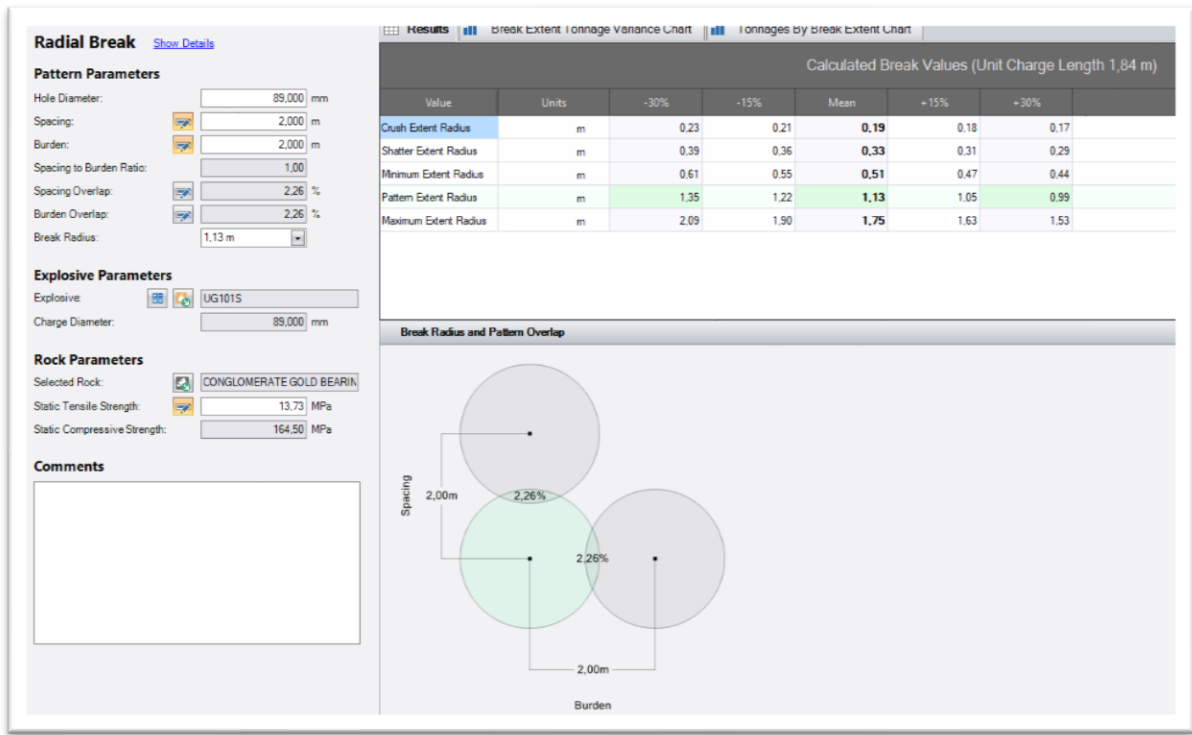
APPENDIX 7.16: RING PATTERN ITERATION AND SIMULATION FOR S/B RATIO OF 1.0 AND BLASTHOLE DIAMETER OF 76MM (AEGIS DRILL AND BLAST UNDERGROUND SOFTWARE, 2019)



Evaluation Table for – 100 4W Cut04 LHP 7EMB

Statistics	Range	Value	Parameter Gauge	Result
Break Overlap Burden	2% - 12%	0.0%		✘
Break Overlap Spacing	2% - 12%	0.0%		✘
Reflection Point	23.42 MPa - 280.63 MPa	104.93 MPa		✔
Ratio of Radial Break t...	45% - 75%	31.63%		✘
Break Angle	80° - 90°	75.68°		✘
Powder Factor Mass	0.4 kg/tonne - 0.8 kg/tonne	0.30 kg/tonne		✘
Energy Factor Mass	1.52 MJ/tonne - 3.04 MJ/tonne	1.16 MJ/tonne		✘

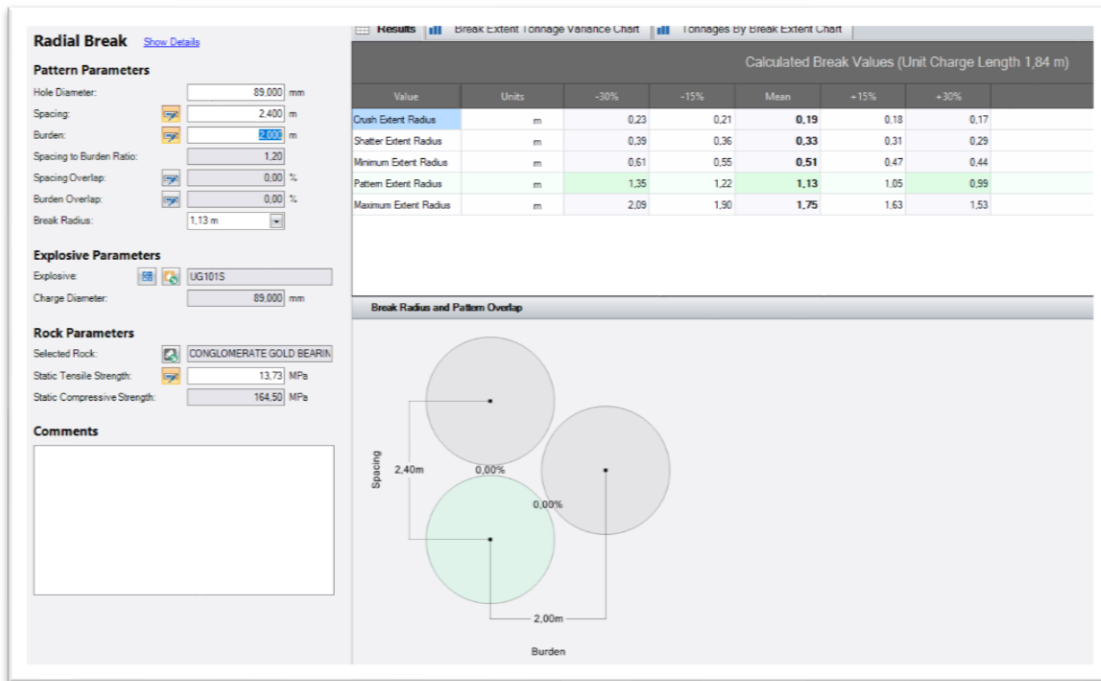
APPENDIX 7.17: RING PATTERN ITERATION AND SIMULATION FOR S/B RATIO OF 1.0 AND BLASTHOLE DIAMETER OF 89MM (AEGIS DRILL AND BLAST UNDERGROUND SOFTWARE, 2019)



Evaluation Table for - 100 4W Cut04 LHP 7EMB

Statistics	Range	Value	Parameter Gauge	Result
Break Overlap Burden	2% - 12%	2.3%		✓
Break Overlap Spacing	2% - 12%	2.3%		✓
Reflection Point	23.42 MPa - 280.63 MPa	187.62 MPa		✓
Ratio of Radial Break t...	45% - 75%	56.31%		✓
Break Angle	80° - 90°	82.38°		✓
Powder Factor Mass	0.4 kg/tonne - 0.8 kg/tonne	0.77 kg/tonne		✓
Energy Factor Mass	1.55 MJ/tonne - 3.09 MJ/tonne	3.00 MJ/tonne		✓

APPENDIX 7.18: RING PATTERN ITERATION AND SIMULATION FOR S/B RATIO OF 1.2 AND BLASTHOLE DIAMETER OF 89MM (AEGIS DRILL AND BLAST UNDERGROUND SOFTWARE, 2019)



Evaluation Table for - 100 4W Cut04 LHP 7EMB

Statistics	Range	Value	Parameter Gauge	Result
Break Overlap Burden	2% - 12%	0,0%		✘
Break Overlap Spacing	2% - 12%	0,0%		✘
Reflection Point	23,42 MPa - 280,63 MPa	187,62 MPa		✔
Ratio of Radial Break t...	45% - 75%	56,31%		✔
Break Angle	80° - 90°	82,38°		✔
Powder Factor Mass	0,4 kg/tonne - 0,8 kg/tonne	0,77 kg/tonne		✔
Energy Factor Mass	1,55 MJ/tonne - 3,09 MJ/tonne	3,00 MJ/tonne		✔

APPENDIX 7.19: RING PATTERN ITERATION AND SIMULATION FOR S/B RATIO OF 1.4 AND BLASTHOLE DIAMETER OF 89MM (AEGIS DRILL AND BLAST UNDERGROUND SOFTWARE, 2019)

Radial Break [Show Details](#)

Pattern Parameters

Hole Diameter: mm

Spacing: m

Burden: m

Spacing to Burden Ratio:

Spacing Overlap: %

Burden Overlap: %

Break Radius: m

Explosive Parameters

Explosive:

Charge Diameter: mm

Rock Parameters

Selected Rock:

Static Tensile Strength: MPa

Static Compressive Strength: MPa

Comments

Results | Break Extent | Tonnage Variance Chart | Tonnes by Break Extent Chart

Calculated Break Values (Unit Charge Length 1,84 m)

Value	Units	-30%	-15%	Mean	+15%	+30%
Crush Extent Radius	m	0.23	0.21	0.19	0.18	0.17
Shatter Extent Radius	m	0.39	0.36	0.33	0.31	0.29
Minimum Extent Radius	m	0.61	0.55	0.51	0.47	0.44
Pattern Extent Radius	m	1.35	1.22	1.13	1.05	0.99
Maximum Extent Radius	m	2.09	1.90	1.75	1.63	1.53

Break Radius and Pattern Overlap

Evaluation Table for - 100 4W Cut04 LHP 7EMB

Statistics	Range	Value	Parameter Gauge	Result
Break Overlap Burden	2% - 12%	0,0%		✘
Break Overlap Spacing	2% - 12%	0,0%		✘
Reflection Point	23,42 MPa - 280,63 MPa	187,62 MPa		✔
Ratio of Radial Break t...	45% - 75%	56,31%		✔
Break Angle	80° - 90°	82,38°		✔
Powder Factor Mass	0.4 kg/tonne - 0.8 kg/tonne	0,77 kg/tonne		✔
Energy Factor Mass	1,55 MJ/tonne - 3,09 MJ/tonne	3,00 MJ/tonne		✔

APPENDIX 7.20: RING PATTERN ITERATION AND SIMULATION FOR S/B RATIO OF 1.6 AND BLASTHOLE DIAMETER OF 89MM (AEGIS DRILL AND BLAST UNDERGROUND SOFTWARE, 2019)

Radial Break [Show Details](#)

Pattern Parameters

Hole Diameter: 89,000 mm

Spacing: 3,200 m

Burden: 2,000 m

Spacing to Burden Ratio: 1.60

Spacing Overlap: 0.00 %

Burden Overlap: 0.00 %

Break Radius: 1,13 m

Explosive Parameters

Explosive: UG101S

Charge Diameter: 89,000 mm

Rock Parameters

Selected Rock: CONGLOMERATE GOLD BEARIN

Static Tensile Strength: 13.73 MPa

Static Compressive Strength: 164.50 MPa

Comments

Results | Break Extent Tonnage Variance Chart | Tonnages By Break Extent Chart

Calculated Break Values (Unit Charge Length 1,84 m)

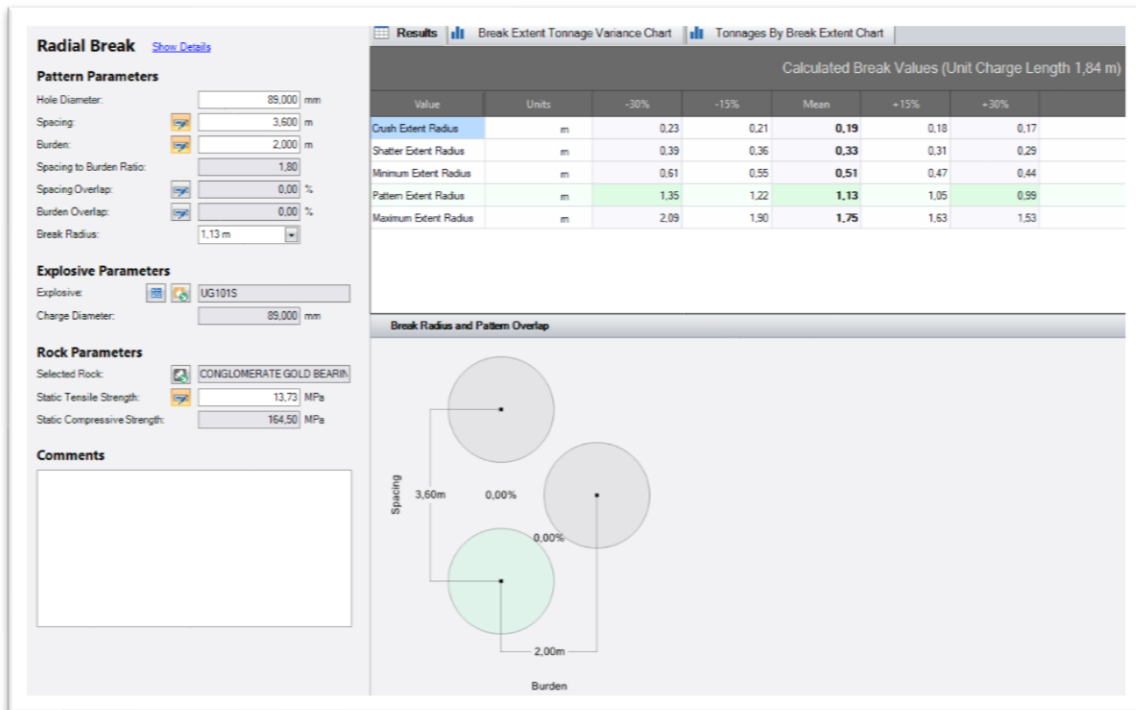
Value	Units	-30%	-15%	Mean	+15%	+30%
Crush Extent Radius	m	0.23	0.21	0.19	0.18	0.17
Shatter Extent Radius	m	0.39	0.36	0.33	0.31	0.29
Minimum Extent Radius	m	0.61	0.55	0.51	0.47	0.44
Pattern Extent Radius	m	1.35	1.22	1.13	1.05	0.99
Maximum Extent Radius	m	2.09	1.90	1.75	1.63	1.53

Break Radius and Pattern Overlap

Evaluation Table for - 100 4W Cut04 LHP 7EMB

Statistics	Range	Value	Parameter Gauge	Result
Break Overlap Burden	2% - 12%	0,0%		✘
Break Overlap Spacing	2% - 12%	0,0%		✘
Reflection Point	23,42 MPa - 280,63 MPa	187,62 MPa		✔
Ratio of Radial Break t...	45% - 75%	56,31%		✔
Break Angle	80° - 90°	82,38°		✔
Powder Factor Mass	0.4 kg/tonne - 0.8 kg/tonne	0,77 kg/tonne		✔
Energy Factor Mass	1,55 MJ/tonne - 3,09 MJ/tonne	3,00 MJ/tonne		✔

APPENDIX 7.21: RING PATTERN ITERATION AND SIMULATION FOR S/B RATIO OF 1.8 AND BLASTHOLE DIAMETER OF 89MM (AEGIS DRILL AND BLAST UNDERGROUND SOFTWARE, 2019)



Evaluation Table for - 100 4W Cut04 LHP 7EMB

Statistics	Range	Value	Parameter Gauge	Result
Break Overlap Burden	2% - 12%	0.0%		✘
Break Overlap Spacing	2% - 12%	0.0%		✘
Reflection Point	23,42 MPa - 280,63 MPa	187,62 MPa		✔
Ratio of Radial Break t...	45% - 75%	56,31%		✔
Break Angle	80° - 90°	82,38°		✔
Powder Factor Mass	0.4 kg/tonne - 0.8 kg/tonne	0,77 kg/tonne		✔
Energy Factor Mass	1,55 MJ/tonne - 3,09 MJ/tonne	3,00 MJ/tonne		✔

APPENDIX 7.22: RING PATTERN ITERATION AND SIMULATION FOR S/B RATIO OF 2.0 AND BLASTHOLE DIAMETER OF 89MM (AEGIS DRILL AND BLAST UNDERGROUND SOFTWARE, 2019)

Radial Break [Show Details](#)

Pattern Parameters

Hole Diameter: mm

Spacing: m

Burden: m

Spacing to Burden Ratio:

Spacing Overlap: %

Burden Overlap: %

Break Radius: m

Explosive Parameters

Explosive:

Charge Diameter: mm

Rock Parameters

Selected Rock:

Static Tensile Strength: MPa

Static Compressive Strength: MPa

Comments

Results | Break Extent Tonnage Variance Chart | Tonnages By Break Extent Chart

Calculated Break Values (Unit Charge Length 1,84 m)

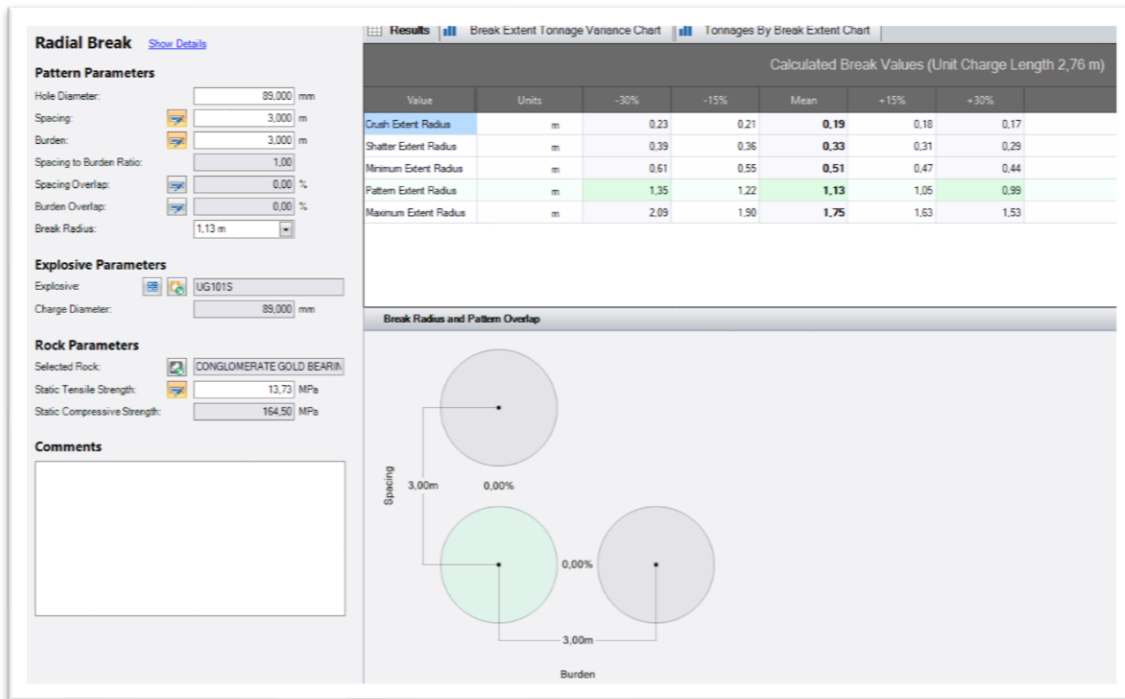
Value	Units	-30%	-15%	Mean	+15%	+30%
Crush Extent Radius	m	0.23	0.21	0.19	0.18	0.17
Shatter Extent Radius	m	0.39	0.36	0.33	0.31	0.29
Minimum Extent Radius	m	0.61	0.55	0.51	0.47	0.44
Pattern Extent Radius	m	1.35	1.22	1.13	1.05	0.99
Maximum Extent Radius	m	2.09	1.90	1.75	1.63	1.53

Break Radius and Pattern Overlap

Evaluation Table for - 100 4W Cut04 LHP 7EMB

Statistics	Range	Value	Parameter Gauge	Result
Break Overlap Burden	2% - 12%	0,0%		✘
Break Overlap Spacing	2% - 12%	0,0%		✘
Reflection Point	23,42 MPa - 280,63 MPa	187,62 MPa		✔
Ratio of Radial Break t...	45% - 75%	56,31%		✔
Break Angle	80° - 90°	82,38°		✔
Powder Factor Mass	0.4 kg/tonne - 0.8 kg/tonne	0,77 kg/tonne		✔
Energy Factor Mass	1,55 MJ/tonne - 3,09 MJ/tonne	3,00 MJ/tonne		✔

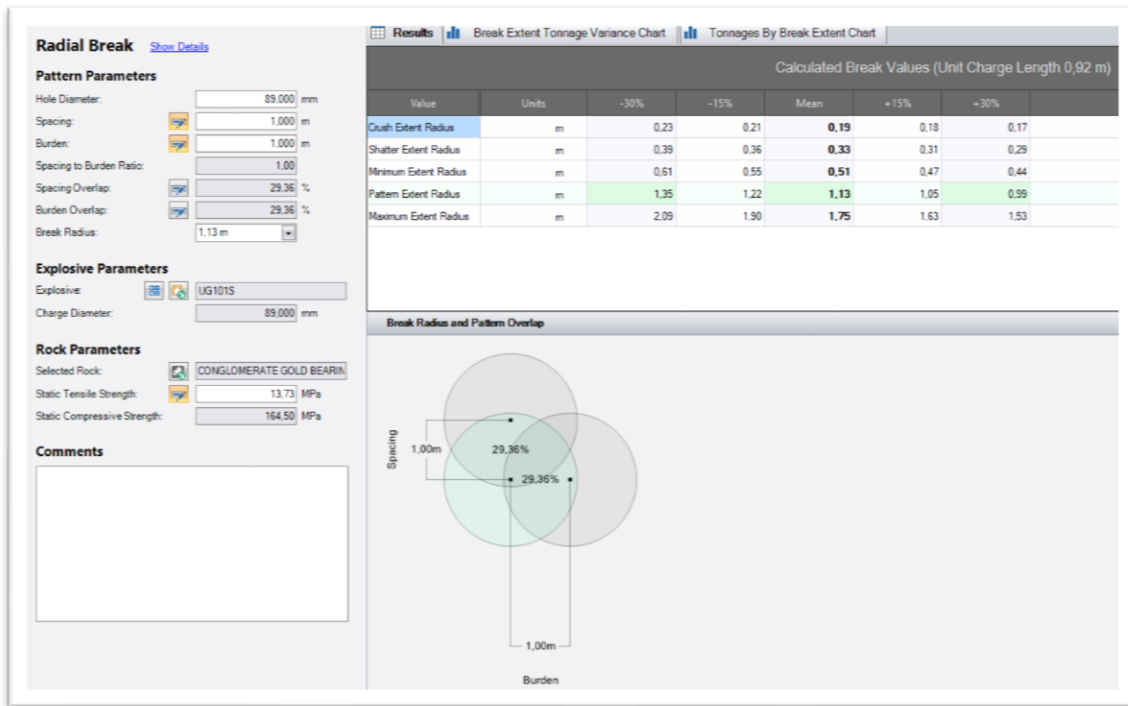
APPENDIX 7.23: RING PATTERN ITERATION AND SIMULATION FOR S/B RATIO OF 1.0 WITH BURDEN AND SPACING OF 3M AND BLASTHOLE DIAMETER OF 89MM (AEGIS DRILL AND BLAST UNDERGROUND SOFTWARE, 2019)



Evaluation Table for - 100 4W Cut04 LHP 7EMB

Statistics	Range	Value	Parameter Gauge	Result
Break Overlap Burden	2% - 12%	0,0%		✘
Break Overlap Spacing	2% - 12%	0,0%		✘
Reflection Point	23,42 MPa - 280,63 MPa	125,08 MPa		✔
Ratio of Radial Break t...	45% - 75%	37,54%		✘
Break Angle	80° - 90°	78,20°		✘
Powder Factor Mass	0.4 kg/tonne - 0.8 kg/tonne	0,39 kg/tonne		⚠
Energy Factor Mass	1,55 MJ/tonne - 3,09 MJ/tonne	1,50 MJ/tonne		⚠

APPENDIX 7.24: RING PATTERN ITERATION AND SIMULATION FOR S/B RATIO OF 1.0 WITH BURDEN AND SPACING OF 3M AND BLASTHOLE DIAMETER OF 89MM (AEGIS DRILL AND BLAST UNDERGROUND SOFTWARE, 2019)



Evaluation Table for – 100 4W Cut04 LHP 7EMB

Statistics	Range	Value	Parameter Gauge	Result
Break Overlap Burden	2% - 12%	29,4%		✘
Break Overlap Spacing	2% - 12%	29,4%		✘
Reflection Point	23,42 MPa - 280,63 MPa	375,24 MPa		✘
Ratio of Radial Break ...	45% - 75%	112,62%		✘
Break Angle	80° - 90°	86,31°		✔
Powder Factor Mass	0.4 kg/tonne - 0.8 kg/tonne	2,80 kg/tonne		✘
Energy Factor Mass	1,55 MJ/tonne - 3,09 MJ/tonne	10,85 MJ/tonne		✘

